ÇARPIŞMA SONRASI GELİŞEN A-TİPİ MAGMATİZMA'NIN JEOKİMYASAL VE JEOKRONOLOJİK ÖZELLİKLERİ (KEBAN-ELAZIĞ-TÜRKİYE)

THE GEOCHEMICAL AND GEOCHRONOLOGICAL PROPERTIES OF POST-COLLISION A-TYPE MAGMATISM (KEBAN-ELAZIĞ-TURKEY)

Mehmet Ali ERTÜRK, Abdullah SAR, Mustafa Eren RİZELİ

Fırat Üniversitesi, Mühendislik Fakültesi, Jeoloji Mühendisliği Bölümü

Özet

Bu çalışmada, Keban-Elazığ-Türkiye bölgesindeki Geç Kretase-Orta Eosen yaşlı Keban Magmatik Kayaçları'nın petrografik, jeokimyasal ve jeokronolojik özellikleri incelenmiştir. İnceleme alanındaki magmatik kayaçlar siyenit porfir ve kuvars monzonitlerle temsil edilmektedir. Petrografik olarak, holokristalen doku gösteren kayaçların esas mineral parajenezlerini K-feldispat (Mega-fenokristal) + plajiyoklas ± amfibol ± biyotit ± kuvars mineralleri oluşturur. İkincil mineral fazları kalsit, serisit, klorit ve epidot mineralleri ile temsil edilmektedir. Aksesuar mineral fazları ise sfen, apatit, zirkon, granat, pirit, florit ve opak minerallerinden oluşmaktadır. Bazı analiz sonuçlarına göre SiO_2 (% 60.09 – 64.37), Al_2O_3 (% 15.75 – 17.96), Fe_2O_3 (% 1.18 – 5.30), MgO (% 0.09 – 0.92) CaO (% 2.07 – 4.27), Na_2O (% 0.80 – 4.93), K_2O (% 4.69 – 13.42),TiO_2 (% 0.22 – 0.37), P_2O_5 (% 0.05 – 0.26), Na_2O+ K_2O (% 8.22 – 14.22), Zr (200.9 – 665.4 ppm), Hf (4.6 – 18.4 ppm), Ta (1.5 – 2.7 ppm), Nb (24 – 56 ppm) değerleri arasında değişmektedir. İncelenen örnekler kondrite göre normalize edilmiş nadir toprak element desenlerine göre hafif nadir toprak elementleri (HNTE) ağır nadir toprak elementlerine (ANTE) göre daha fazla zenginleşme gösterirken, ilksel mantoya göre normalize edilmiş iz element desenlerine göre ise büyük iyon yarıçapına sahip elementler (BİYE), yüksek alan enerjisine sahip elementlere (YAEE) göre daha fazla zenginleşme göstermektedir. LA-ICPMS zirkon U-Pb yaşlandırması göre kristalizasyon yaşları 46.1 ± 0.5, 76.3 ± 0.3, 76.36 ± 0.34 ve 77.4 ± 0.3 My. arasındadır (Geç Kretase-Orta Eosen). İncelenen kayaçlar A-tipi granitoid alanlarına düşmekte olup şoşonitik karakterlidir. İncelenen kayaçların tektonik ortam diyagramlarında post-collisional (çarpışma sonrası gelişen) bölgesine düşmektedir. Arazi, petrografi, jeokimyasal ve jeokronoloji çalışmalarına göre Keban Magmatik Kayaçları'nın çarpışma sonrası gelişmiş magmatizma niteliğinde olduğu düşünülmektedir.

Anahtar Kelimeler: Çarpışma sonrası magmatizma, Geç Kretase-Orta Eosen, Keban, Elazığ.

Abstract

In this study, the petrographic, geochemical and geochronological characteristics of Late Cretaceous-Middle Eocene Keban igneous rocks were examined in Keban-Elazığ-Turkey. Igneous rocks in the study area are represented by syenite porphyry and quartz monzonites. Petro-graphically, the main mineral paragenesis of rocks showing holocrystalline texture are K-feldspar (Mega-phenocrystalline) + plagioclase ± amphibole ± biotite ± quartz minerals. Secondary mineral phases are represented by calcite, sericite, chlorite and epidote minerals.

Accessory mineral phases consist of sphene, apatite, zircon, garnet, pyrite, fluorite and opaque minerals. According to some analysis results, SiO_2 (60.09 – 64.37 wt.%), Al_2O_3 (15.75 – 17.96 wt.%), Fe_2O_3 (1.18 – 5.30 wt.%), MgO (0.09 – 0.92 wt.%) CaO (2.07 – 4.27 wt.%), Na_2O (0.80 – 4.93 wt.%) , K_2O (4.69 – 13.42 wt.%), TiO_2 (0.22 – 0.37 wt.%), P_2O_5 (0.05 – 0.26 wt.%), $Na_2O + K_2O$ (8.22 – 14.22), Zr (200.9 – 665.4 ppm), Hf (4.6 – 18.4 ppm), Ta (1.5 – 2.7 ppm), Nb (24 – 56 ppm) ranges between values. The chondrite normalized rare earth element (REE) patterns display enrichment of light rare earth elements (LREE) compared to the heavy rare earth elements (HREE). The primitive mantle normalized trace element patterns indicate that the large ion lithophile elements (LILE) enriched compared to the high field strength elements (HFSE). According to LA-ICPMS zircon U-Pb crystallization ages ranges between 46.1 ± 0.5, 76.3 ± 0.3, 76.36 ± 0.34 and 77.4 ± 0.3 My. (Late Cretaceous-Middle Eocene). In the tectonic environment diagrams the studied rocks fall into the post-collisional fields (developing after collision).

These rocks fall into the A-type granitoid areas and are of shoshonitic character. It falls into the post-collisional region (developed after collision) in the tectonic environment diagrams of the rocks studied. According to the the field, petrography, geochemical and geochronological studies are evaluated together, Keban Magmatic rocks are thought to have the characteristics of post-collision developed magmatism.

Keywords: Post-collision magmatism, Late Cretaceous-Middle Eocene, Keban, Elazığ.

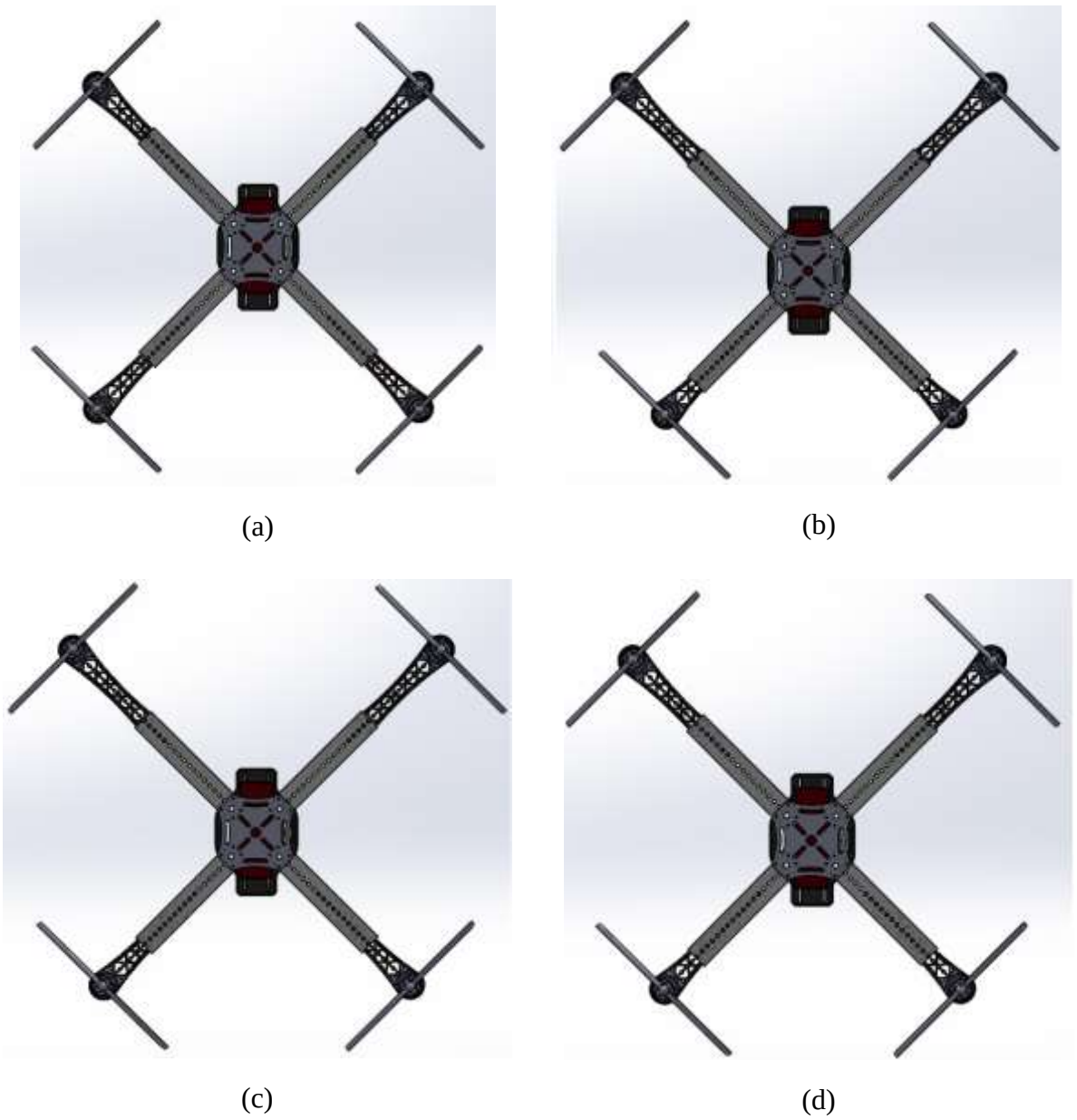

(a) (b)

(c) (d)

Figure 4: (a) Initial situation, (b) %50 differential and %50 collective morphing, (c) %50 differential and %25 collective morphing, (d) %25 differential and %50 collective morphing

3. RESULT AND DISCUSSION

With differential and collective morphing, the quadrotor mass does not change. Only moments of inertia obtained from solid-body modeling change. Inertia moments are obtained from the models drawn in the Solidworks program. In the table below, the inertia and mass information of Figure 2 are given.

Table 2: Differential and collective morphing moment of inertia change

State	m(kg)	Ix(kg*m^2)	Iy(kg*m^2)	Iz(kg*m^2)
Figure 2 (a)	0.60292	0.03595	0.03543	0.02027
Figure 2 (b)	0. 60292	0.03596	0.03564	0.02049
Figure 2 (c)	0. 60292	0.03527	0.03490	0.01906
Figure 2 (d)	0. 60292	0.03659	0.03622	0.02170

PID coefficients are considered constant in all cases of differential and collective morphing. PID coefficients are given in Table 3.

Table 3: PID coefficients

State	P	I	D
Differential and collective morphing	50	5	50

Simulation results in Matlab / Simulink environment are given below.

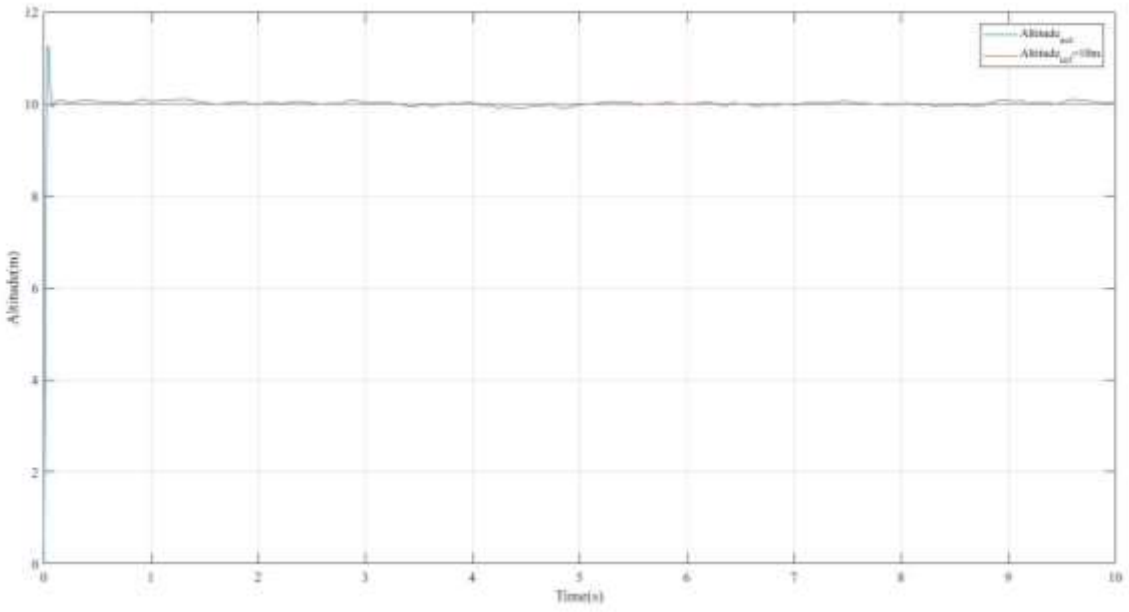

(a)

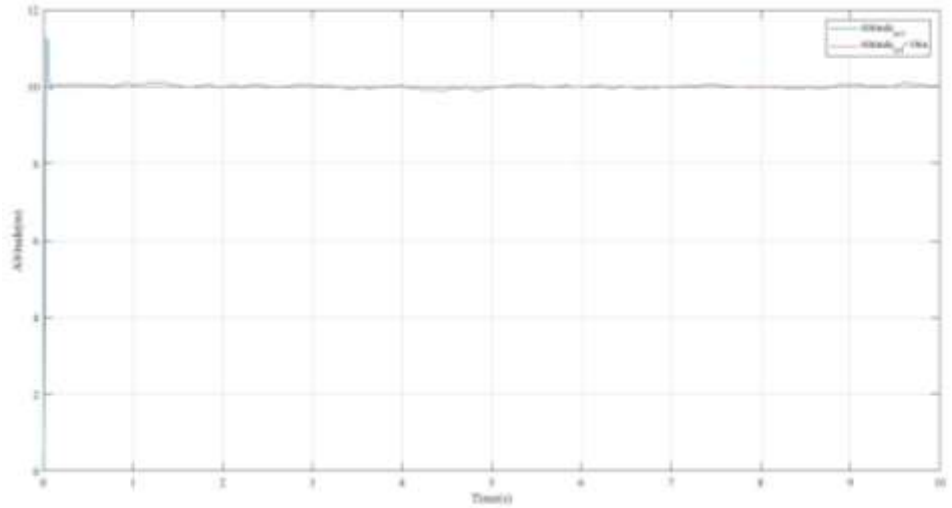

(b)

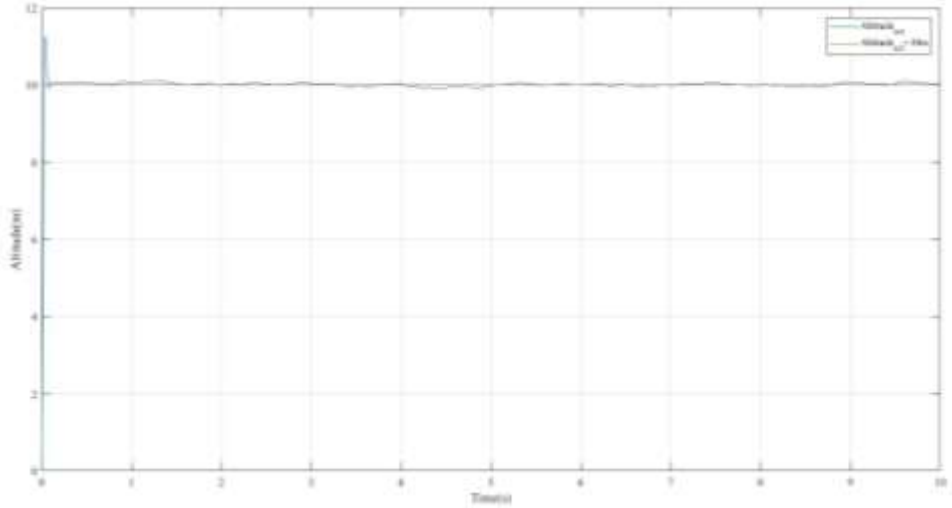

(c)

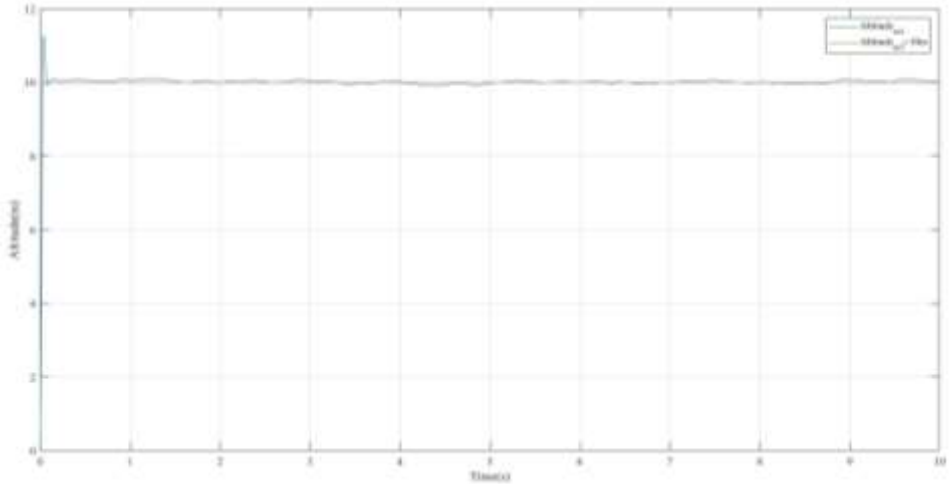

(d)

Figure 5: (a) Initial situation simulation, (b) %50 differential and %50 collective morphing simulation, (c) %50 differential and %25 collective morphing simulation, (d) %25 differential and %50 collective morphing simulation

4. CONCLUSIONS

In this study, the effect of differential and collective morphing on quadrotor hover flight was investigated. The dynamic model was created using the Newton-Euler approach. The quadrotor model was drawn in the Solidworks program. Simulations were made using the state space model approach in Matlab / Simulink environment with the parameters taken from here. PID algorithm is used for quadrotor control.

According to the simulation results, differential and collective morphing did not affect the quadrotor hover flight. The reason for this is that the value sent as input in the space model is not affected by the moments of inertia. Differential and collective morphing does not affect hover flight can be seen by examining the design performance criteria rise time, settling time and overshoot values. Design performance criteria are given in Table 4.

Table 4: Differential and collective morphing design performance criteria

	Initial situation	%50 differential and %50 collective morphing	%50 differential and %25 collective morphing	%25 differential and %50 collective morphing
Rise Time	0.0187 second	0.0187 second	0.0187 second	0.0187 second
Settling Time	0.0667 second	0.0667 second	0.0667 second	0.0667 second
Overshoot	14.4%	14.4%	14.4%	14.4%

REFERENCES

[1] G. O. Vargas, C. Hintz, L. R. G. Carrillo, F. M. Palacios, and E. S. E. Quesada, "Dynamic modeling of a multi-rotorcraft uas with morphing capabilities," in *2015 International Conference on Unmanned Aircraft Systems (ICUAS)*, 2015: IEEE, pp. 963-971.

[2] A. Desbiez, F. Expert, M. Boyron, J. Diperi, S. Viollet, and F. Ruffier, "X-Morf: a crash-separable quadrotor that morfs its X-geometry in flight," in *2017 Workshop on Research, Education and Development of Unmanned Aerial Systems (RED-UAS)*, 2017: IEEE, pp. 222-227.

[3] T. Avant, U. Lee, B. Katona, and K. Morgansen, "Dynamics, Hover Configurations, and Rotor Failure Restabilization of a Morphing Quadrotor," in *2018 Annual American Control Conference (ACC)*, 2018: IEEE, pp. 4855-4862.

[4] D. Falanga, E. Mueggler, M. Faessler, and D. Scaramuzza, "Aggressive quadrotor flight through narrow gaps with onboard sensing and computing using active vision," in *2017 IEEE international conference on robotics and automation (ICRA)*, 2017: IEEE, pp. 5774-5781.

[5] Y. Bai, "Control and Simulation of Morphing Quadcopter," Saint Louis University, 2017.

[6] A. Marks, J. F. Whidborne, and I. Yamamoto, "Control allocation for fault tolerant control of a VTOL octorotor," in *Proceedings of 2012 UKACC International Conference on Control*, 2012: IEEE, pp. 357-362.

[7] S. Bouabdallah, "Design and control of quadrotors with application to autonomous flying," Epfl, 2007.

THE EFFECT OF COLLECTIVE AND DIFFERENTIAL MORPHING ON LONGITUDINAL FLIGHT IN QUADROTORS

Lecturer Oguz KOSE

Gumushane University, Kelkit College of Aydın Dogan

Assoc. Prof. Tugrul OKTAY

Erciyes University, Department of Aeronautical Engineering

Abstract

Four-rotor unmanned aerial vehicles (UAV) known as quadrotors are popular platforms in recent years. They are used in many areas from military to civil use. While it is used in border and port security in the military field, it is used in works such as search and rescue, hobby, cinema, photography, firefighting and mapping in the civil field. These devices are preferred because pilots eliminate the risk of life. In this article, the effect of collective and differential morphing of unmanned aerial vehicle known as quadrotor on longitudinal flight is discussed. Morphing is a developmental feature that has recently been used in unmanned aerial vehicles. In this study, morphing quadrotor is done by lengthening and shortening the arm lengths. Collective and differential morphing are studied separately. Along with morphing, quadrotor modelling and control was also done. Although it is simple in structure, it has a complex structure in terms of model and control. Newton-Euler method was used for the dynamic model. Non-linear motion equations have been converted to linear state. The full quadrotor model was drawn in the Solidworks program. Mass and inertia information was obtained from this model. Simulation model was created by using state space model approach in Matlab / Simulink environment. Proportional integral derivative (PID) algorithm was used as the control structure. Collective and differential morphing has been tested in different simulations. The results are given in comparison with the design performance criteria. In scope, this study is one of the rare studies on morphing in the literature.

Keywords: quadorotor, quadcopter, morphing, uav, pid, control, state space model, uav.

1. INTRODUCTION

In the past two decades, unmanned aerial vehicles (UAV) have had a major impact on aviation. As the name implies, unmanned aerial vehicles are powerful aircraft that do not carry cabin crew and can be controlled remotely. Control of unmanned aerial vehicles is carried out using a remote pilot or autonomous control systems. Unmanned aerial vehicles are used in situations such as search and rescue, military operations and fire fighting in disaster damaged areas. Therefore, it minimizes the risk of pilots' life in hazardous areas.

UAVs can be classified into many categories. The unmanned aerial vehicle to be covered in this study will be the quadrotor that enters the rotary wing class. Quadrotor is the unmanned aerial vehicle that can stay in the air with the lifting force produced by four rotors. Quadrotor does not need any runway as it can vertical take-off and land(VTOL). In addition, the

quadrotor has high maneuverability when compared to fixed-wing UAVs. Therefore, it is more advantageous to use it for special tasks.

In this article, collective and differential morphing situation will be discussed during the longitudinal flight of a quadrotor. Morphing is the changes that occur in the quadrotor geometry. Along with Morphing, the flight control system required for the quadrotor will also be designed. In recent years, many studies have been done on quadrotor control and morphing. K. Habib (2014) in [1] aimed a model for modelling and control. The difference between the real altitude and the desired altitude was the error signal. The manoeuvres of the unmanned aerial vehicle were achieved with differential equation and state space model. PID control was used as a controller. But the model had a lack of high overshoot. Li et. al. (2011) in [2] proposed a model that perceives the dynamic response of the unmanned aerial vehicle. He used PID control for the position and orientation of the aircraft. Due to the incompatibility between the PID control gains, the model was also unstable. C. Hintz et al. in [3] made a quadrotor study with morphing feature. With this study, the quadrotor was working in narrow spaces by changing its geometry. It was used in the cave and out of the reach of people. A. Desbiez et al. in [4] worked on the quadrotor that changed the arm angles. With the signal sent from the ground station to the quadrotor, he could change the angles from the center of the quadrotor. T. Oktay and O. Kose [5-7] designed a quadrotor with collective morphing feature both during longitudinal and vertical flight. This quadrotor provided morphing with the lengthening and shortening of the arms. PID algorithm is used as control system.

2. MATERIAL AND METHODS

A quadrotor consists of four rotors and propellers as seen in Figure 1. Each rotor creates rhythm force. If the sum of the four rotor thrust forces is greater than the weight of the quadrotor, the quadrotor starts to rise from the ground.

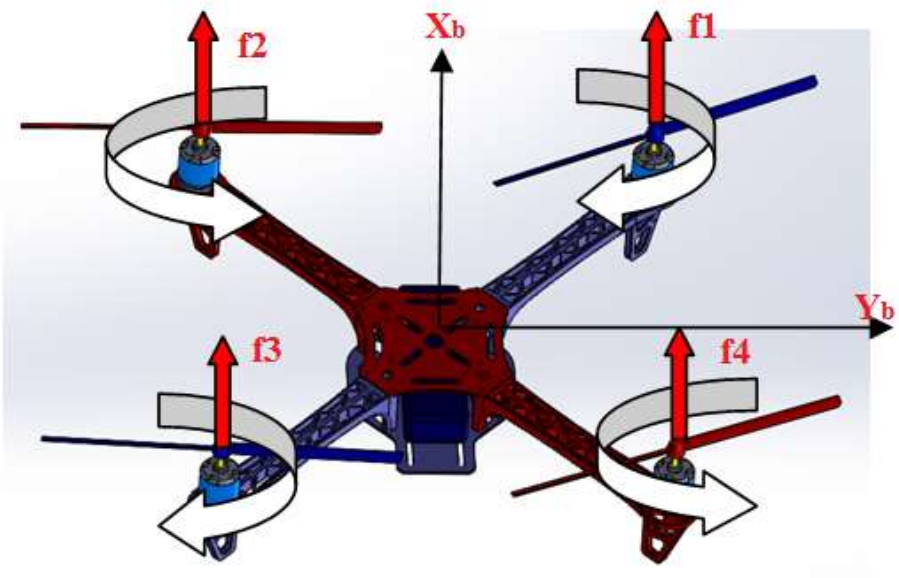

Figure 6: Quadrotor

The longitudinal flight to be covered in this study takes place on the quadrotor Y axis. In this study, an X-type quadrotor is used. For longitudinal movement, the speed of the front rotors should be reduced while the speed of the rear rotors should be increased. Figure 2 shows the longitudinal movement.

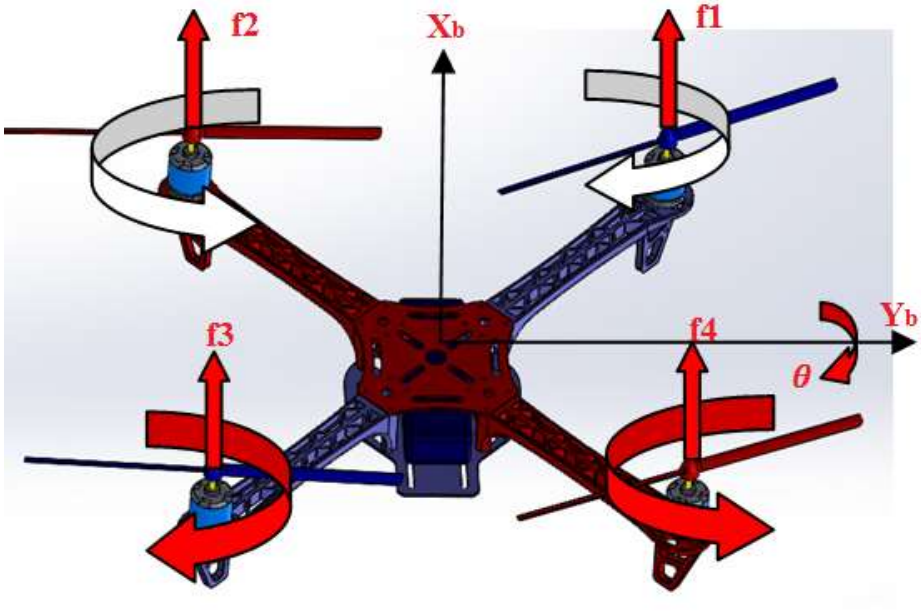

Figure 7: Quadrotor longitudinal flight

2.1 Quadrotor Dynamic Model

Newton-Euler approach is used to create the quadrotor dynamic model. The following views are valid for this approach[8, 9].

• Quadrotor structure is rigid and symmetrical,

• Propellers of quadrotor are rigid,

•Quadrotor thrust and drag force are proportional to the rotor speed square,

• Ground effect in the quadrotor is neglected.

Quadrotor has a non-linear structure as a dynamic structure. The non-linear structure has twelve equations, including both longitudinal and lateral movements. These equations can be divided into two parts and used separately for longitudinal and lateral motion. Non-linear equations are converted to linear equations by various methods. The equations used for longitudinal flight are given below.

$$\dot{x} = u \tag{1}$$

$$\dot{z} = w \tag{2}$$

$$\dot{u} = -g\theta \tag{3}$$

$$\dot{\boldsymbol{w}} = \frac{\boldsymbol{f_t}}{\boldsymbol{m}} \tag{4}$$

$$\dot{\boldsymbol{q}} = \frac{\boldsymbol{\tau_y}}{\boldsymbol{I_y}} \tag{5}$$

$$\dot{\boldsymbol{\theta}} = \boldsymbol{q} \tag{6}$$

Where, x, z and θ are linear and angular positions. u, w and q are linear and angular velocity.

In order to apply the given equations within the model, an input value must be given to the equations. The input value used for the longitudinal flight is given below.

$$\boldsymbol{\tau_y = U_3 = bl}(\Omega_1^2 - \Omega_2^2 - \Omega_3^2 + \Omega_4^2) \tag{7}$$

Where l the distance between any rotor and the center of the quadrotor, b is the thrust factor, Ω is propeller speed.

2.2 State Space Model and Control System

State space model is the expression of a physical system in first order differential equations with input, output and state variables in matrix form. Quadrotor state space model is expressed by linear motion equations. In general, the state space model of a system is indicated by the following expression.

$$\dot{x} = Ax(t) + Bu(t)$$

$$y = Cx(t) + Du(t)$$

Where x(t) state vector, u(t) control or input vector, y(t) output vector, A system matrix, B input matrix, C output matrix and D feed forward matrix.

In this case, the quadrotor forward flight state space model would be as shown below.

$$\begin{bmatrix} \dot{x} \\ \dot{z} \\ \dot{u} \\ \dot{w} \\ \dot{q} \\ \dot{\theta} \end{bmatrix} = \begin{bmatrix} 0 & 0 & 1 & 0 & 0 & 0 \\ 0 & 0 & 0 & 1 & 0 & 0 \\ 0 & 0 & 0 & 0 & 0 & -g \\ 0 & 0 & 0 & 0 & 0 & 0 \\ 0 & 0 & 0 & 0 & 0 & 0 \\ 0 & 0 & 0 & 0 & 1 & 0 \end{bmatrix} \begin{bmatrix} x \\ z \\ u \\ w \\ q \\ \theta \end{bmatrix} + \begin{bmatrix} 0 & 0 \\ 0 & 0 \\ 0 & 0 \\ 1/m & 0 \\ 0 & 1/I_y \\ 0 & 0 \end{bmatrix} \begin{bmatrix} f_t \\ \tau_y \end{bmatrix}$$

$$y = \begin{bmatrix} 0 & 0 & 0 & 0 & 0 & 0 \\ 0 & 0 & 0 & 0 & 0 & 0 \\ 0 & 0 & 0 & 0 & 0 & 0 \\ 0 & 0 & 0 & 0 & 0 & 0 \\ 0 & 0 & 0 & 0 & 0 & 0 \\ 0 & 0 & 0 & 0 & 0 & 1 \end{bmatrix} \begin{bmatrix} x \\ z \\ u \\ w \\ q \\ \theta \end{bmatrix}$$

The state space model represents the inertia moment in the input matrix. Inertia moment is a diagonal matrix. This matrix is produced because the quadrotor's four arms are symmetrical and aligned on the x and y axes. The inertia matrix is as shown below.

$$I = \begin{bmatrix} I_x & 0 & 0 \\ 0 & I_y & 0 \\ 0 & 0 & I_z \end{bmatrix} \quad (8)$$

PID control is a continuous control law or procedure that combines proportional, integral, and derivative basic control effects. The duration of the error is constantly present in the control command in this control. PID control is generally known as the simplest controller. It provides adequate, robust and appropriate control in many industrial application areas. For PID controller design, parallel architecture has been used[10].

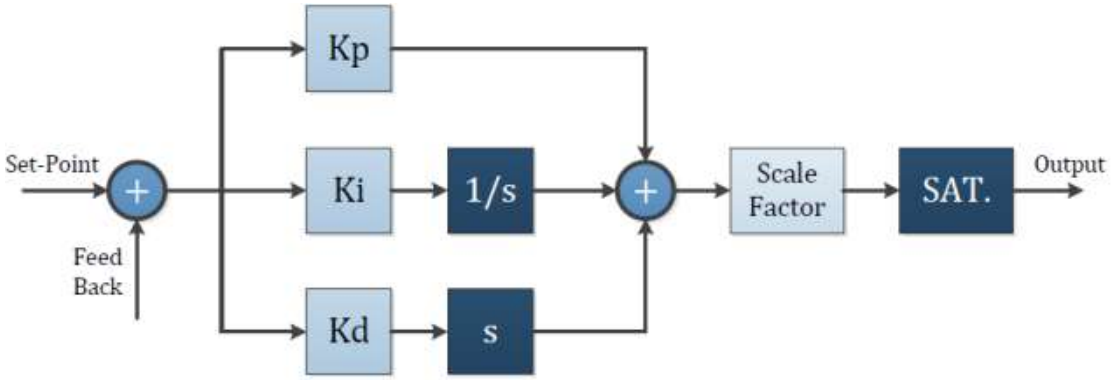

Figure 8: PID architecture

PID control is an audit effect that combines the advantages of the three main audit effects within a single unit. Integral effect reduces the steady state error that may occur in the system to zero. Derivative effect increases the response rate of the system.

2.3 Morphing System

The researchers realized that many years ago, birds changed their body geometries to perform various manoeuvres during their flight. The process of changing this body geometry is called morphing. Morphing is a developmental feature that has recently been used in unmanned aerial vehicles. Morphing in unmanned aerial vehicles takes place in the form of changing body geometry as in birds. There are two types of morphing available in the literature:

• Active morphing

• Passive morphing

If the quadrotor performs morphing during flight, it is called active morphing. If morphing is done while the quadrotor is on the ground, it is called passive morphing. In this study, active morphing will be discussed.

The quadrotor lengthens or shortens all four arms simultaneously and in the same amount during active morphing. Differential and collective morphing are discussed together in this study. Arm lengths were taken into account while morphing was performed. For example, the back arms perform 50% differential morphing while the forearms perform 50% collective morphing. The figures below show differential and collective morphing.

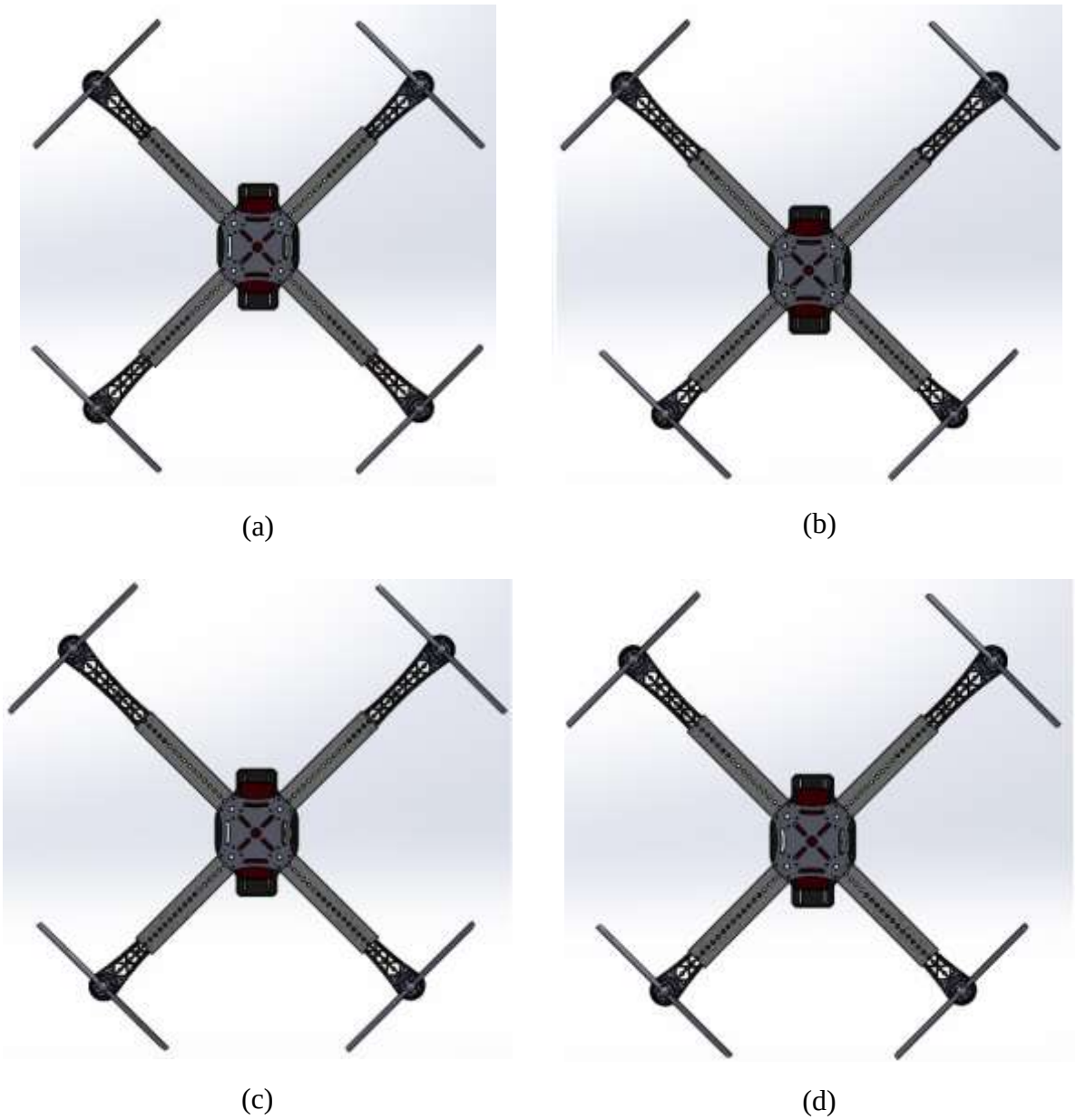

(a) (b)

(c) (d)

Figure 9: (a) Initial situation, (b) %50 differential and %50 collective morphing, (c) %50 differential and %25 collective morphing, (d) %25 differential and %50 collective morphing

3. RESULT AND DISCUSSION

The quadrotor mass does not change in both collective and differential morphing. Since the solid-body model changes in the morphing process, the moment of inertia changes. In the case

of collective and differential morphing in Figure 4, when the mass is kept constant and morphing is applied, the moment of inertia change is given in Table 1.

Table 5: Collective and differrential morphing moment of inertia change

State	m(kg)	Ix(kg*m^2)	Iy(kg*m^2)	Iz(kg*m^2)
Figure 4 (a)	0.60292	0.03595	0.03543	0.02027
Figure 4 (b)	0. 60292	0.03596	0.03564	0.02049
Figure 4 (c)	0. 60292	0.03527	0.03490	0.01906
Figure 4 (d)	0. 60292	0.03659	0.03622	0.02170

PID coefficients for longitudinal flight were chosen same values for both non-morphing and morphing cases. These values are given below.

Table 6: PID coefficients

State	P	I	D
Differential and collective morphing	50	0.3	1

Simulation results in Matlab / Simulink environment are given in Figures 5.

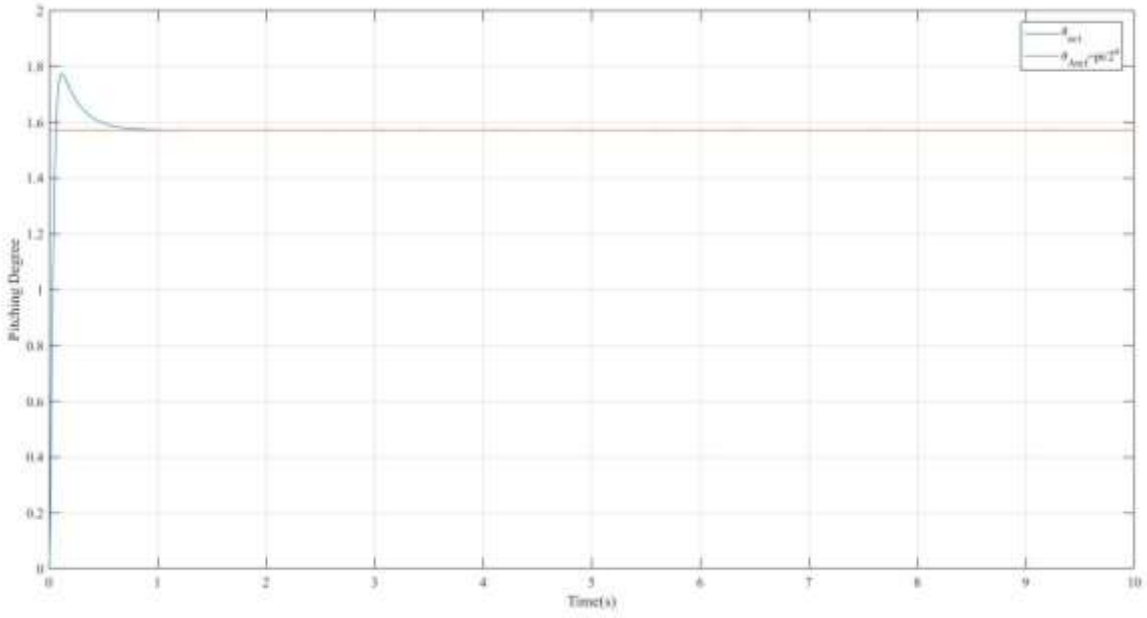

(a)

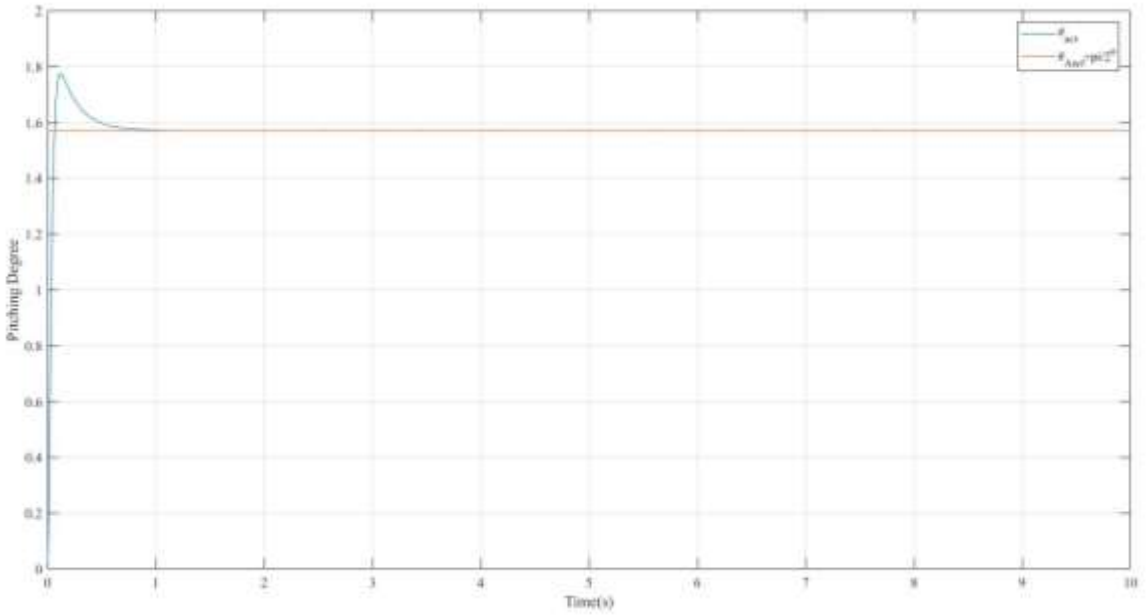

(b)

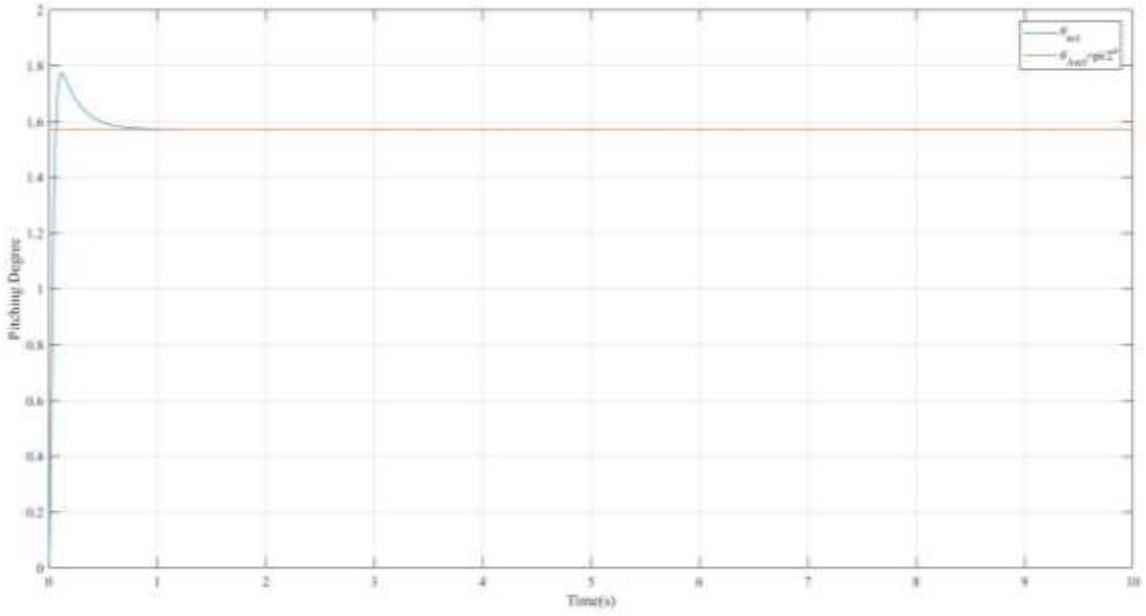

(c)

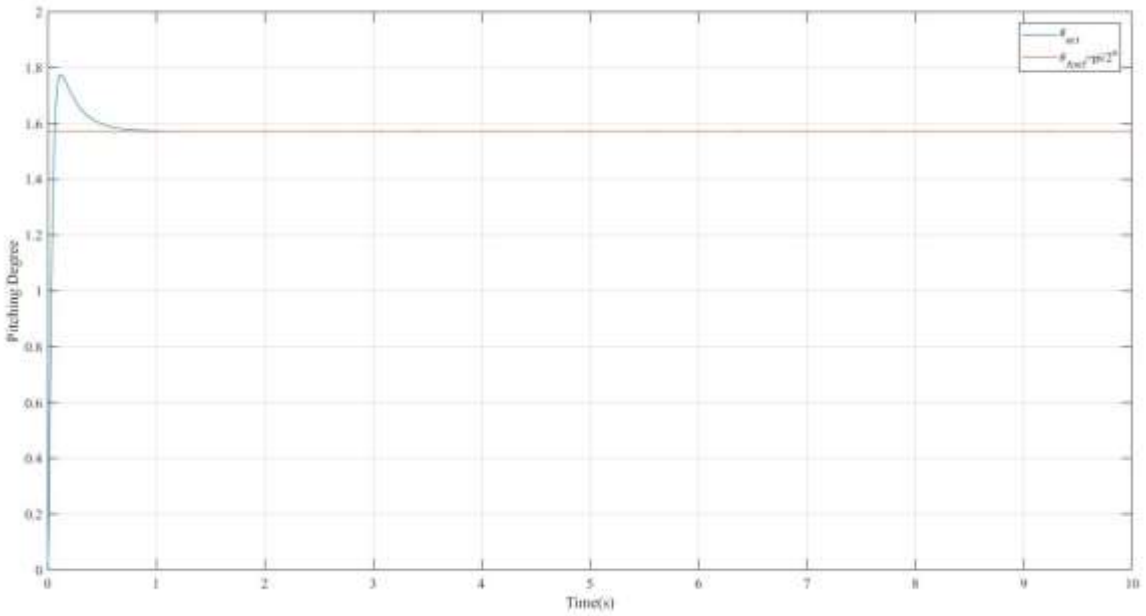

(d)

Figure 10: (a) Initial situation simulation, (b) %50 differential and %50 collective morphing simulation, (c) %50 differential and %25 collective morphing simulation, (d) %25 differential and %50 collective morphing simulation

4. CONCLUSIONS

In this study, the effect of both collective and differential morphing on longitudinal flight was investigated. The quadrotor dynamic model was created using the Newton-Euler approach. The model was drawn in the Solidworks program. Simulations were made in the Matlab / Simulink environment with the parameters taken from the model. State space model approach was used in simulations. The PID algorithm was used as the control system.

According to the simulation results, differential and collective morphing had an impact on longitudinal flight. The reason for this effect is that the Iy value, which is the moment of inertia, is an entry into the state space model. This value changes in every morphing situation. This was determined by examining the design performance criteria rise time, settling time and overshoot values. Table 3 differential and collective morphing design performance criteria are given.

Table 7: Differential and collective morphing design performance criteria

	Initial situation	%50 differential and %50 collective	%50 differential and %25 collective	%25 differential and %50 collective
Rise Time	0.0435 sec	0.0437 sec	0.0429 sec	0.0444 sec
Settling Time	0.462 sec	0.463 sec	0.459 sec	0.467 sec
Overshoot	13%	13.1%	13%	13.1%

REFERENCES

[1] M. K. Habib, W. G. A. Abdelaal, and M. S. Saad, "Dynamic modeling and control of a quadrotor using linear and nonlinear approaches," 2014.

[2] J. Li and Y. Li, "Dynamic analysis and PID control for a quadrotor," in *2011 IEEE International Conference on Mechatronics and Automation*, 2011: IEEE, pp. 573-578.

[3] C. Hintz, C. Torno, and L. R. G. Carrillo, "Design and dynamic modeling of a rotary wing aircraft with morphing capabilities," in *2014 International Conference on Unmanned Aircraft Systems (ICUAS)*, 2014: IEEE, pp. 492-498.

[4] A. Desbiez, F. Expert, M. Boyron, J. Diperi, S. Viollet, and F. Ruffier, "X-Morf: a crash-separable quadrotor that morfs its X-geometry in flight," in *2017 Workshop on Research, Education and Development of Unmanned Aerial Systems (RED-UAS)*, 2017: IEEE, pp. 222-227.

[5] T. Oktay and O. Kose, "The Effect of Collective Morphing on the Longitudinal Flight in Quadcopter," presented at the MAS INTERNATIONAL EUROPEAN CONGRESSON MATHEMATICS, ENGINEERING, NATURAL ANDMEDICAL SCIENCES-III, Şanlıurfa, 2019.

[6] T. Oktay and O. Kose, "The Effect of Collective Morphing on the Lateral Flight in Quadcopter," presented at the Umteb 6. Uluslararasi Mesleki ve Teknik Bilimler Kongresi, Iğdır, 2019.

[7] T. Oktay and O. Kose, "The Effect of Collective Morphing on the Vertical Flight in Quadcopter," in *MAS INTERNATIONAL EUROPEAN CONGRESSON MATHEMATICS, ENGINEERING, NATURAL ANDMEDICAL SCIENCES-III*, Şanlıurfa, 2019, pp. 1-10.

[8] A. Marks, J. F. Whidborne, and I. Yamamoto, "Control allocation for fault tolerant control of a VTOL octorotor," in *Proceedings of 2012 UKACC International Conference on Control*, 2012: IEEE, pp. 357-362.

[9] S. Bouabdallah, "Design and control of quadrotors with application to autonomous flying," Epfl, 2007.

[10] K. J. Åström and T. Hägglund, *Control PID avanzado*. Pearson, Madrid, 2009.

INVESTIGATION OF HARDNESS AND WEAR PROPERTIES OF Ni-B COATINGS ANNEALED AT DIFFERENT TEMPERATURES

FARKLI SICAKLIKLARDA TAVLANAN Ni-B KAPLAMALARIN SERTLİK VE AŞINMA ÖZELLİKLERİNİN İNCELENMESİ

Erhan DURU

Res. Asst, Sakarya University Engineering Faculty, Metallurgy and Materials Engineering

Fatih DOĞAN

PhD student, Sakarya University Institute of Natural Science, Metallurgy and Materials Engineering

Mehmet UYSAL

Assist. Prof. Dr., Sakarya University Engineering Faculty, Metallurgy and Materials Engineering

Serdar ASLAN

Assist. Prof. Dr., Sakarya University Engineering Faculty, Metallurgy and Materials Engineering

Hatem AKBULUT

Prof. Dr., Sakarya University Engineering Faculty, Metallurgy and Materials Engineering

Özet

Bu çalışmada akımsız kaplama prosesi ile çelik altlık malzeme üzerine biriktirilen Ni-B alaşım kaplamalarının Ar gazı ortamında 2 saat boyunca oda sıcaklığındaki ve farklı ısıl işlem sıcaklıklarındaki (300^{o}C, 400^{o}C, 500^{o}C) morfolojileri, faz yapıları, sertlikleri ve aşınma özellikleri incelenmiştir. Ni-B alaşım kaplamalarının yüzey morfolojileri ve kesit görüntüleri taramalı elektron mikroskobu (SEM) görüntülendi ve faz yapıları X-ışın kırınımı (XRD) ile analiz edildi. Isıl işlem öncesi ve ısıl işlem sonrası kaplamaların sertlik değerleri nanoindentation sertlik cihazı ile hesaplandı. Aşınma ve sürtünme testleri kuru kayma aşınma yöntemiyle oda sıcaklığında (25^{o}C), 300 metre boyunca, 5N normal yük altında, 25 mm/s kayma hızında gerçekleştirildi. Kaplamaların yüzey morfolojileri yoğun ve homojen karnabahar yapısında olduğu gözlendi. Kaplamalar ısıl işlem öncesi amorf yapıda iken ısıl işleme tabi tutulduklarında nikel tamamen kristalize oldu ve nikel borid (Ni_3B ve Ni_2B) fazları oluştu. Isıl işlem sonrası oluşan bu fazlar nikel matrisin tane büyümesini engelleyerek kaplamanın sertliğini arttırdı ve kaplama yüzeyinin aşındırıcı ile temas alanını azaltarak aşınma direncini geliştirdi. Aşınma testlerinden sonra her bir kaplamanın aşınma miktarı ve sürtünme katsayısı hesaplandı, aşınma yüzey görüntüleri SEM ile incelendi ve aşınma sonrası oluşan aşınma izlerinin elemental analizi enerji dağılım spektroskopisi (EDS) ile yapıldı. Isıl işlem sıcaklığının 400^{o}C'ye arttırılmasıyla kaplamanın sertlik değeri ve aşınma direnci arttı. Kaplamaların aşınma yüzeyleri genellikle abrasif aşınma oluşurken 500^{o}C sıcaklıkta ısıl işlem

görmüş kaplamanın aşınma yüzeyinde ayrıca adhezif aşınma oluştu. Isıl işlem görmüş kaplamanın aşınma miktarı ve sürtünme katsayısı, ısıl işlem görmemiş kaplamaya göre daha düşük olduğu hesaplanmıştır. 400ºC ısıl işlem görmüş Ni-B kaplama, endüstriyel uygulamalarda kullanılmakta olan sert krom kaplama ile karşılaştırıldığında daha yüksek sertlik ve daha iyi aşınma direnci göstermiştir.

Anahtar Kelimeler: Ni-B kaplama, ısıl işlem, sertlik, aşınma.

Abstract

In this study, the morphology, phase structures, hardness and wear properties of Ni-B alloy coatings deposited on the steel substrate by electrodeposition process at room temperature and different annealing temperatures (300ºC, 400ºC, 500ºC) for 2 hour in Ar gas medium were investigated. Surface morphologies and cross-sectional images of Ni-B alloy coatings were monitored by scanning electron microscopy (SEM) and phase structures were analyzed by X-ray diffraction (XRD). The hardness values of the coatings as-deposited and annealed were calculated with the nanoindentation hardness device. Wear and friction tests were carried out by dry sliding wear method at room temperature (25ºC) for 300 meters, under 5N normal load, at 25 mm/s sliding speed. It was observed that the surface morphologies of coatings were dense and homogeneous cauliflower. When the coatings were in amorphous structure as-deposited, annealed nickel completely crystallized and nickel borid (Ni_3B and Ni_2B) phases occurred. Phases formed after heat treatment prevent the crystal growth and thus increasing the hardness of the coating and improving the wear resistance by reducing the contact area of the coating surface with the abrasive. After the wear tests, the wear rate and friction coefficient of each coating were calculated, the surface images of the wear tracks were examined by SEM, and the elemental analysis of the wear tracks was done by energy dispersive spectroscopy (EDS). By increasing the anneal temperature to 400ºC, the hardness and wear resistance of the coating increased. Wear tracks of the coatings are generally abrasive, while adhesive wear has also occurred on the wear track, which has been heat treatment at 500ºC. The wear rate and friction coefficient of the annealed coating were calculated to be lower than that of the as-deposited coating. The 400ºC heat treated Ni-B coating showed higher hardness and better wear resistance compared to the hard chrome coating used in industrial applications.

Keywords: Ni-B coating, heat treatment, hardness, wear.

1. INTRODUCTION

In surface coating technology, electroless Ni based coatings is used as an alternative to hard chrome coating due to its superior mechanical and tribological properties and homogeneously distributed surface coating. Pure nickel, alloy and composite coatings have gained great importance in the past few decades. Especially the electroless Ni-P and Ni-B alloyed coatings are being investigated more for industrial applications (Sahoo P, 2011). Sodium borohydride, which is used as a reducing agent in the electroless Ni-B coating process, improves the

hardness and wear resistance of the material more than Ni-P coatings (Das S K, 2011). Due to the mechanical properties of micro-structural problems, microstructure, phase transformation, tribological properties and corrosion resistance of Ni-B coatings continue to be investigated. The electroless Ni-B coating process takes place by reducing nickel ions to the substrate material surface immersed in the bath solution containing reducing agent and metal ion salts (Mallory, 1990). The heat treatment applied after the surface coating process improves the morphology, phase structure, hardness and tribological properties of the material. While the mechanical properties of the coating increase with heat treatment, the corrosion resistance decreases (Vitry, 2012). Although the hardness and wear resistance of the substrate deposited with Ni-B electroless coating increases, the heat treatment applied to the material affects the development of the material strength (Krishnaveni, 2005). Generally, the hardness of the material is equivalent to the hardness of the chrome plating at 400^{o}C±50 heat treatment temperature for about 1 hour under vacuum. The increase in material hardness is thought to be nickel borides (Ni_3B, Ni_2B) formed after heat treatment. Ni-B coatings are heat treated at different temperatures to increase the phase diversity in the crystal. It is stated that the boron content is important in the formation of Ni_3B and Ni_2B crystal phases after heat treatment in the studies of the coatings related to heat treatment. The agglomeration of Ni_3B crystals when the heat treatment temperature is over 500^{o}C causes a decrease in material hardness (Dervos, 2004). It has also been reported that Ni_2B phase decomposes while Ni_4B_3 phase forms at high temperature (Takahasi, 1980). The grain growth of the heat-treated coatings is low and accordingly there is an increase in the hardness of the material. The microstructure, coating thickness and oxide layer of the coating play an important role on the tribological behavior of Ni-B coatings (Vitry, 2011). In the present industrial applications, it is thought that the electroless Ni-B coatings will be a suitable surface deposition process to reduce the wear of the mechanical parts at high temperatures and to extend their service life under severe conditions. In this study, Ni-B electroless plating was deposited on the mild carbon steel surface to improve the mechanical and tribological properties of the material by using electroless coating technique. The surface hardness and wear resistance of the coating at room temperature and different annealing temperatures (300^{o}C, 400^{o}C and 500^{o}C) under argon atmosphere for 2 hours were examined.

2. EXPERIMENTAL

Ni-B coatings deposited on 5mm in thickness and 40mm x 30mm sized mild steel substrate. Electroless Ni-B coating bath composition and operating conditions are given in **Table 1**. The samples were abraded from 400 to 1200 SiC sandpaper to remove the surface roughness of the samples. Polished with 1µm alumina to increase adhesion on the substrate. It was then washed with ethanol in the ultrasonic bath for 5 min and dried with hot air. Finally, the samples were immersed in a 1:3 ratio of HCl acid solution before being placed in the coating bath, then washed with ethanol and distilled water. After the reaction in the coating solution was completed, the samples were washed first with ethyl alcohol and then with distilled water. The sample was then air dried.

Table 8. Electroless Ni-B coating bath composition and operating conditions.

Chemical composition	Concentration
$NiCl_2.6H_2O$	20 g/L
$NaBH_4$	1 g/L
$C_2H_8N_2$	90 mL/L
NaOH	90 g/L
Pb $(NO_3)_2$	0,015 g/L
Operating Conditions	
Bath temperature	92±2 °C
pH	14
Deposition time	60 min.
Agitating speed	400 rpm

After coating process, heat treatment of the deposited samples was performed at different annealing temperatures (300°C, 400°C, 500°C) for 2 hour fixed annealing time in argon gas medium. The surface morphologies and cross-sectional images of the coatings were analyzed using JEOL 6060-LV scanning electron microscope (SEM). Crystal phases of the coatings as-deposited and annealed were analyzed by X-ray diffraction (XRD) using the Rigaku D/MAX 2000 X-ray generator and filtered radiation of Cu-Kα (1.54059A°) in the 2θ range from 20° to 80° mode at a scanning rate of 1°/min. Hardness was calculated with applying a maximum 50 mN load of indentation speed is kept constant 10 s by Anton Paar Nanoindentation tester: NHT^3 with Berkovich-type diamond indenter. The hardness of the samples was measured 5 times from the cross-section and the averages of the measurements were taken. Tribological tests were carried out against the Al_2O_3 ball of 6mm diameter, with dry sliding wear at 25°C±2 room temperature, 45±5 relative humidity environment by CSM Instruments TRB 18-317 device. After the wear tests carried out at a sliding speed of 25cm/s under 5N load at 300 m sliding distance, the friction coefficients and wear rates of the samples were calculated, and the wear traces of the samples were analyzed with SEM images.

3. RESULTS AND DISCUSSION

XRD patterns of Ni-B deposited samples annealed at room temperature, 300°C, 400°C and 500°C are shown in **Figure 1**. In the literature, crystal nickel formation and precipitation of borides have been reported after heat treatment (Pal, 2011). While only amorphous Ni broad

peak is observed at room temperature, sharp crystal phases (Ni, Ni_3B, Ni_2B) peaks are formed after the heat treatment. The main sharp peak of the nickel corresponds to the plane (111), while the short peaks indicate the planes (200) and (220). It also shows that there is no phase transition in the coating as-deposited at room temperature. In the sample annealed at 300°C for 2 hours, the crystalline Ni_3B phases were formed together with the weak crystal Ni phase. When the heat treatment temperature is increased to 400°C, it is seen that the peak density of crystal Ni_3B increases and the Ni_2B peaks are formed. The formation of pure nickel crystal and precipitation of nickel borides show that the transformation of Ni-B alloy at 400°C (Malfatti, 2012). Also, the reduction of Ni (fcc) peak density could be explained by the formation of a numerous of dense and narrow peaks corresponding to several reflections of the Ni_3B crystal phases (Vitry, 2009). When the heat treatment temperature is increased to 500°C, the peak density of nickel borid phases decreases and the peak density of the nickel crystal increases (Sankara, 2004).

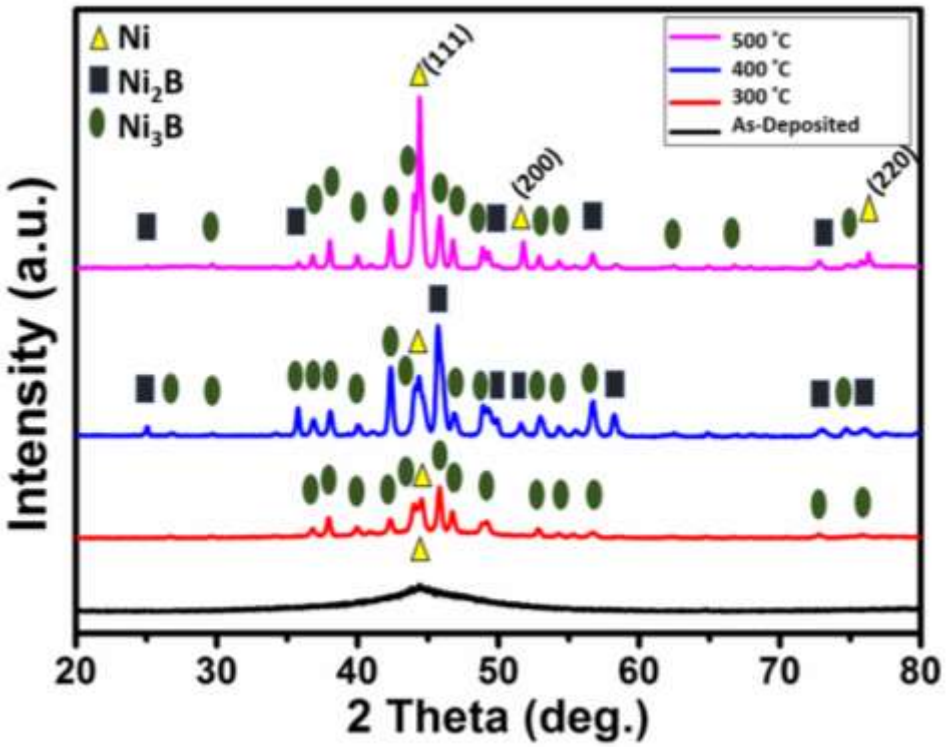

Figure 1. XRD pattern of as-deposited and annealed (300°C, 400°C, 500°C) samples.

The surface morphologies and cross-sectional images of Ni-B electroless coatings that are heat treated at different temperatures (300°C, 400°C and 500°C) are shown in **Figure 2**, respectively. Ni-B electroless coatings were heat treated to increase the hardness and wear resistance. Surface morphology of all Ni-B coatings are cauliflower-like. The cauliflower structure is a morphology that occurs in electroless coatings, and it reduces the friction coefficient of the coating due to its self-lubricating feature (Sahoo, 2011). When increasing the annealing temperature to 400°C, it is seen that the coating surface is denser and homogeneous. In addition, there is an increase in grain boundaries with the crystallization of deposits (Çelik, 2016).

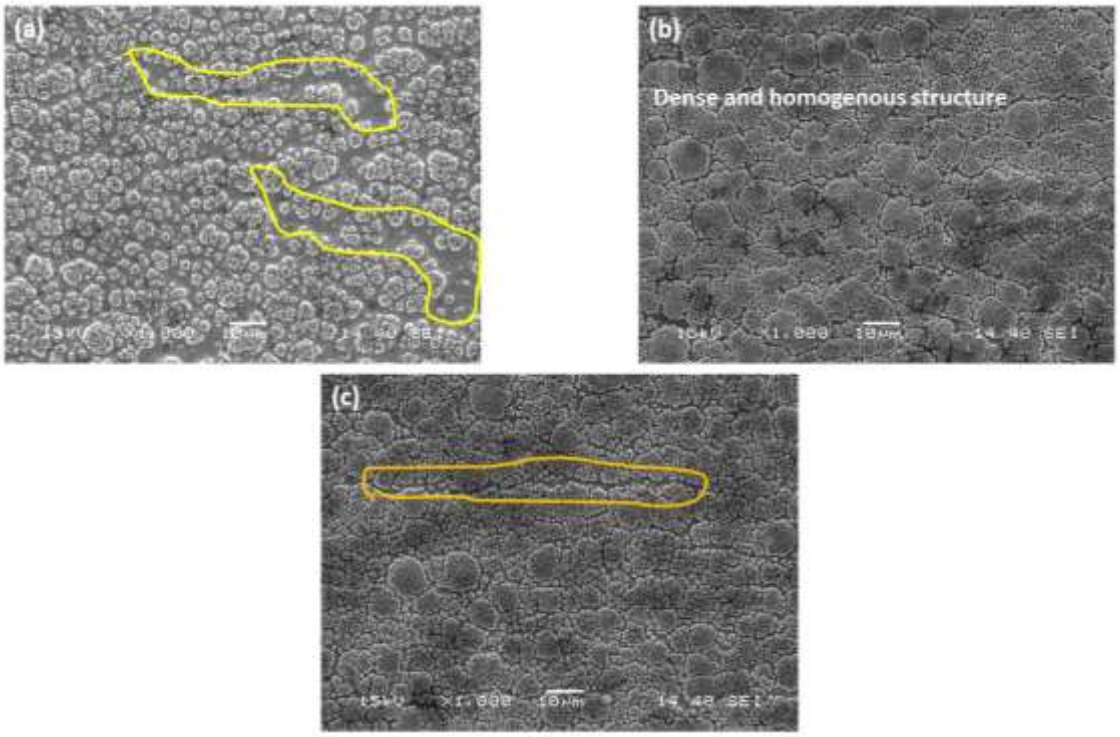

Figure 2. Surface morphology images of Ni-B electroless coatings annealed at different temperatures (300°C, 400°C, 500°C), respectively.

Cross-sectional images of coatings annealed at different temperatures are given in **Figure 3**, respectively. As seen in the figure, columnar growth occurred in the coating cross-section and the coating thickness was measured ~20 µm. There is no separation in the adhesion of the coating to the substrate, and cracks and pores are not observed. It is seen that the column structure formed in the cross section of the coating annealed at 400°C is more intense and compatible with the surface morphology (Kundu, 2014).

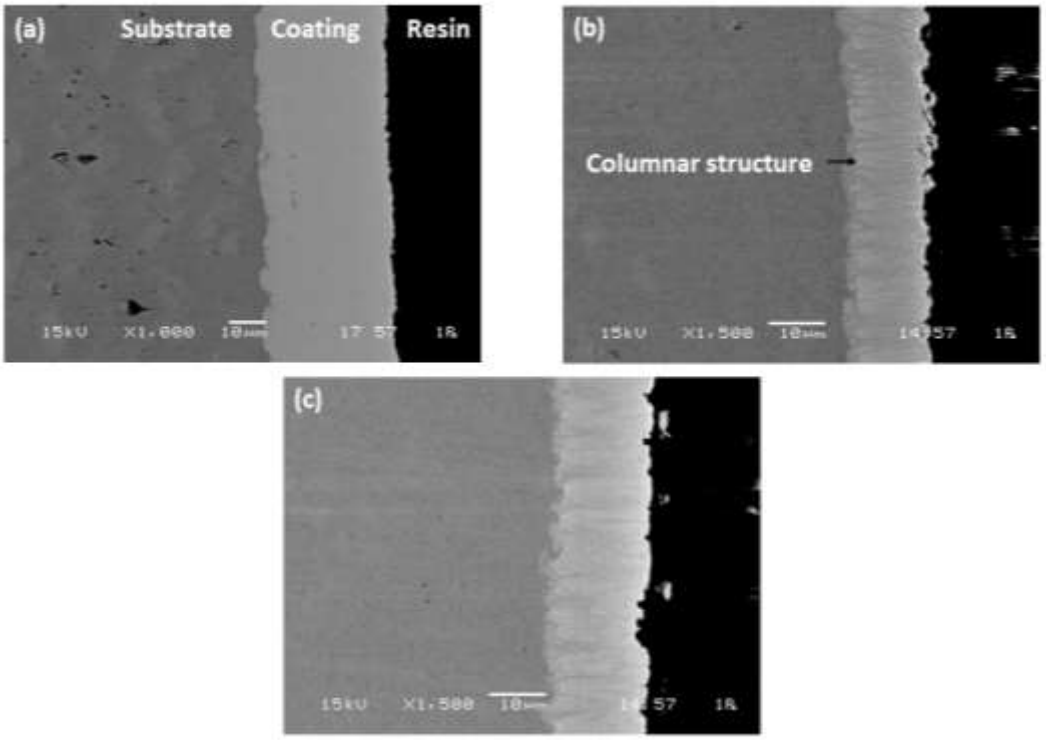

Figure 3. Cross-section images of coatings annealed at different temperatures (300°C, 400°C, 500°C), respectively.

Figure 4 shows the effect of the annealing temperature of the deposits of Ni-B on the coating hardness. By increasing the heat treatment temperature, the coating hardness first increased and then decreased. The increase in coating hardness and elastic modulus given in **Table 1** is of great importance for the crystal nickel boride phases. It is seen that the hardness results and XRD data are compatible. The hardness value of the sample annealed at 300°C was measured as 840 HV. Increasing hardness to 1150 HV by increasing the heat treatment temperature to 400°C is related Ni_3B and Ni_2B precipitation of hard phases. Hard nickel borides particles are formed by precipitate hardening (Krishnaveni, 2005). When the heat treatment temperature is increased to 500°C, the decrease in coating hardness to 1030 HV was related to the increase of nickel crystal density and the decrease of nickel borid phase density. The softening of the coating at high temperatures is related to the reduction of Ni_3B particles in the hardening sites by conglomeration. Thus, the boron moves away from the alloy and the coating hardness decreases with the soft nickel phase formed in the matrix (Nava, 2013). The precipitation hardening that occurs with microstructural changes after heat treatment is compatible with the literature (Balaraju, 2016).

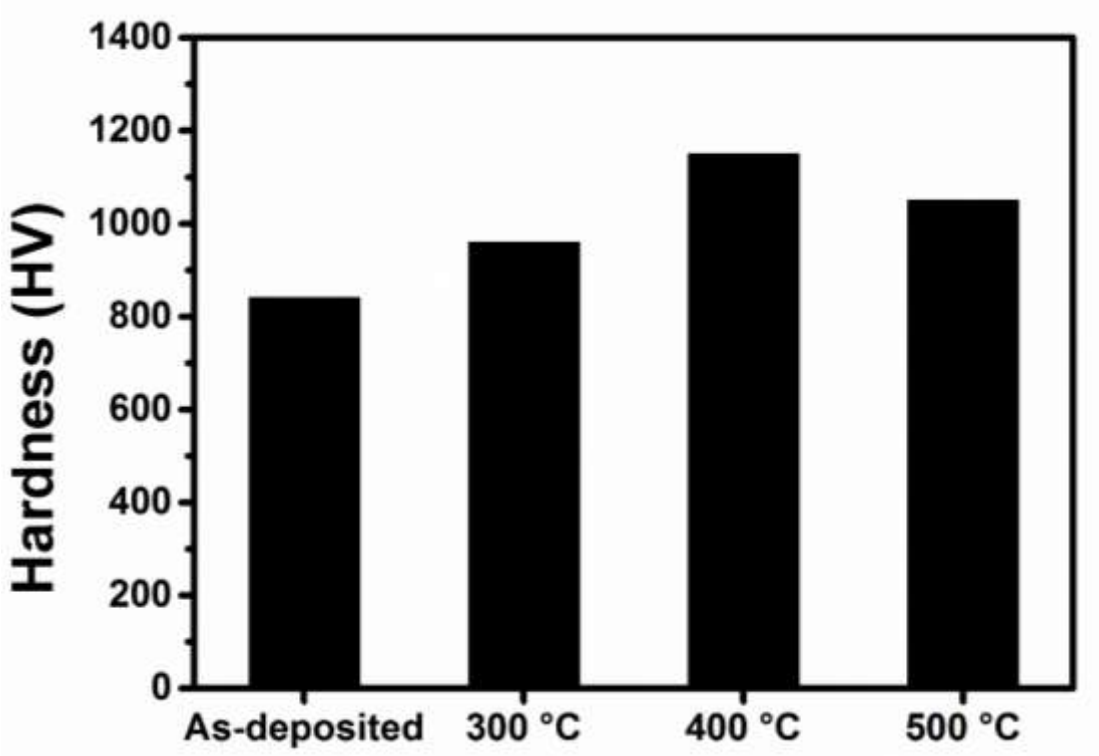

Figure 4. Hardness of as-deposited and annealed coatings.

SEM images of wear traces after dry sliding wear tests of samples treated at different temperatures are given in **Figure 5**. Abrasive grooves in the abrasion trace of the annealed coating at 300^{o}C carry the material to the edge of the abrasion path and form cracks in the abrasion trace. As seen in **Figure 5b**, the Ni-B coating annealed at 400^{o}C preserves its nodular cauliflower structure during the sliding wear. Nickel borides deposited on the wear track prevent crack propagation over wear. As seen in the wear trace of the sample annealed at 500^{o}C (**Figure 5c**), the residues formed due to the rough surface caused the formation of large cracks. In addition, grain coarsening and microstructural heterogeneities could lead to increment of cracked areas on the wear surface and increased wear rate of the coating (Balaraju, 2016). High magnification SEM pictures were taken from the regions marked with red to examine the wear marks in detail.

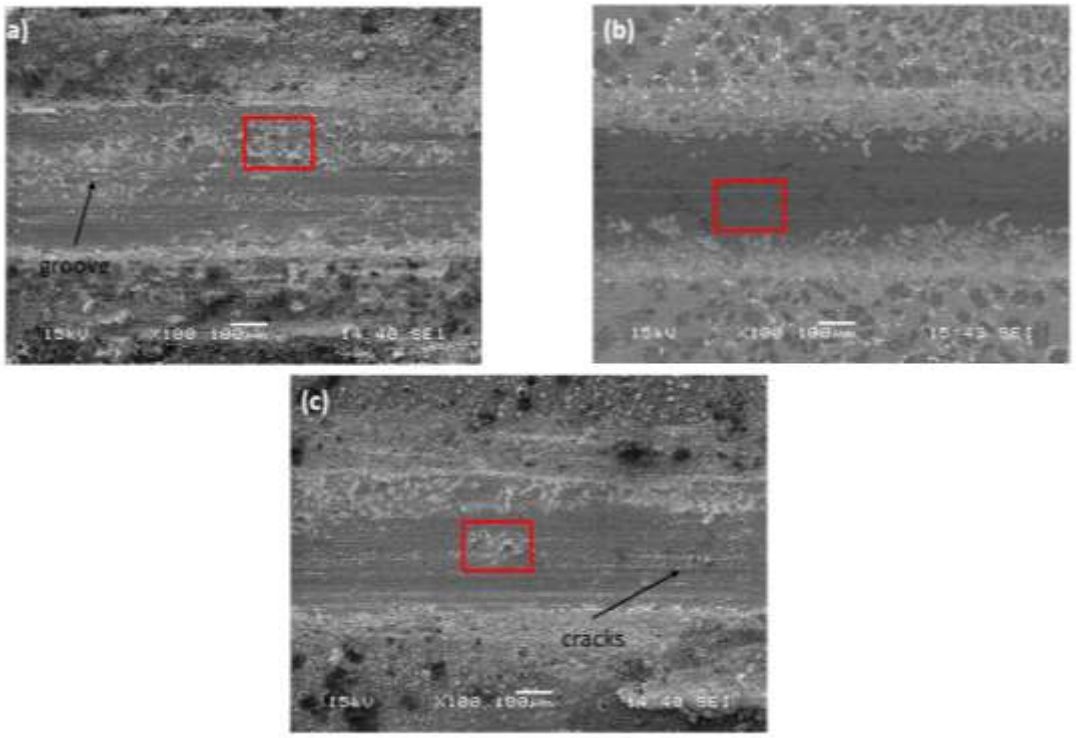

Figure 5. Wear traces images of annealed coatings at different temperatures (300°C, 400°C, 500°C), respectively.

High magnification SEM micrographs of Ni-B coating wear marks annealed at 300°C, 400°C and 500°C are given in **Figure 6**. Although phase transformations occur in the sample annealed at 300°C, there are cracks on the wear surface due to the insufficient lubricating borides. As seen in F**igure 6b**, the crushed columnar areas on the wear surface of the sample annealed at 400°C function as load bearing areas, improving the wear resistance of the coating. Columnar growth observed in cross-sectional view of the coating, nodular structure and lubricant nickel borides on the coating surface have reduced the contact area with the counter surface and improved wear resistance. The increased surface hardness with the precipitation of nickel crystal and nickel borides formed with heat treatment increases the plastic resistance of the coating (Krishnaveni, 2005). It is also seen that the load is carried by the nodules and the deformation on the wear surface is minimal. Crushed nodules on the wear surface explain the amount of wear and friction coefficient. The better mechanical properties of the annealed coating at 400°C are explained by the fact that the crystal phases formed after heat treatment prevent grain growth. In addition, crushing nodules on the wear surface shows high plastic deformation throughout the sliding wear. As seen in **Figure 6c**, delamination type abrasion with plates separation is observed in the wear trace of the sample annealed at 500°C. Adhesive wear mechanism occurs due to the attractive forces formed between the Ni-B coating and the counter surface. In addition, high shear stress on contact of the wear zone with the hard-counter surface causes the formation of micro cracks. The rough surface formed by the crack on the surface increasing the stress accumulation increases the friction coefficient of the coating and causes material loss (Mukhopadhyay, 2018).

Adhesion wear mechanism on the wear surface causes high material separation and wear residues. Borid phases in the hardening areas at 500ºC heat treatment was conglomeration and their number decrease of hardening sites. As this causes grain coarsening and the coating to soften, dislocation increases between the particles, thereby reducing the hardness and wear resistance of the coating (Krishnaveni, 2005). The crack growth observed on the wear surface of the sample annealed at 500ºC is related to the reduction of plastic deformation and the effect of residual particles (Balaraju, 2016). As the high temperature annealing applied to the coating exceeded the yield strength of the coating, it caused serious adhesion and wear losses. The relationship between the deposits formed after heat treatment and the tribological behavior of the coating surface is specified in the literature (Sanakara Narayanan, 2004).

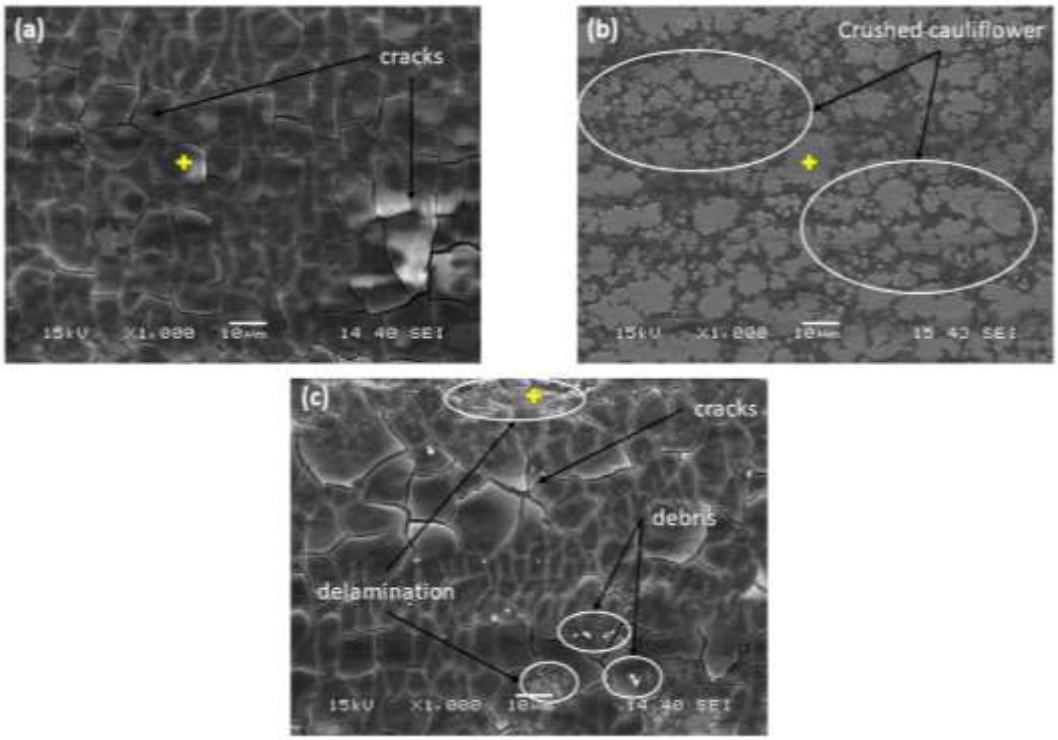

Figure 6. High magnification SEM micrographs of annealed coatings at different temperatures (300ºC, 400ºC, 500ºC), respectively.

EDS spectra of the worn surfaces of Ni-B coatings that are heat treated at 300ºC, 400ºC and 500ºC are shown in **Figure 7**. EDS analyzes were performed in yellow highlighted SEM wear image areas. The high oxide peaks formed by EDS analysis of the wear surface of the sample annealed at 400ºC prove that there is a protective oxide layer on the wear surface. The formation of the oxide layer observed in the crushed areas prevents the material loss of the coating. As seen in **Figure 7c**, the sample is annealed at 500ºC and it is confirmed by the low oxygen percentage that the protective oxide layer that plays an important role in reducing the friction and wear in EDS analysis. Also, the appearance of the aluminum peaks supports the layer transferred from the counter surface to the wear surface by adhesion. In the EDS analysis of the coatings annealed at 500ºC, the percentage of aluminum is higher than the other coatings, resulting in the formation of micro-cracks with strong adhesive strength and

the spread of these cracks. Due to rough wear morphology, the formation of coarse graining in the coating increases the ductility of the material and causes the oxide layer to break (Mukhopadhyay, 2018).

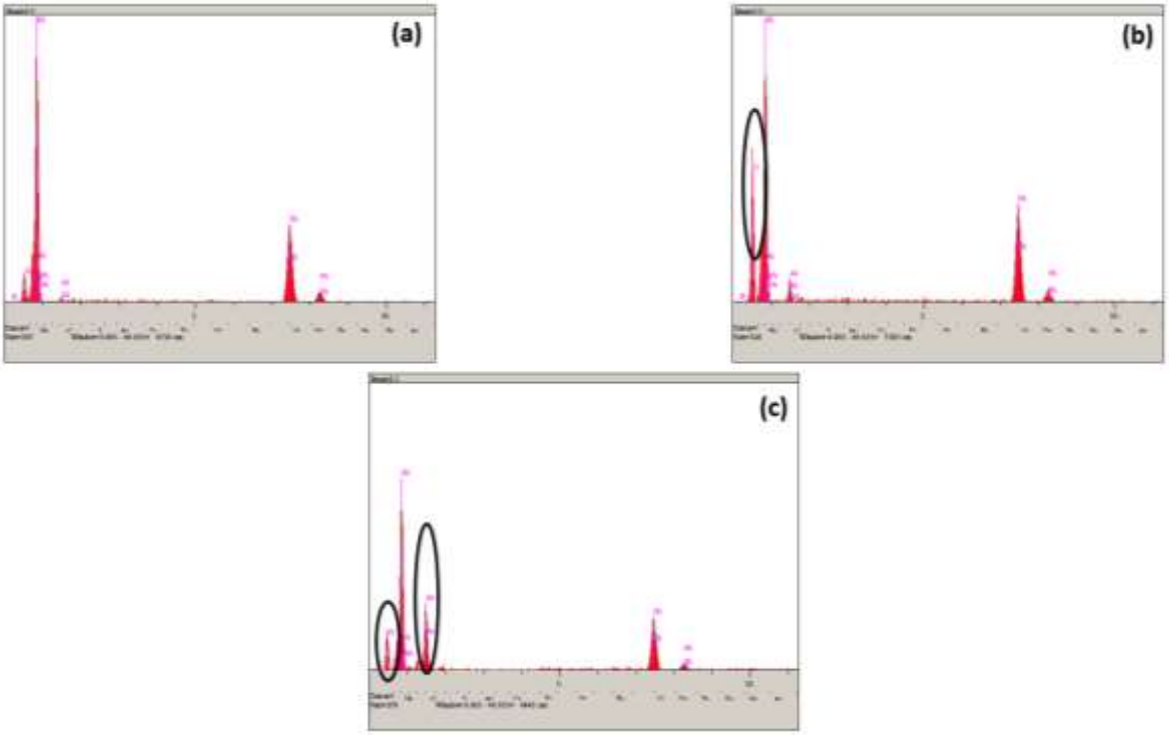

Figure 7. EDS spectra of coatings annealed at (a) 300°C, (b) 400°C, (c) 500°C, respectively.

The wear rates and friction coefficient values calculated after the wear tests of the heat-treated samples are given in **Figure 8**. It was observed that Ni-B coatings initially increased friction coefficients and then reached equilibrium. When the samples annealed at 300°C and 400°C are compared, it is seen that the increase in heat treatment improves the wear resistance of the coating. The friction coefficient of the coating annealed at 300°C has reached equilibrium after 200 meters and is the highest compared to other samples. By increasing the heat treatment temperature from 300°C to 400°C, there is a considerable reduction in the coefficient of friction of the coating. Although the friction coefficient of the annealed coating at 400°C reaches equilibrium after 50 meters, the presence of boron in the lubricant function reduces wear. The columnar growth of the coating reduces the contact area with the counter surface in wear tests. Also, columnar growth is to prevent adhesive wear by retaining lubricant borides (Balaraju, 2016). Nickel boride precipitates formed in the heat-treated coating significantly reduced the friction coefficient due to their high hardness and plastic deformation (Kanta, 2009). Coarse grained structures formed in the sample annealed at 500°C cause roughness on the coating surface and the friction coefficient of the coating increases. Because of the high heat treatment temperature worsens the wear process, rough surface wear and abrasion residues are formed. This causes the coefficient of friction to increase.

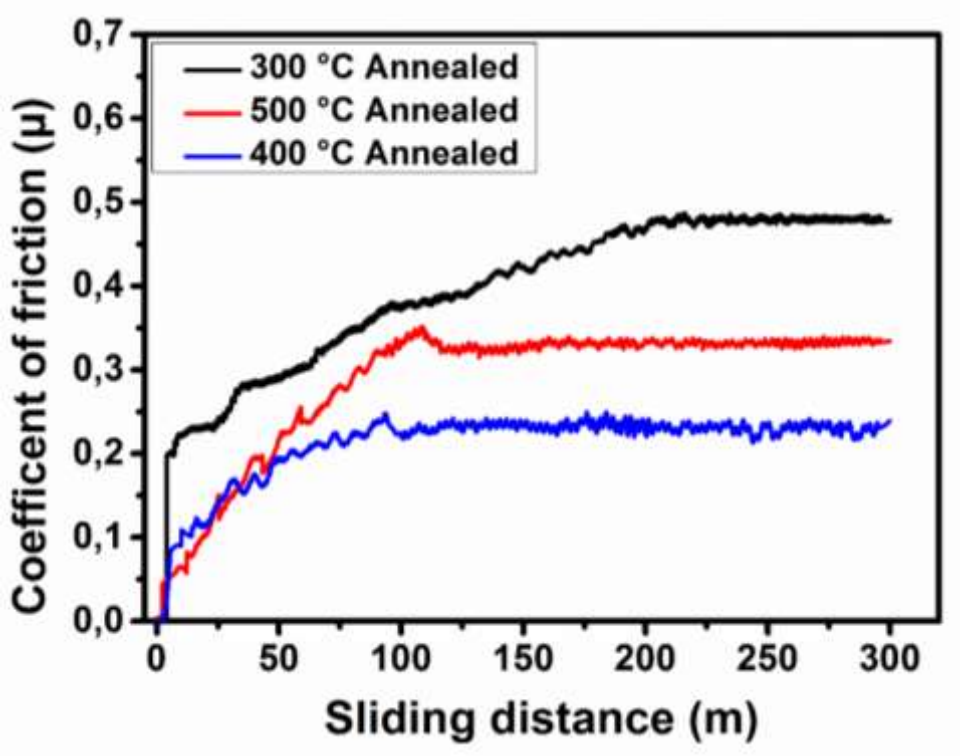

Figure 8. Coefficient of frictions with sliding distance at different annealed coatings.

The wear rates calculated after the wear tests of the heat-treated samples are given in **Figure 9**. The low wear rate in the 400°C heat treated sample relates to the nickel particle size and grain refinement described by the Orowan mechanism. However, by increasing the heat treatment temperature to 500°C, wear rate increases. The deterioration in the coating precipitated by heat treatment causes an increase in wear rate. Also, the increase in wear rate is related to the microstructural change in high annealing temperatures (Balaraju, 2016). In addition, grain coarsening caused by aggregation of boride phases in the sample annealed at 500°C increases the wear rate of the coating (Mukhopadhyay, 2018).

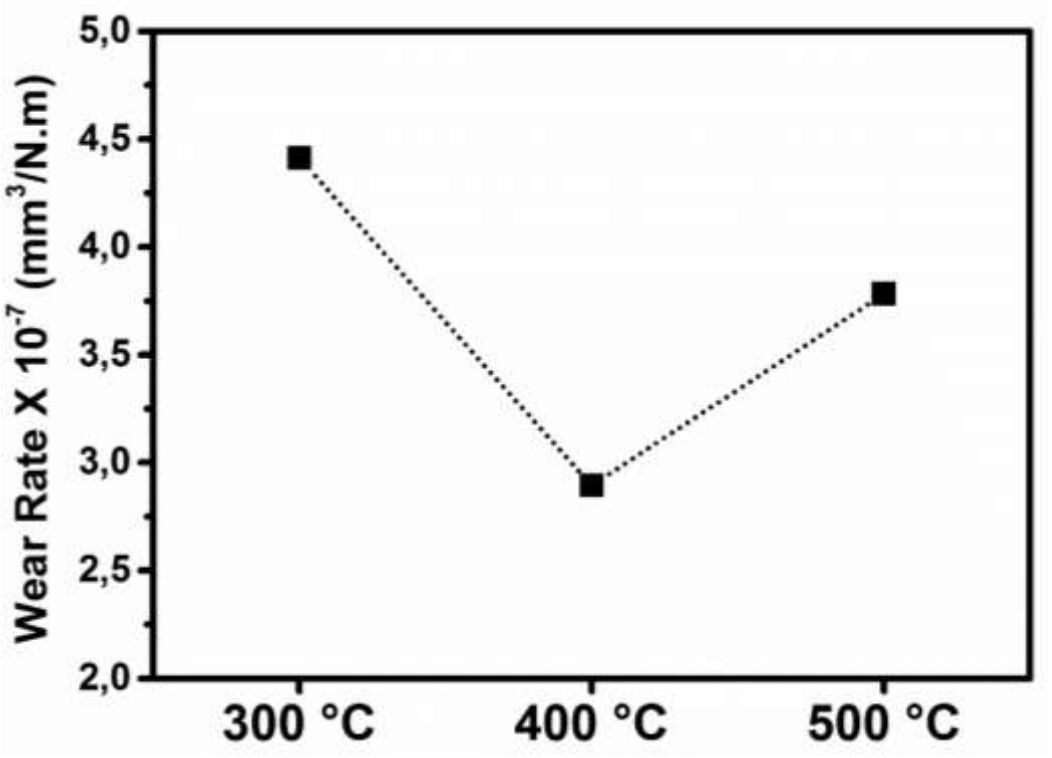

Figure 9. The effect of heat treatment applied to coatings on the wear rate.

4. CONCLUSION

Mechanical and tribological properties of samples with different annealed temperatures of Ni-B alloy coating deposited on mild steel were investigated. The surface morphologies of the coatings are typical nodular cauliflower-like structures. XRD results showed that the Ni-B alloy coatings became crystalline after heat treatment. The most Ni_3B peak formation in the sample annealed at 400°C resulted in increased hardness and low wear in the coating. The highest hardness value of Ni-B coating was obtained due to the formation of Ni_3B and Ni_2B crystal phases in the 400°C annealed sample. Coating hardness decreased due to the decomposition of the Ni_3B crystal by increasing the annealing temperature. The increase in the hardness of the heat-treated coating is directly related to the increase of the wear resistance of the sample. Decrease in coating hardness was observed due to grain coarsening by increasing the heat treatment temperature to 500°C. Tribological behaviors of Ni-B coatings which were subjected to heat treatment at different temperatures were examined. With the precipitation of nickel borid crystal phases formed after heat treatment, the hardness of the Ni-B coating increased, and the wear resistance improved. The wear rate and friction coefficient values calculated after dry sliding wear tests. The wear amount and friction coefficient values were observed to be better at 400°C compared to other coatings. Grain coarsening and deposits formed in the coating annealed at 500°C negatively affected the tribological behavior of the material. In addition, the wear resistance of the coating has weakened as the crack formations observed on the wear surface cause fatigue wear. It can be

stated that the microstructure of the annealed coating at 400°C, the phase transformation and the oxide layer formed on the wear surface provide the improvement of the mechanical and tribological properties of the coating.

ACKNOWLEDGEMENTS

This work has been supported by the National Boron Research Institute of Turkey (Grant No: 2017-31-07-25-001) and Scientific Research Projects Unit for the Sakarya University (Grant No. 2016-50-02-007), Turkey.

REFERENCES

1. Balaraju J. N., Priyadarshi A., Kumar V., Manikandanath N. T., Praveen Kumar P., Ravisankar B., 2016, "Hardness and wear behaviour of electroless Ni–B coatings", Mater. Sci. Tech. 32:1654-1665.

2. Çelik İ., Karakan M., Bülbül F., 2016, "Investigation of structural and tribological properties of electroless Ni–B coated pure titanium", Proc. IMechE. Part J: J. Engineering Tribology 230:57-63.

3. Das S. K., Sahoo P., 2011, "Electrochemical Impedance Spectroscopy of Ni-B Coatings and Optimization by Taguchi Method and Grey Relational Analysis", Port. Electrochim. Acta. 29: 211-231.

4. Dervos, C.T., Novakovic, J. and Vassiliou, P., 2004, "Vacuum heat treatment of electroless Ni-B coatings", Mater Lett., 58: 619-623.

5. Kanta A.-F., Vitry V., Delaunois F., 2009, "Wear and corrosion resistance behaviours of autocatalytic electroless plating," J. Alloy Compd., 486(1-2):L21-L23, DOI: http://doi.org/10.1016/j.jallcom.2009.07.038.

6. Krishnaveni K., Sankara Narayanan T. S. N., Seshadri S. K., 2005, "Electroless Ni-B coatings: preparation and evaluation of hardness and wear resistance," Surf. Coatings Technol., 1: 115-121, DOI: http://doi.org/10.1016/j. surfcoat.2004.01.038.

7. Kundu S., Das S., Kand Sahoo P., 2014, "Properties of electroless nickel at elevated temperature-a review" Procedia Eng., 97: 1698-706.

8. Malfatti C.F., Ferreira J.Z., Olveira C.T., Rieder E.S., Bonino J.P., *Materials and Corrosion*, 63: 36-43.

9. Mallory G., Hajdu J. B., 1990, "*Electroless Plating: Fundamentals and Applications"*, Noyes Publ. New York, 1990.

10. Mukhopadhyay A., Barman T. K., Sahoo P., 2018, "Effects of Heat Treatment on Tribological Behavior of Electroless Ni–B Coating at Elevated Temperatures", Surf. Rev. and Let., 25(2): 1-22, DOI: 10.1142/S0218625X18500142.

11. Nava D., Dávalos C.E., Martínez-Hernández A., Manríquez F., Meas Y., Ortega-Borges R., Pérez-Bueno J.J., Trejo G., 2013, "Effects of Heat Treatment on the Tribological and Corrosion Properties of Electrodeposited Ni-P Alloys", Int. J. Electrochem. Sci., 8: 2670-2681.

12. Pal S., Verma N., Jayaram V., Biswas S. K., Riddle Y., 2011, "Characterization of phase transformation behavior and microstructural development of electroless Ni-B coating", Mater. Sci. Eng. A. 528(28): 8269-8276.

13. Sahoo P., Das S.K., 2011, "Tribology of electroless nickel coating", Mater. Des. 32: 1760-1775.

14. Sankara Narayanan T.S.N., Seshadri S.K., 2004, "Formation and characterization of borohydride reduced electroless nickel deposits", J. Alloys Compd. 365: 197-205.

15. Takahasi M., Tateno Y., Koshimura M., 1980, Jpn. J. Appl. Phys. 19: 2335.

16. Vitry V., 2009, "Electroless nickel-boron deposits: Synthesis, formation and characterization; Effect of heat treatments; Analytical modeling of the structural state", Université de Mons, Bélgica.

17. Vitry, V. Kanta A-F. and Delaunois F., 2011, "Mechanical and wear characterization of electroless nickel-boron coatings", Surf. Coat. Technol. 206: 1879-1885.

18. Vitry V., Kanta A-F., Delaunois F., 2012, "Application of nitriding to electroless nickel-boron coatings: Chemical and structural effects; mechanical characterization; corrosion resistance", Mater. Des. 39: 269-278.

ქლოროგენული მჟავების როლი, როგორც ბუნებრივი თერაპიული კომპონენტი, ინფლაქტაციის ჩასახშობად

ივანკა ასლანიკაშვილი

მაგისტრის ხარისხი, თბილისის სახელმწიფო უნივერსიტეტი

ანოტაცია

ანთება ქსოვილის პათოლოგიის ან არანორმალობის ნიშანი იყო იმისთვის, რომ სიგნალიზაცია მიეწოდებინა სისტემას. NSAID– ების თერაპიულ გამოყენებას აქვს გარკვეული გვერდითი მოვლენები. ამ კვლევამ გამოიკვლია ქლოროგენის მჟავის, როგორც ბუნებრივი თერაპიული ნაერთის პოტენციური როლი ანთების სამიზნის ჩახშობის მიზნით, მაგალითად COX-2, ურთიერთქმედების მოდელის გამოყენებით. კვლევაში გამოყენებული კვლევის მეთოდი იყო მოლეკულური დოკინგური მიდგომა, რომელიც აკავშირებს ლიგანდსა და ცილას. ცილოვანი მონაცემების შესახებ მოცემულია ცილოვანი მონაცემების ბანკი (ID: 6 კოქსი), და ქლოროგენური მჟავა, რომელიც მიღებულია PubChem– დან (CID: 1794427). ჩვენ დავათავსეთ COX-2 და ქლოროგენური მჟავა Hex 8.0.0 გამოყენებით. ქლოროგენური მჟავისა და COX-2 მოლეკულური ურთიერთქმედების ვიზუალიზაცია და ანალიზი ხორციელდება Discovery Studio Client 4.1 პროგრამული უზრუნველყოფის გამოყენებით. ქლოროგენის მჟავა ძალიან გამტარია და ადვილად შეიწოვება ლიპინსკის ხუთივე წესის საფუძველზე. საინტერესოა, რომ ჩვენ აღმოვაჩინეთ, რომ თხუთმეტი ამინომჟავა შეკრული იყო ქლოროგენის მჟავასთან, რომელიც წყალბადის ბორბლით და ვან დერ ვალალთან არის წარმოქმნილი. ლიგანდის პროტეინს შორის ურთიერთქმედება იწვევს დამაკავშირებელ ენერგიას -327.59 კკალ / მოლი. ქლოროგენის მჟავა ასრულებს პოტენციურ როლს ანთების გზის ინჰიბირებაში COX-2 ინჰიბირებით. ამ სტატიაში ვარაუდობენ, რომ ქლოროგენის მჟავას აქვს პოტენციალი, როგორც ანთების საწინააღმდეგო საშუალება, COX-2– ის, როგორც ანთებითი შუამავლის ჩახშობის მიზნით.

საკვანძო სიტყვები: ქსოვილის პათოლოგია, გვერდითი მოვლენები, მოლეკულური დოკინგი, ქლოროგენური მჟავა

ოჯახის დეკორატიული თევზი წევრების ფილოლოგია

ირინე სილაგაძე,

საქართველოს უნივერსიტეტი, Msc. დ.

ანოტაცია

Labridae არის თევზის დიდი და მრავალფეროვანი ოჯახი. ლაბრიდას ქვეშ მდებარე მრავალი სახეობა ინდონეზიურ მარჯნის რიფებში ცხოვრობს. ამასთან, დასავლეთის ჯავის სამხრეთ სანაპიროდან ლაბრადებში არსებობს დეკორატიული თევზის მრავალფეროვნების შესახებ შეზღუდული სამეცნიერო მტკიცებულება. კვლევის მიზანს წარმოადგენდა ინფორმაციის მიწოდება სახეობათა მრავალფეროვნებისა და ფილოგენეტიკური ურთიერთობების შესახებ დასავლეთის ჯავის სამხრეთ სანაპიროზე მდებარე თევზისებრი თევზის ოჯახის სახეობებს შორის. ეს კვლევა ჩატარდება მიზნობრივი შერჩევის კვლევის მეთოდის გამოყენებით. დაკვირვებულ პარამეტრებში შედის მორფომეტრიული და მერიალისტური პერსონაჟები და ევოლუციური ურთიერთობები სახეობებს შორის Labridae- ს ოჯახში, რომელიც შეგროვებულია სამხრეთ სანაპიროდან სუკაბუმსა და გარუტში, დასავლეთის ჯავა. მორფოლოგიური მონაცემები აღწერილი იქნება აღწერილურად, მორფომეტრიული და მერიალისტური მონაცემების საფუძველზე. სახეობათა დონეზე იდენტიფიკაცია ხდება იდენტიფიკაციის ხელმისაწვდომი სახელმძღვანელოს მითითებით. ფილოგენეტიკური ურთიერთობები სტატისტიკურად გაანალიზდება PAUP 4.0-ში განხორციელებული კლასტიკური მეთოდის გამოყენებით მაქსიმალური დაზოგვის ალგორითმის გამოყენებით. კლადოგრამას აქვს თანმიმდევრულობის ინდექსი 0.563, რაც მიუთითებს დაბალ ჰომოპლაზზე და ამტკიცებს, რომ ხე ყველაზე ეკონომიური იყო. ლაბრიდემ შექმნა მონოფიზიტური განძი Acanthurus maculiceps- სთან შედარებით, ხოლო Cheilio inermis იყო მთავარი სახეობა, ხოლო სხვები წარმოებულები.

საკვანძო სიტყვები: ლაბრადები, მორფომეტრია, ფილოგენე

نمونه های نوآوری در نرسنگ

მრავალფეროვანი წყაროების დეფორმირებული სახელმწიფო

ლეონიდ კუპრავა,

განმცხადებელი, სოხუმის სახელმწიფო უნივერსიტეტი

ანოტაცია

სტატიაში მოცემულია ცილინდრული და კონუსური კომპრესიული ზამბარების მუდმივი დენის დატვირთვის პროცესის პროცესის კომპიუტერული სიმულაციის შედეგები, ტორსიონარული და ტორსიული წყლები, დისკის წყაროები. გამოითვლება ფერადი კონტურები ეკვივალენტური სტრესის, გადაადგილებისა და მასალის დეფორმაციის შესახებ გაზაფხულის მოდელებზე. მასალის ყველაზე დატვირთული მოცულობა განისაზღვრა საგაზაფხულო სტრესის დეფორმაციის დროს. პირველი ხრახნი, რომელზეც გაზაფხულის მხარეა, ძაბვას მაქსიმალურად დეფორმირებული ხდის.

საკვანძო სიტყვები: დატვირთვა, სტრესი, დეფორმაცია, კოჭა

СЕМЕЙНОЕ ВОСПИТАНИЕ И ПСИХОЛОГИЯ

Светлана Думбадзе

Студентка Грузинского общественного института

Аннотация

В статье рассматриваются причины развода и профилактические меры по разрешению семейных разводов. В контексте факторов распада семьи и предложений были объявлены профилактические меры для использования семейного развода.

Ключевые слова: семья, психологическая психология, семья, психологи, психологи, психологи

АРАЛАС ЕСЕПТЕРДІҢ ЖУЫҚ ШЕШІМІ

Гүлмира Теңдібаева

Қорқыт Ата атындағы Қызылорда мемлекеттік университеті

Аңдатпа

Бұл жұмыста алдымен екінші ретті дифференциалдық теңдеудің типі анықталады және ол канондық формада азаяды, содан кейін толқындық теңдеу үшін аралас есеп айнымалыларды бөлу әдісімен, вариативті итерация әдісімен және Адомиан ыдырау әдісімен шамамен шешіледі. Барлық осы әдістер нақты шешімге ауысатын функциялар тізбегін қамтамасыз етеді. Барлық жағдайларда бірдей нәтижелер алынды, бірақ Адомиан ыдырау әдісі өте қарапайым және ыңғайлы болды.

Түйінді Сөздер: Қосымша Мәлімдеме, Вола Қабылдау, Сарапты Сараптау Әдісі, Вариациялық Ітерация Әдісі, Әдістемелік Құралдар Әдісі, Әрекет Шешімі

АНАЛИЗ ЧИСЛА БИМОЛЕКУЛЯРНЫХ РЕАКЦИЙ

Гульбахор Алимджонова

Ташкентский государственный технический университет

Аннотация

В исследовании проблема бимолекулярной реакции под названием «Брюссель» решается численно. После некоторого упрощения получается нелинейная система из двух или трех неизвестных простых дифференциальных уравнений, которая зависит только от одного параметра (например,?). Структурированная задача Коши была решена прецизионным методом с непрерывным шагом в Рунге-Кутте четвертого уровня. Анализируются проблемы единичных точек, устойчивости и поворота границы, а также графика траекторий в пространстве и проекций в плоскостях на различные значения параметров. Брюссельская проблема, связанная с ГДР, также была решена.

Ключевые слова: бимолекулярная реакция, брюсселятор, обычная система полезных инструментов, значимый цикл, стабильность.

ҚОСЫМША БІЛІМ ОРТАЛЫҚТАРЫНДАҒЫ МОБИЛЬДІ ТӘСІЛДЕУ ТӘРТІБІ

Т. Алдабергенова & И. Юсупова

Санкт-Петербург мемлекеттік университеті

Аңдатпа

Оқушылардың көзқарастары мен білімін қалыптастыруға ынталандыру үшін мобильді оқытуға дайындық - бұл технологияны білім беру ортасына интеграциялаудың жаңа бағыты. Мобильді құрылғыларды сәтті енгізу оқуды жақсартуға мүмкіндік береді. Бұл тұрғыда дәстүрлі оқытудың күшті жақтары мен мобильді оқытудың күшті жақтарын біріктіретін оқыту ортасы перспективалы бағыт ретінде қарастырылуы мүмкін. Бұл құжаттың мақсаты - бұл оқу ортасының білім алуға, оқудағы жетістіктері мен оқушылардың көзқарастарына әсерін анықтау үшін мультимедиялық араласудың оқу ортасына тиімді интеграциясын зерттеу. Осы әдебиетке шолу жасағанда, рецензияланған журналдың жиырма екі мақаласы алдын ала анықталған критерийлерге сәйкес таңдалды (мысалы, сандық зерттеулерді қолдана отырып жүргізілген зерттеулер, мысалы, квази-эксперименттік және эксперименттік зерттеулер және т.б., мысалы, аралас зерттеулер). әдісі, кейс-стади және т.с.с., соның ішінде деректерді жинау процедурасындағы сандық аспекті қоса алғанда) және осы мақалалардан олардан сенімді және маңызды ақпаратты алу үшін мұқият талдаңыз. Алынған нәтижелер мобильді технологиялардың аралас оқыту ортасына енуі студенттердің білімін жағымды түрде игеруіне айтарлықтай әсер ететіндігін көрсетеді, дегенмен рецензияланған мақалаларда олардың оқуға айтарлықтай әсерін көрсетпейтін эмпирикалық нәтижелер аз. Оқушылардың қарым-қатынасына қатысты, студенттердің пікірлері бойынша, студенттердің араласқан білім беру ортасында мобильді технологияны академиялық мақсаттар үшін қолдануға ынталандырылды.

Түйін сөздер: аралас оқыту, ұтқыр оқыту, оқу нәтижелері, академиялық үлгерім, көзқарас

შავი ზღვის გაზის ჰიდრატების საბადოების წარმოქმნის გეოლოგიური და თერმობარული პირობების თავისებურებები და მათი განვითარების პერსპექტივები

ირაკლი არჩუაძე,

სოხუმის სახელმწიფო უნივერსიტეტი

ბსტრაქტული

აქტუალურობის შედეგად გაირკვა, რომ აუცილებელია შავი ზღვის გაზის ჰიდრატის საბადოების მოზიდვა ინდუსტრიულ განვითარებაში, როგორც ბუნებრივი გაზის ალტერნატივა. ამას წინ უნდა უძღოდეს მათი არსებობის გეოლოგიური და თერმობარული თავისებურებების იდენტიფიცირება და სინთეზი. აღინიშნა, რომ გაზის ჰიდრატების წარმოქმნა ხდება გარკვეულ თერმობარულ პირობებში, გაზის ჰიდრატის შემქმნელი აგენტის არსებობით, რომელსაც გააჩნია ჰიდრატების წარმოქმნა, ისევე როგორც საკმარისი რაოდენობით წყალი, რომელიც აუცილებელია კრისტალიზაციის პროცესის დასაწყებად. გაზის ჰიდრატების დაგროვება, როგორც წესი, არ ხდება თავისუფალ სივრცეში - ზღვის წყალში, არამედ ზღვის ფსკერის კლდეებში. ბუნებრივი გაზის ჰიდრატების ფორმირების პროცესში მნიშვნელოვანი როლი ენიჭება თერმობარულ პარამეტრებს, აგრეთვე გეოლოგიურ გარემოს თვისებებსა და მახასიათებლებს, რომლებშიც, ფაქტობრივად, ხდება ჰიდრატების წარმოქმნის პროცესი და ჰიდრატების შემდგომი დაგროვება. აღინიშნა, რომ შავი ზღვის გაზის ჰიდრატების ფორმირებისა და დაგროვების წყარო ძირითადად კატაგენტური (ღრმა) გაზია, მაგრამ დიაგენეტიკური გაზი ასევე მონაწილეობს გაზის ჰიდრატების საბადოების ფორმირების პროცესში.

საკვანძო სიტყვები: გაზის ჰიდრატის საბადო, განვითარება, გეოლოგიური თავისებურებები

ბიოაგროქიმიური მახასიათებელი ქიმიური ინდუსტრიის პირობებში ნიადაგების ტექნოგენური დაბინძურებაა

თამარ ელიავა,

გორის სახელმწიფო სასწავლო უნივერსიტეტის ლექტორი

ბსტრაქტული

ნიადაგის ფიზიკურ-ქიმიური თვისებები (pH, ორგანული ნივთიერებების შემცველობა, კატიონის გაცვლის უნარი). მძიმე ლითონების მთლიანი და მობილური ფორმების განაწილების კანონზომიერება შოსტკას სუმის რეგიონის ტერიტორიაზე ქიმიური ინდუსტრიის გავლენის ქვეშ და მის ფონზე. ბიოაგროქიმიურმა ინდიკატორებმა მოიპოვეს მიკროსკოპული სოკოების და მათი სახეობების შემცველობა, ნიადაგების შესწავლის ყველაზე დამახასიათებელი, რაც შეიძლება გამოყენებულ იქნას, როგორც დამატებითი კრიტერიუმი ეკოლოგიური და გეოქიმიური კვლევებისთვის.

საკვანძო სიტყვები: ნიადაგის ფიზიკურ-ქიმიური თვისებები, ორგანული ნივთიერებების შემცველობა, კატიონის გაცვლის უნარი

TOPYRAQTY'N SHOGU QASIETININ DEGRADATIONSON BOLZHAU ƏDISTERI TURALY

Arman Tolipov

Toshkent Davlat Politexnika Universiteti o'qituvchisi

Fizika va mexanika to'plamlari to'qnashuvlari to'plami va ularni ishlatishda ishlatiladigan matraslar qora rangga aylantirilgan. Temengi qobilyatingizni tyynyn bolshayu uchin ğaldaliq boyınsha masstingiz jagdayyyn baqalaudy zheke raskalasynyn kurudy eken nosqasyn qarastyrdy. Tabiғi ylғaldylyқtyң tabiғi kүyden sudyң tolyқ қanuғu zhaғdayyna deyin өsuinің bolzhamdy kүyin belgileu қazhettiligi dəleldendi zhane dəleldendi.Memlekettің Ush өlshemdi gradatsiyasy қoldanylady, Foundation 30 zhane 60% ylғaldylyқtyң zhoғarylauy kүydің əlsiz zhane ortasha өzgeruine səykes keledi. Lesstің salystyrmaly shөguinің fizikalyқ kүyine zhane bəlshekterdің məlsherinің taraluynyң naқty fraktsiyalaryna təueldiligi, shөgindilerdің қybylys retinde microaggregates қүrylymynyң zhane onyң tozuynyң erekshelikterimen Bailanys rastaldy. Mikroagregat - ydyrauy qurlimik beriktik kysymyna zagyn satylarinda zhredi.

To'ylangan so'zlar: bolzham, apatlik jarayoni

ОЦЕНКА МИНИМАЛЬНОГО РИСКА ПО МАКСВЕЛЛУ

Д. Бороденко

старший преподаватель, Институт транспорта и связи

Аннотация

Смещение по длине возникает, когда вероятность включения единицы популяции в выборку связана со значением измеряемой переменной. Например, отбор проб ткани Кокса (1969). В этой статье дан генезис распределения Максвелла смещения по длине. Оценки минимального риска по его шкале были получены при квадрате погрешности, предупредительной и двух других функциях потерь с помощью цензурированной выборки типа II. Относительная эффективность была рассчитана для сравнения.

Ключевые слова: распределение Максвелла с большой длиной, функция потерь, функция риска, оценки MMSE, функция потери квадрата ошибок

خشونت خانگی و سالمندان

Nafisa Begum

University of Faryab

چکیده

خشونت خانگی ، که تصور می شود در طول تاریخ بشر وجود داشته است ، یکی از معضلات اجتماعی در سده ای که در آن زندگی می کنیم نیز می باشد. اگرچه خشونت همه افراد جامعه را دربر می گیرد اما برخی از گروه ها که از نظر خشونت آسیب پذیری بیشتری دارند. یکی از این گروه ها سالمندان هستند. نفوس سالمندان از نظر سهم خود در کل نفوس در سراسر جهان به دلیل افزایش اوسط طول عمر و کاهش باروری در حال افزایش است. در ترکیه، در سال 2006 اوسط طول عمر 71.5 می باشد. آسیب های جسمی و روانی ناشی از خشونت عواقب بارزی دارد. علاوه بر این ، روابط اجتماعی زنان در معرض خشونت را رو به وخامت می گذارد ، توانایی آنها برای مشارکت در زندگی اجتماعی و اقتصادی ،احقاق حقوق خود و مشارکت آنها در سازوکارهای تصمیم گیری آسیب می بیند و مشارکت آنها در زندگی اجتماعی و اقتصادی بسیار کاهش می یابد. در نتیجه؛ رویکرد اجتماعی برای جلوگیری از خشونت و استثمار از اهمیت زیادی برخوردار است. هر جامعه ای باید از طریق برنامه های دولت ، قانون و مقررات ، رسانه ها ، سازمان های رسمی و داوطلبانه ، مؤسسات آموزشی و غیره علیه خشونت تلاش کند.

کلمات کلیدی: خشونت خانگی ، سالمندان ، خشونت ، استثمار از سالمندان

LEGAL REGULATIONS OF INTERNATIONAL MARITIME SECTOR

Noorullah Beigi

Jawzjan University

Abstract

Undoubtedly, maritime transport is an important part of the world economy, given that 90% of international shipping is by sea. It is an important activity for the transportation of agricultural products, energy, manufactured goods and many other goods safely and securely from around the world. Because maritime transport is connected to the computer system with electronic advances and continues to operate through electronic communications, the creation of secure cyber systems is an important requirement for the continued security of these activities. In this paper, the effects of cyber threats on the maritime sector and the legal regulations of international law in this area will be assessed in general.

Keywords: Maritime, Cyber Hazards, Cyber Hazard Management

LIMITATION OF ROTARY WING UNMANNED AERIAL VEHICLE PROPULSION SYSTEM ENERGY USING ANFIS

ANFIS KULLANARAK DÖNER KANATLI INSANSIZ HAVA ARACI ITKI SISTEM ENERJISININ SINIRLANDIRILMASI

Lec. Hüseyin ŞAHİN

Ankara Yıldırım Beyazıt University, Meslek Yüksekokulu, Uçak Teknolojisi

Dr. Mehmet KONAR

Erciyes University, Faculty Of Aeronautics And Astronautics, Aircraft Electric and Electronic

Assoc. Prof.Tuğrul OKTAY

Erciyes University, Faculty Of Aeronautics And Astronautics, Aircraft Engineering

Abstract

Rotary wing unmanned aerial vehicles (UAVs) can perform many military and civilian duties as a developing science in aviation. Today, most rotary wing unmanned aerial vehicles use electric batteries as the primary energy source of the propulsion system. It reveals the security weaknesses of the electric unmanned aerial vehicles due to their high energy needs. When electrically powered devices consume more power than factory data, they can cause fire due to excessive heat and leave permanent damage. To prevent damage to electrical components, they must operate at permissible working forces and conditions. In this study, the aim is to limit the electric power consumption of the electric rotary unmanned aerial vehicle in the propulsion system and to operate the propulsion system safely, efficiently and effectively. For this purpose, firstly, with the help of RCbenchmark's 1580 model dynamometer, propulsion system tests were carried out with different combinations of propulsion systems of UAV. Using the different ANFIS model, the thrust force prediction was made. In the created models, the number of revolutions per minute of the brushless motor, the diameter of the impeller, the pitch of the impeller and the current are determined as input parameters, and the thrust force produced by the motor is determined as the output parameter. Model with 4 input and 1 output parameter was created. The system required for the safe operation of the engine was created by using the data obtained from the propulsion system test.

Keywords: UAV, Propulsion, ANFIS, Current Limitation.

Özet

Döner kanatlı insansız hava araçları havacılıkta gelişen bir bilim dalı olarak askeri ve sivil birçok görevi yerine getirebilmektedir. Günümüzde çoğu döner kanatlı insansız hava araçlarında itki sisteminin temel enerji kaynağı olarak elektrik bataryaları kullanmaktadır. Elektrikli insansız hava araçlarının yüksek enerji ihtiyaçları nedeni ile güvenlik zafiyetlerini ortaya çıkarmaktadır. Elektrikle çalışan aletler fazla güç harcadıkları zaman aşırı ısı nedeni ile yangın ortaya çıkartabildikleri gibi kalıcı hasarlar bırakabilirler. Elektrikli malzemelerin hasar

görmesini önlemek için izin verilen çalışma güçlerinde ve koşullarında çalışmaları gerekmektedir. Bu çalışmada elektrikli döner kanatlı insansız hava aracını itki sistemindeki elektrik güç tüketiminin sınırlandırılması yapılarak itki sisteminin güvenli, verimli ve etkili çalışmasını amaçlamaktadır. Bu amaç için öncelikle RCbenchmark firmasının 1580 model dinamometresi yardımı ile bir motorun değişik itki sistem kombinasyonları ile itki sistem testleri gerçekleştirilmiştir. İtki sistem testlerinden elde edilen veriler ANFIS modelleri yardımıyla itki tahmini yapılmıştır. Bu süreçte farklı bulanık mantık modelleri oluşturulmuştur. Oluşturulan modellerde fırçasız motorun dakikadaki devir sayısı, pervane çapı, pervane hatvesi ve motorun çektiği akım değerleri giriş parametreleri olarak belirlenmiştir ve motorun ürettiği itki kuvveti çıkış parametresi olarak belirlenmiştir. 4 giriş 1 çıkış parametresine sahip model oluşturulmuştur. İtki sistem testinden elde edilen veriler kullanılarak motorun güvenli çalışabilmesi için gerekli olan sistem oluşturulmuştur.

Anahtar Kelimeler: İHA, İtki, ANFIS, Akım Kısıtlama

1. INTRODUCTION

Rotary wings UAVs are automatic controlled or remote controlled aircraft that can fly from everywhere with the help of upward propellers. Rotary wing UAVs can fulfill the requirements of their applications in the military and civilian fields. The rotary wings UAVs that have the ability to take off vertically require many tasks such as surveillance, search and rescue, aerial imaging, and package delivery. Areas such as aviation, robotic, electronic, hardware, and software contributed to the development of UAVs. Many rotary wing UAVs use it as the main source of the electricity source for reasons such as fuel and maintenance costs. [1-3]

According to their duties, unmanned aerial vehicles can be designed in different sizes. The design of the propulsion system must be unique because of many different sizes of aircraft, from mini to megaplanes. Many parameters should be taken into consideration while designing the propulsion system. The optimization problem examined in this study is to find the optimum combination of thrust system components to meet the safety requirements of rotary wing aircraft powered by electric brushless DC (BLDC) motor. Typical electric UAVs consist of four components: propeller, BLDC motor, electronic speed control (ESC) and battery. Traditional designing of propulsion system is tried to be found by trial and error method. [4-5]

The propulsion system is a critical and indispensable system for UAV. The thrust force which is necessary to maintain a flight provides by propulsion system. The performance and utility of the aircraft largely depends on the components used in the propulsion system. The propulsion system, which is one of the most important stages while designing UAV, determines many flight performance parameters such as the flight time, size and payload capacity of the UAV. [6-7]

One of the most common damages in rotary wing UAVs are electrical damages. These damages bring important consequences, such as the engine, ESC or battery being burnt. If these parts are not operated in accordance with the manufacturer's data, they may cause permanent damage. [8-9]

Due to environmental factors such as increased fuel costs, carbon dioxide emissions and noise, electric power systems have become popular. Along with the developments in electric power sources, electric propulsion systems have been used more in practical applications in UAVs. [10-11]

2. RESEARCH AND FINDINGS

2.1. Adaptive Neuro-Fuzzy Inference System (ANFIS)

The Adaptive Neuro-Fuzzy Inference System (ANFIS) technique was originally presented by Jang in 1993.[12] ANFIS uses machine learning methods which are both Fuzzy Logic and Artificial Neural Networks (ANN) together. ANFIS; apply the parameters of Fuzzy Inference System (FIS) with ANN learning method. The advantages of using ANFIS;

- easy implement
- can use If-Then method
- fast and accurate learning

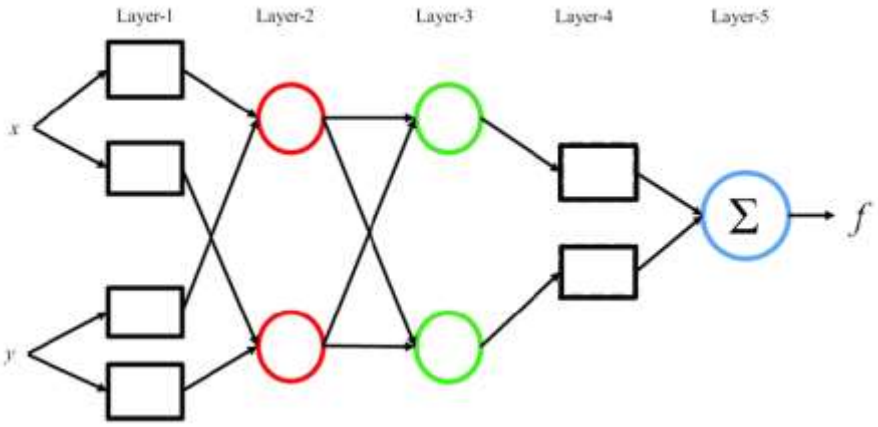

Figure 1. Diagram of ANFIS

ANFIS consists of 5 layers. These are; blurring, operating rule, normalization, clarification and collection.

Fuzzy inference method is a kind of artificial intelligence method. Fuzzy logic can used to control complex and simple systems. Fuzzy logic can choose the solution of difficult and complex system problems. Some of these application areas are; medicine, transport, robot systems, artificial intelligence. [13]

Fuzzy logic basically allows defining values that fall between traditional evaluations such as true-false, 1-0 or yes-no. It is an advanced version of the classical logic method. It can also be

defined as very valuable logic. Fuzzy logic is a naturalization method of the machine or system. Contrary to the classical logic, fuzzy logic not only contains 1 and 0, but also contains values such as 0,5. In fuzzy logic, sharp transitions between values are prevented and the system becomes smarter. [14-15]

The most basic concept of fuzzy systems are fuzzy sets. Similar to classical logic methods, fuzzy logic systems, intersection, union and complements are performed. Fuzzy logic methods may be a suitable method for complex processes when there is no simple mathematical model, nonlinear problems and specialist information processing will be done. However, if the traditional method gives a good result or there is a sufficient mathematical model, fuzzy logic may not be able to create a feasible model. [16]

2.2. Experimental Study and Simulation

RCbenchmark 1580 model dynamometer was used to measure the thrust force in the experimental phase of the study. Make a calibration before using this dynamometer for test provides more accurate and precise results. RC benchmark 1580/1585 installation manual written by Tyoto Robotics Company was used for the installation and calibration process. Consumed electrical energy and produced thrust force were measured by using dynamometer.

Figure 2. Experimental study

With the help of the computer interface of the dynamometer used to measure the consumption of electric power by the BLDC and the thrust produced by the system are recorded. Thus, the performance parameters of the propulsion system for the UAV were examined. The propulsion system test of the EMAX GT-2815 BLDC motor with 10x50, 11x45 and 11x80 propellers has been carried out. The signals required for the move of the BLDC were produced by the 30A ESC unit by the computer interface.

6 signals were sent from the computer interface to the ESC unit between 1000µs to 2000 µs for each propulsion system configuration and the test was repeated 3 times to give accurate results. When excessive force is applied or speed increase (acceleration) on BLDC is consume more electric power. Therefore it is waited for 2 seconds after each signal is sent and the wrong current data is prevented.

The propeller diameter (Pd), propeller pitch (Pp), the number of revolutions per minutes (RPM) of the BLDC and the electric current value (A) were determined as the input parameters of the fuzzy logic model. The thrust force created by the propulsion system is determined as the output parameter of the model. The representation of the created model is given in figure 3.

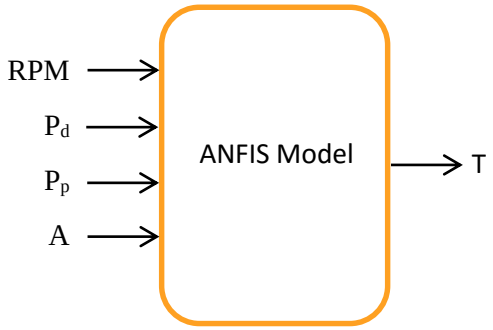

Figure 3. System model structure

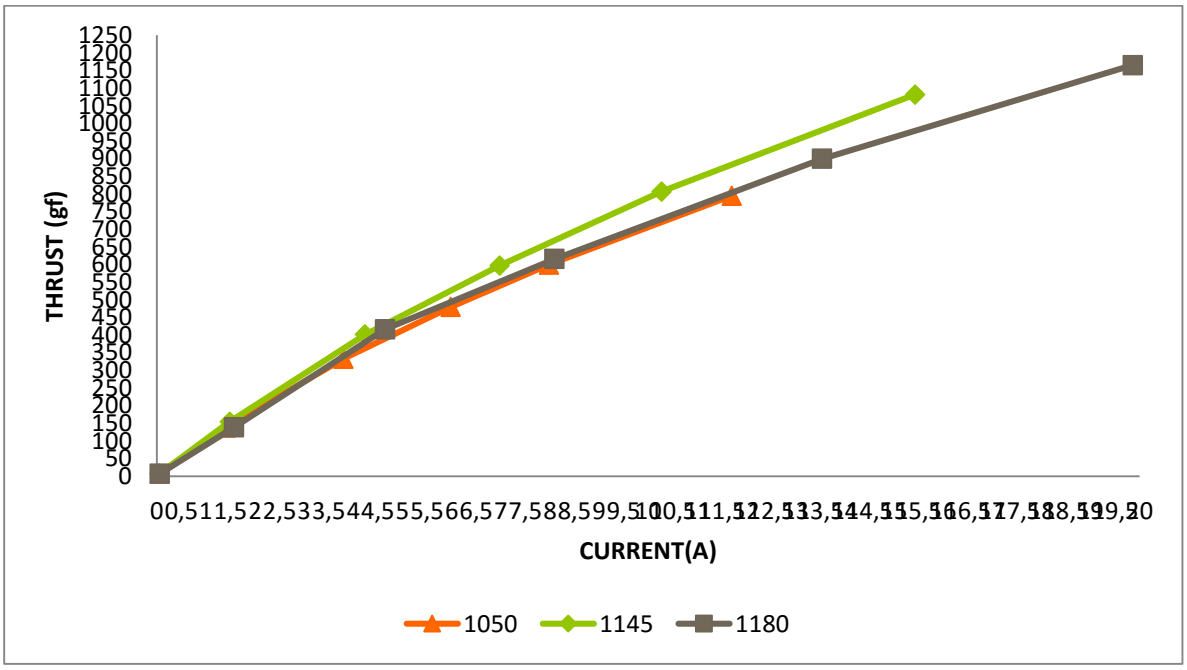

Figure 4. Current-Thrust Force graphs of propellers

With the help of the dynamometer that measure the thrust force, 45 data sets out of 54 data sets were used as training data and 9 data sets were used for test data. 3.8, 5.9 and 11.7 ampere current values of the 10x50 propeller, 7.98, 5.94 and 11.7 ampere current values of the 11x45 propeller and 1.6, 13.49 and 4.58 ampere values of the 11x80 propeller were used for testing.

For this study, Minimum Square Error (MSE) was used to compare system performance. The training and test data obtained in the simulation results are shown in the table. The low MSE indicates that the model's true values. The results of the education and test data obtained in the simulations of the different models are given in table 1. It is seen that the best model is in the 3-rule system with the lowest MSE. Percentage error values in the test data are given in figure 5.

Table 1. Performance comparison of different models

Kural Sayısı	MSE	
	Eğitim	Test
2	2.6881e+01	7.0887e-01
3	1.1384e+01	1.6476e+00
4	1.8006e-01	1.9660e+00

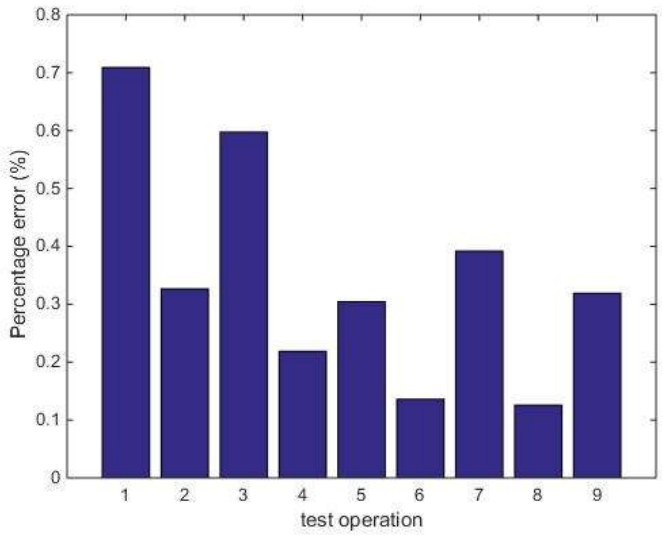

Figure 5. Percentage error values of test operation data

3. RESULT

One of the most important phases of designing UAVs are the propulsion system design. The designed propulsion system must meet all safety requirements. When designing the propulsion system, the electrical power requirements of the system must be taken into. In this study, propulsion system is designed by considering the electrical power consumption. Thanks to the limiting electrical power consumption of the BLDC motor, the propulsion system has been made safer. The thrust force produced by the power limitation system was estimated by the fuzzy inference method.

KAYNAKLAR

1. Valavanis, K. P., & Vachtsevanos, G. J. (2015). Handbook of Unmanned Aerial Vehicles (pp. 1–3022). Springer Netherlands. https://doi.org/10.1007/978-90-481-9707-1
2. Leutenegger, S., Hürzeler, C., Stowers, A. K., Alexis, K., Achtelik, M. W., Lentink, D., Oh, P. Y., & Siegwart, R. (2016). Flying robots. In Springer Handbook of Robotics. https://doi.org/10.1007/978-3-319-32552-1_26
3. Kardasz, P, Doskocz, J. Drones and Possibilities of Their Using. Journal of Civil & Environmental Engineering, 2016; 6(3). https://doi.org/10.4172/2165-784x.1000233
4. Dai, X, Quan, Q, Ren, J, & Cai, K, Y. An analytical design-optimization method for electric propulsion systems of multicopter UAVs with desired hovering endurance. IEEE/ASME Transactions on Mechatronics. 2019, pp. 1-11.
5. Dai, X, Quan, Q, Ren, J, & Cai, K, Y. Efficiency optimization and component selection for propulsion systems of electric multicopters. IEEE Transactions on Industrial Electronics, 2019, 66(10), 7800–7809. https://doi.org/10.1109/TIE.2018.2885715
6. Şahin, H, Oktay, T, Konar, M. Anfis Based Thrust Estimation of a Small Rotary Wing Drone. Europian Journal of Science and Technology, 2020; 18, pp. 738-742. DOI: 10.31590/ejosat.694721
7. Sahin, H, & Oktay, T, & Konar, M, (2020). İnsansız Hava Aracı İtki Gücünün Tahmini. Uluslararası 5 Ocak Uygulamalı Bilimler Kongresi, 3 - 05 January 2020: Adana, Türkiye,
8. Avanzini, G, de Angelis, E, L, Giulietti, F. Optimal Performance and Sizing of a Battery-powered Aircraft. Aerospace Science and Technology 2016. https://doi.org/10.1016/j.ast.2016.10.015
9. Gabriel, D. L., Meyer, J., & Du Plessis, F. (2011). Brushless DC motor characterisation and selection for a fixed wing UAV. IEEE AFRICON Conference. https://doi.org/10.1109/AFRCON.2011.6072087
10. Konar, M. GAO Algoritma Tabanlı YSA Modeliyle İHA Motorunun Performansının ve Uçuş Süresinin Maksimizasyonu. European Journal of Science and Technology, 2019; 15: pp. 360–367. https://doi.org/10.31590/ejosat.529093
11. Hwang, M. H, Cha, H, R, Jung, S, Y. Practical Endurance Estimation For Minimizing Energy Consumption of Multirotor Unmanned Aerial Vehicles. Journal of Energies, 2018; 11(9): pp. 1–10. https://doi.org/10.3390/en11092221
12. J.-S.R. Jang, "ANFIS: Adaptive-Network-Based Fuzzy Inference System," IEEE Trans. Systems, Man, and Cybernetics, vol. 23, no. 3, pp. 665-684, May/June 1993
13. Sivanandam, S. N., Sumathi, S., & Deepa, S. N. Introduction to Fuzzy Logic using MATLAB. In Introduction to Fuzzy Logic using MATLAB. Berlin Heidelberg: Springer, 2007.
14. Konar, M, Bağiş, A. Uçuş Kontrol Sistemi Hız Parametresinin Adaptif Ağ Yapili Bulanik Sonuç Çikarım Sistemi Kullanilarak Belirlenmesi. 2009 IEEE 17th Signal Processing and Communications Applications Conference, SIU 2009. https://doi.org/10.1109/SIU.2009.5136565

15. Badr, B, M, Eltamaly, A, M, Alolah, A, I. Fuzzy Controller for Three Phases Induction Motor Drives. 2010 IEEE Vehicle Power and Propulsion Conference; 2010. https://doi.org/10.1109/VPPC.2010.5729080
16. Williams, J, K. Introduction to Fuzzy Logic. Artificial Intelligence Methods in the Environmental Sciences. 2009. pp. 127–151.

ANALYSIS AND EVALUATION STUDY OF SELF-COMPACTING CONCRETE

Mohamad Khaled Abed Elrahim

Master student, Near East University, Department of Civil and Environmental Engineering

Abstract

Concrete is considered one of the most important elements in the construction sector and the demand for its raw materials or the mixture that consists of it (sand, steel, and coarse aggregate) is increasing with time and with the expansion of architecture in the current era, In addition to huge quantities of waste and residue as a result of demolished construction projects that may lead to environmental damage with drainage of environmental resources from minerals and water And rocks etc. The depletion of natural resources may lead to earthquakes and landslides. This problem has posed a challenge for researchers and work to explore alternatives to reduce the use of environmental raw materials, Emiroglu et al., (2012) and Gammel et al., (2011) did a test on concrete by replacing its original ingredient with some other constituents and realized that there was an increase in the compressive strength of the concrete. Researchers have discovered the self-compacting concrete SCC. This paper aims to study and analyses the Self-Compacting Concrete, types of materials used in the SCC and compare it with the normal concrete in different parts. In addition to analyzing the impact of substitution SCC on preserving the environment and its resources by showing the advantages and disadvantages of using the self-compacting concrete. The study of SCC consist many types of tests which will give an overview about the performance of SCC. As a result of this study it can be said that the SCC it has many advantages that reduce environmental risk and conserve natural resources.

Keywords: Self-Compacting Concrete, Environment, Advantages and Normal Concrete.

1. INTRODUCTION

Concrete is a very important ingredient in the construction sector and it's constant in demand (especially its constituents - sand, steel and coarse aggregate) could lead to land degradation, depletion of natural minerals, lower ground water table and rock disintegration which could cause natural disasters like earthquakes and landslides. These problems have made researchers to dig deep into other means that could replace the original ingredients. Emiroglu et al., (2012) and Gammel et al., (2011) did a test on concrete by replacing its original ingredient with some other constituents and realized that there was an increase in the compressive strength of the concrete. Concrete can be mixed in various ways depending on its usage to give a desire workability, durability and mechanical work rate. According to Duff Abrams (1923), he attested to the fact that the most importamt factor in determining the strength of SCC concrete is the water/cement ratio (w/c). Meaning, the concrete gets higher strength when the (w/c) is low and vice-versa. A low water/cement ratio provides a cement with enhanced strength, lower permeability, resistance to weathering and a better bonding agent between concrete and reinforcement, reduce

shrinkage and cracking, decrease in both volumes change from wetting and drying. It is also important to note that the strength of a concrete varies on a number of factors like quality and quantity of the constituents and the curing environment. SCC mixture can be gauged by the volume or weight - with the aim of a desired workability in mind. Strength is one thing, but workability is another. Workability is the property of a freshly mixed SCC that determines its working characteristics. This means that the easiest way to, mix, place, and compact and finish the mixing id by considering the characteristics above. Some factors that can affect workability in SCC includes cementing materials quality, concrete consistency, water content, admixtures and a particular percentage of air. Additionally, to achieve a good and desirable SCC mixture that is durable and mechanically sound, there's a need for consolidation and curing. Consolidation is the reinforcement of the concrete materials to avoid low compressive strength, by increasing the density of the concrete and making it durable. Curing on the other hand is the ability to maintain a required moisture, temperature and time to allow the concrete achieve a desired or intended purpose.

2. SELF-COMPACTING CONCRETE

2.1. Fundamental guidelines for SCC Mixture

SCC was.first processed in Japan around 29 years back so as to accomplish strong concrete structures. Starting now and into the foreseeable future, a few examinations have been finished to realize a logical blend design for a slandered concrete, which is essentially indistinguishable to ordinary cement. SC Concrete is portrayed so no supplemental inside or outside vibration is required for the compression. It is packing itself alone because of its own weight and remove the air molecules while spilling in the formwork. In structural members with abnormal state of fortress it fills also absolutely all spaces and holes. SC concrete streams like "nectar" and after setting it has a flat concrete level. SCC incorporates of indistinguishable parts from vibrated standard concrete, which are cement, grains, water, added substances and admixtures. In standard, the characteristics of the fresh and hardened SC Concrete, which rely upon the mix design, ought not be unique in relation to ordinary cement. One remarkable thing is the consistency. SC concrete must have a slump stream sf of approx. sf > 65 cm. subsequent to pulling the stream concrete. We should contemplate decrease of the water-powder-proportion w/p, constraint of the course totals content Vg, and the utilization of superplasticizer.

2.2. Types of SCC

1. The powder type SCC: is recognized by a lot of ash which is between 550 and 650 kg/m3. The paste goes about as a 'greasing up' coat that admissible distortion, which carrying.the granules in a condition of cut off. This keep up the plastic consistency and increases the segregation resistance. The.yield point. is set up by the joining of additives

2. Viscosity type SCC: has lower amount of powder, 350 to 450 kg/m3, a high water/concrete proportion and high water/powder proportion. VMAs (viscosity. modifying.agent) work by modifying the concrete structure at a microscopic level, advancing viscosity, yet avoiding stream. The.yield point. is commonly directed by the expansion of additives

3. Combination type.of SCC: joins elements from both powder SCC's and VMA SCC's. The powder quantity varies in a range of 450 to 550 kg/m3.

2.3. Uses

- Bridges and on pre-cast sections.
- Raft construction and pile foundation.
- Highly stable and durable retaining wall.
- Repairs and renewal constructions.

2.4. Merits of SCC

The benefits that are obtained from the use of SCC cannot be overemphasized. It serves the following purposes; a few are listed below:

- reduces employments
- improve building ability
- join to reinforcing steel
- speed up project schedules
- stream in complex forms
- reduces voids in high reinforced areas
- excellent durability and strength
- permits easier pumping procedure
- excellent surface finishes
- rapid placement without vibration
- reduce noise level that results from mechanical vibrators
- it is recommended for deep sections
- makes a regular surface

2.5. Materials used in SC concrete

1. Cement: ordinary Portland cement

2. Aggregates: the size of the aggregates is not more than 20mm.the best choice of the shape of aggregates are round or spherical.

The fine aggregates utilized in self-compacting concrete can be natural or artificial aggregates with regular grade. The general use of fine aggregates is the aggregates with less than 0.125mm (particle size)

3. Water: The quality of water is the same as in reinforced concrete and stressed concrete construction.

4. Mineral admixtures:

It utilized shift dependent on the blend design and properties required. Distinctive mineral admixtures are recorded beneath.

- Ground Granulated Blast Furnace Slag (GGBS**):** promote the flow characteristics of SCC.
- Fly ash: The fine particles asset to fill the pores. This improves the quality and durability of the SCC structures.
- Silica Fumes**:** increment the mechanical characteristics of the SCC structure.
- Stone Powder: The utilization of stone powder in SCC is utilized to improve the powder content of the blend.

5. Chemical admixtures: New superplasticizers are utilized in SCC blend design. So as to promote the frost and overflow resistance of the concrete structure, air entraining operators are utilized. To control the setting time, retarders are utilized.

2.6. Properties of SCC

- **Filling ability:** the SCC concrete is subjected to the following test such as Droop test (slump flow) and V-funnel to measure it filling ability and limit. This is attained when there's a free flow of the mixture in filling the empty spaces in the structural platform corresponding to its personal weight**.**
- **Passing ability:** the possibility of a SCC mixture can be measured or detected using the following technique such as U-box, Fill box and J-ring procedures. The idea is to check the limit of the mixture under its own very weight in relation to how it flows into restricted spaces of material - e.g. steel bars
- **Segregation resistance:** The reduction of segregation or a total resistance is attained when the filling and passing limit possess a homogenous structure throughout the procedures of the usage.

2.7. Test method

1. Slump flow test:

This test was established to elucidate the flow of the concrete horizontally without any form of hindrance. This was first made use of in Japan in checking the effectiveness of a deluged concrete. The procedure that would be used to decide the slump flow depends on the strategic procedures. The radii of the concrete's circle are yardstick for gauging the concrete's filling ability.

➢ **Tools:**

- truncated cone template with diameters (200mm at the bottom ,100mm at the upper part and with a height equal to 300mm)
- Base plate of a hardened, (area equal to 700mm square)
- Ladle
- Scale
- Stopwatch

Fig1: equipment for flow slump experience (Prof. Dr. Nabeel Al-Bayati, 2017)

Fig2: Slump flow and T50cm experience (Prof. Dr. Nabeel Al-Bayati, 2017)

2.8. V funnel test (V funnel experience and V funnel at T 5 min):

The experience is made to measure stream capacity i.e. flowability of the concrete. Apart from this, the outcome is impacted likewise by the solid qualities. High stream time can moreover be connected with low deformability due to a high glue consistency, and with high between particle grinding.

➢ **Tools :**

- V-channel
- Pail
- Shovel
- Ladle
- Stopwatch
- 12 liter of concrete

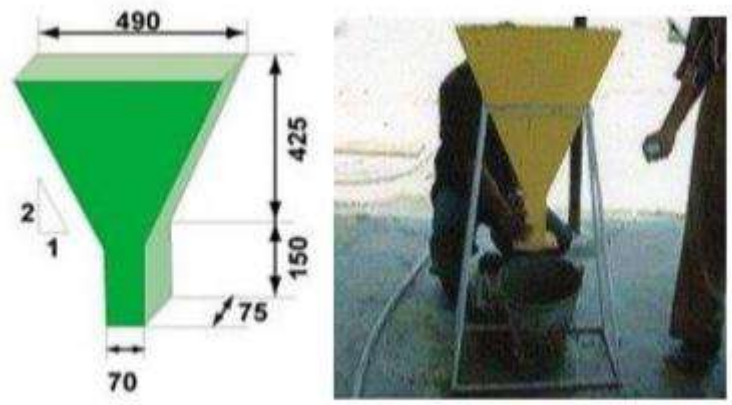

Fig 3: V- channel tool (Prof. Dr. Nabeel Al-Bayati, 2017)

Results:

This experience estimates the naivety of stream of concrete, as the flow time is less, the flow capacity is more.10 secs is convenient flow time for SC concrete. Following 5 minutes of settling, isolation of solid will demonstrate a less constant stream with an expansion in stream time.

2.9. L Box Test on Self Compacting Concrete:

Generally, this experiment is very appropriate and utilizable for research and construction usage - because it checks the filling and passing ability of SCC and resistance to segregation can be externally distinguished.

➢ **Tools**

- L box
- Stopwatch
- Ladle
- Shovel
- 14 liter of concrete

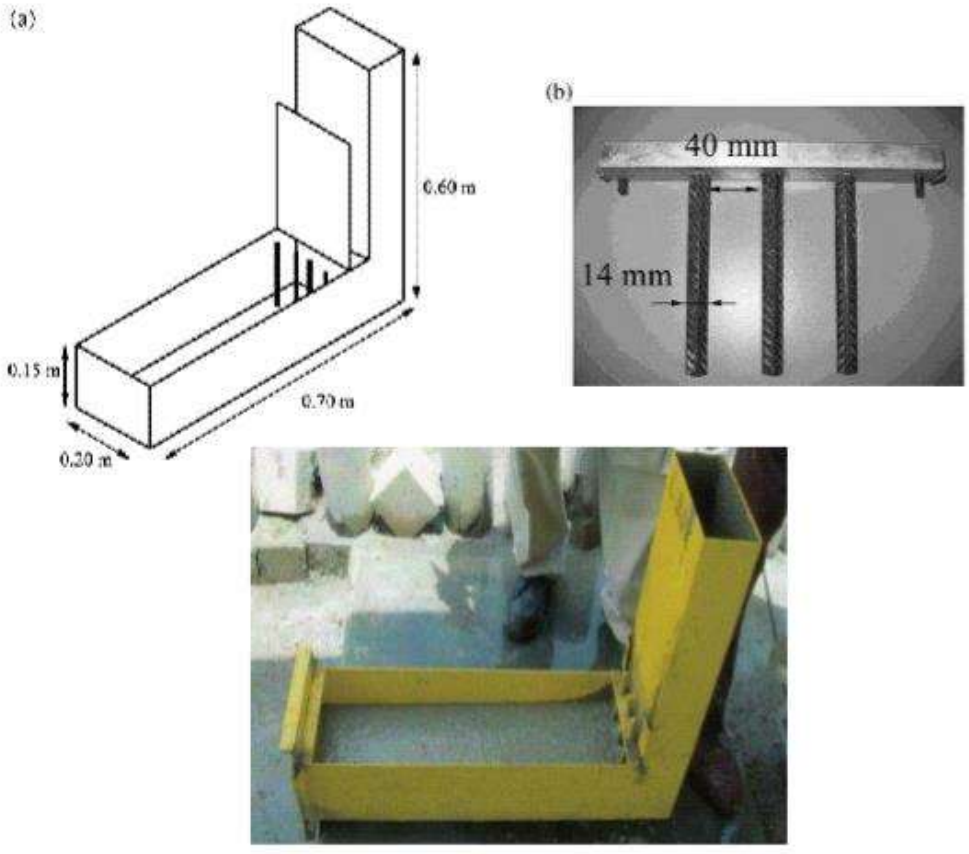

Fig4: L box tool (Prof. Dr. Nabeel Al-Bayati, 2017)

Result:

If H2/H1 = 1, this simply implies that the concrete mixtures flow unrestricted like water; meaning the mixture is flat. Therefore, this indicates the best stream of the concrete mixture as the value obtained from the test is of near value to the ratio. Although, no tangible value has been meet to fit the correct measurement, but a group of European Union (EU) expert has given an approximated value to show when the concrete mixture is flowable - 0.8, T20 and T40 time.

2.10. U box experience:

A very good determining test is the one being tested here; although, it's very challenging and might be very difficult to produce these things. It gives a decent immediate evaluation

of filling capacity this is actually what the solid needs to do-altered by an unmeasured prerequisite for passing capacity. The 35 mm hole between the areas of fortification might be viewed as excessively close. The inquiry stays open of what filling stature under 30cm is as yet worthy.

➢ **Tools**

- Stopwatch
- Shovel
- Ladle
- 20 liter of concrete

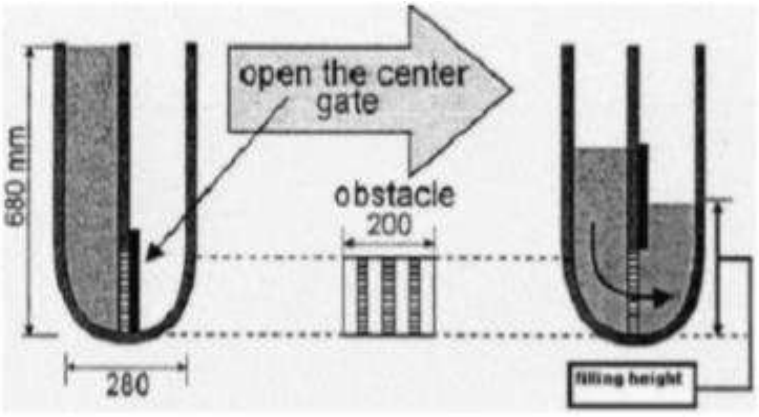

Fig 5: U box tool (Prof. Dr. Nabeel Al-Bayati, 2017)

Results:

Concrete mixture flows as smoothly and steady as water here and when at rest it will be

flat. The best stream and passing capacity of the solid, when the test value is close to the filling height (H1-H2)

2.11. Fill box experience:

If the passing ability and resistance to segregation of the mixture is poor, it is bound to fail in the construction it would be used for or perform below par even if it has a high filling capability. Although, there's a challenge in accommodating the largeness of the device and its eventual expansion, the quality SCC concrete provides is definitely unmatched.

➢ **Tools**

- Fill box
- Ladle ,2 liter
- Scale
- Stopwatch

Fig6: fill box hollow and loaded with cement (Prof. Dr. Nabeel Al-Bayati, 2017)

Results:

On the off chance that the solid streams as uninhibitedly as water, at rest it will be flat, so normal filling rate = 100%.the best self-compacting qualities of the solid, when the experience value is close to 100%. Normal filling rate: normal filling rate F= {(H1+H2)/2*H1} *100%

3. Difference between SC concrete and normal concrete

	Self-Compacting Concrete	Normal Concrete
1	Compaction is experience as the concrete flows on its own weight	Concrete is compacted by vibration machine
2	High workability	Less workablility
3	Altering agents such as super plasticizers and VMA produce high workability	Workability obtained through increased moisture content
4	Visible binding increment in the SCC mixture with the usage of super plasticizers	Very weak cement mixture
5	Percentage of water in the mixture is very low	Percentage of water in the mixture is high
6	There's a very high proportion of cement and fine aggregate content in the mixture	The fines content is less than in SCC
7	Bleeding decreases due to the Lower water content	Bleeding is high
8	Segregation is very low as the increment in the proportion of the fine aggregate provides a uniform mixture	High level of segregation
9	Due to the increase in the addition of fine aggregate contents, there's reduced viscosity	High Viscosity
10	it give good and beautiful finish	Normal finish
11	Great choice for thick reinforcement works	Conventional cement mixture are not advisable for thick reinforcement works as it is not reliable due to its inability to readily compact

Table.1 Difference between SC concrete and normal concrete.

3. CONCLUSION

Convincingly, we can undoubtedly say that the environment is feeling a great toll as result of the constant extraction and utilization of natural aggregates for construction. Inadvertently, the enormous amount of waste materials and rubbles as a result of demolished construction projects and waste generated from several materials is serious cause for concern and needs quick solution. Although, these wastes can be reused or recycled in generating materials that could be used in the concrete production company; which is where SCC comes in as the perfect replacement for conventional cement with

numerous merits. Therefore, it is very necessary to stress the need for SCC in modern day structures. More so, the rate at which SCC would serve a better purpose can't be attained through the mixture; certain ratio of the aggregates has to be increased, but it is necessary to take precautions so has to improve the overall performance of the SCC mixture. Concurrently, there are several improvements been made to create a better standard for SCC to create more durability and develop a better standard for future recommendations.

REFERENCES

[1] Petroski, H. (2009). Engineering: Akashi Kaikyo Bridge. *American Scientist*, *97*(3), 192-196.

[2] Bakhtiarian, A. H., Shokri, M., & Sabour, M. R. Application of Self-Compacting Concrete, Worldwide Experiences.

[3] Ouchi, M., & Hibino, M. (2000). Development, Applications and Investigations of Selfcompacting Concrete. In *International Workshop, Kochi, Japan*.

[4] Aggarwal, P., Siddique, R., Aggarwal, Y., & Gupta, S. M. (2008). Selfcompacting concrete-procedure for mix design. *Leonardo electronic journal of practices and technologies*, *12*, 15-24.

[5] Okamura, H., & Ouchi, M. (2003). Self-compacting concrete. *Journal of advanced concrete technology*, *1*(1), 5-15.

[6] Aggarwal, P., Siddique, R., Aggarwal, Y., & Gupta, S. M. (2008). Selfcompacting concrete-procedure for mix design. *Leonardo electronic journal of practices and technologies*, *12*, 15-24.

[7] Collepardi, M. (2003, October). Self-compacting concrete: What is new. In *Proceedings of the 7th CANMET/ACI Conference on superplasticizer and other chemical admixtures in concrete* (pp. 1-16).

[8] Panda, K. C., & Bal, P. K. (2013). Properties of self compacting concrete using recycled coarse aggregate. *Procedia Engineering*, *51*, 159-164.

[9] Ramanathan, P., Baskar, I., Muthupriya, P., & Venkatasubramani, R. (2013). Performance of self-compacting concrete containing different mineral admixtures. *KSCE journal of Civil Engineering*, *17*(2), 465-472.

23

[10] Nazari, A., & Riahi, S. (2011). Effects of CuO nanoparticles on compressive strength of self-compacting concrete. *Sadhana*, *36*(3), 371.

[11] Desnerck, P., De Schutter, G., & Taerwe, L. (2010). Bond behaviour of reinforcing bars in self-compacting concrete: experimental determination by using beam tests. *Materials and Structures*, *43*(1), 53-62.

[12] Dehn, F., Holschemacher, K., & Weiße, D. (2000). Self-compacting concrete (SCC) time development of the material properties and the bond behaviour. *Selbstverdichtendem Beton*, 115-124.

[13] Cazacu, N., Bradu, A., & Florea, N. (2016). Self Compacting Concrete in Building Industry. *Buletinul Institutului Politehnic din lasi. Sectia Constructii,*

Arhitectura, *62*(1), 85.
[14] Ramanathan, P., Baskar, I., Muthupriya, P., & Venkatasubramani, R. (2013). Performance of self-compacting concrete containing different mineral admixtures. *KSCE journal of Civil Engineering*, *17*(2), 465-472.
[15] Emiroglu, Mehmet & Yildiz, Servet & Kelestemur, Mehmet. (2015). A study on dynamic modulus of self-consolidating rubberized concrete. Computers and Concrete. 15. 795-805. 10.12989/cac.2015.15.5.795.
[16] Gammel, Nanthagopalan, Prakash & Santhanam, Manu. (2011). Fresh and hardened properties of self-compacting concrete produced with manufactured sand. Cement and Concrete Composites. 33. 353-358. 10.1016/j.cemconcomp.2010.11.005.
[17] Al-Bayati, Nabeel. (2017). SELF COMPACTING CONCRETE WITH TESTS.

THE APPLICATION OF PRESSURE DIFFERENCE IN THE LIQUID TRANSFER PURPOSE

Ahmed Ashraf Ezzat Mohamed IBRAHIM & Assist. Prof. Dr. Anoosheh IRAVANIAN

Civil and environmental engineering faculty, Near East university, Near East Boulevard, ZIP: 99138,Lefkoşa / TRNC Mersin 10 - Turkey

Abstract

In the liquid close flow process the liquid is transferred from the point with the high pressure to the point with low pressure. Such a property can be used to transfer the liquid between two points with difference in the level. This study contains applications of this property to transfer liquids. we can control the pressure value between the two points we want to transfer the water between them using the (closed pressure tank) in the destination point. (closed pressure tank) is a full tank connected with the close flow liquid system from the top at the destination point with valve system in the bottom. according to the value of the level difference and the density of the liquid we can set the valve to create the pressure difference inside the tank causing liquid transition. The amount of liquid leaving the tank will be replaced by a new amount via the upper system connection in the top of the tank. such a method can create an infinite liquid transition between two points which can be very useful at the field of Renewable Energy - Environmentally Friendly power stations and for the Industrial heat dissipation purposes. The stiffness, dimensions , and design of the system elements(pipes, tank, valve, connections, extra..) can be changed according to the liquid type and the difference in the level. This study Analyse that system for the case of water liquid.

Keywords: water pump , pressure flow, pumping system, infinity flow.

1. INTRODUCTION

It is known that when it is required to transfer the water between two points with difference in the level we should use a pumping system. The suitable pump type is supposedto be chosen up to the system conditions. The dynamic Pumps specifically the Centrifugal Pumps are most commonly used all over the world. The Positive Displacement Pumps specifically the Lobe Pumps offer different characteristics like an excellent high efficiency. Generally most of the pump types technique is to employ the dynamic energy to increase the pressure. To create this dynamic energy we need to provide the system with required energy which is a cost. This study presents a new liquid transition method without any need for dynamic force. In this method no need to employ an external pressure provider that means we can get rit of the cost of the energy spent by the pumping systems.

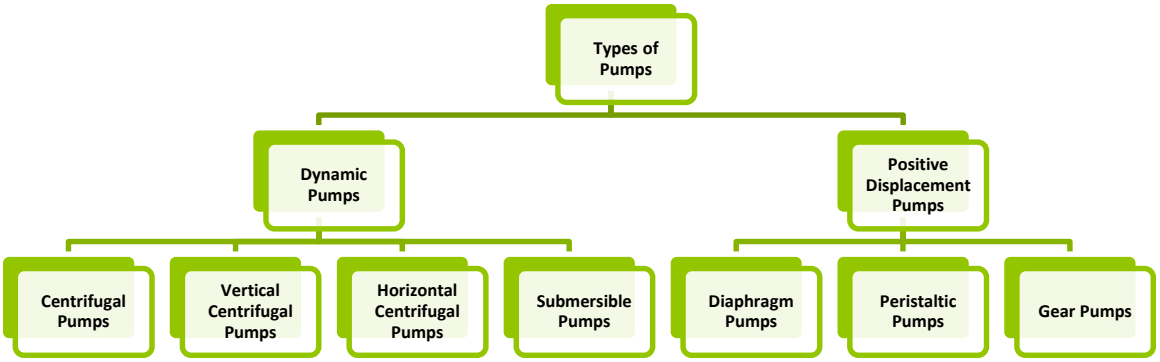

Figure 1. types of the pumps

The pumping system is added to the bernoulli equation providing the required energy to start the water transfer.

$$P_1 + \frac{1}{2}.\rho.v_1^2 + \rho.g.h_1 + P_p = P_2 + \frac{1}{2}.\rho.v_2^2 + \rho.g.h_2 + f_h.\rho.g + P_t$$

The pump pressure (Pp) is added to the left-hand side of the equation and the turbine pressure (Pt) is added to the right. The left part of the equation represents the energy of the point where we want the flow to start ,on the other hand the rightpart of the equation represents the destination point energy. The purpose of thepump is to increase the energy of the left-hand side. In this time the flow startingpoint energy will be bigger than the destination point therefore the flow startsfrom the point with higher energy so pump use can be expressed as addingexternal pressure (Pp) provider tocontrol the flow direction. The aim ofthis study is to control the liquid pressure of one of the flow two points –inthe close flow system - which willenable us to control the flow without adding an external pressure provider thusit is a new liquid transimmition technik.

It is known that (P1) represents the pressure ofthe starting flow point with (h1) leveland (P2) represents the pressure of the destination flow point with (h2) level. If weconsider the liquid velocity to be a neglected value for both of the sides – asthe flow is happening between tanks – also we remove the turbine and the pumpfrom the system ,the minor losses can be neglected for now. The value ofliquid density and the magnitude of the acceleration due to gravity is fixedfor both sides. The equation can be represented like this: :

$$P_1 + \frac{1}{2}.\rho.v_1^2 + \rho.g.h_1 + P_p = P_2 + \frac{1}{2}.\rho.v_2^2 + \rho.g.h_2 + f_h.\rho.g + P_t$$

From this equation it is clear that when this condition is met **(P2<(P1- g* ρ *(h2-h1)))** the flow can occur. The control of (P2) vale enables to control the flow of the system.

2. CLOSED PRESSURE TANK SYSTEM

The required decrease in the pressure of the destination point can be created using the closed pressure tank.

2.1. CLOSED PRESSURE TANK SYSTEM DESCRIBTION

Thedestination point of the flow is going to be fixed to the closed pressure tankwhich can create the gap in pressure values between the two points of the flow causing liquid transition. The mechanism of the closedpressure tank employs the gravity to affect a high density metal cylinderto decrease the pressure. The cylinderis fixed on a path at the vertical sides of the cylinder tank. The path enablesthe cylinder to have free motion because of the gravity. At the left top part of the tank there is one liquid entry.At the right there is one liquid exit. At the left bottom part of the tank there is one liquidentry. At the right there is one liquid exit. The tank works withtwo opposite operations. After the exit opening it is the regulation tank andafter the regulation tank it is the turbine.

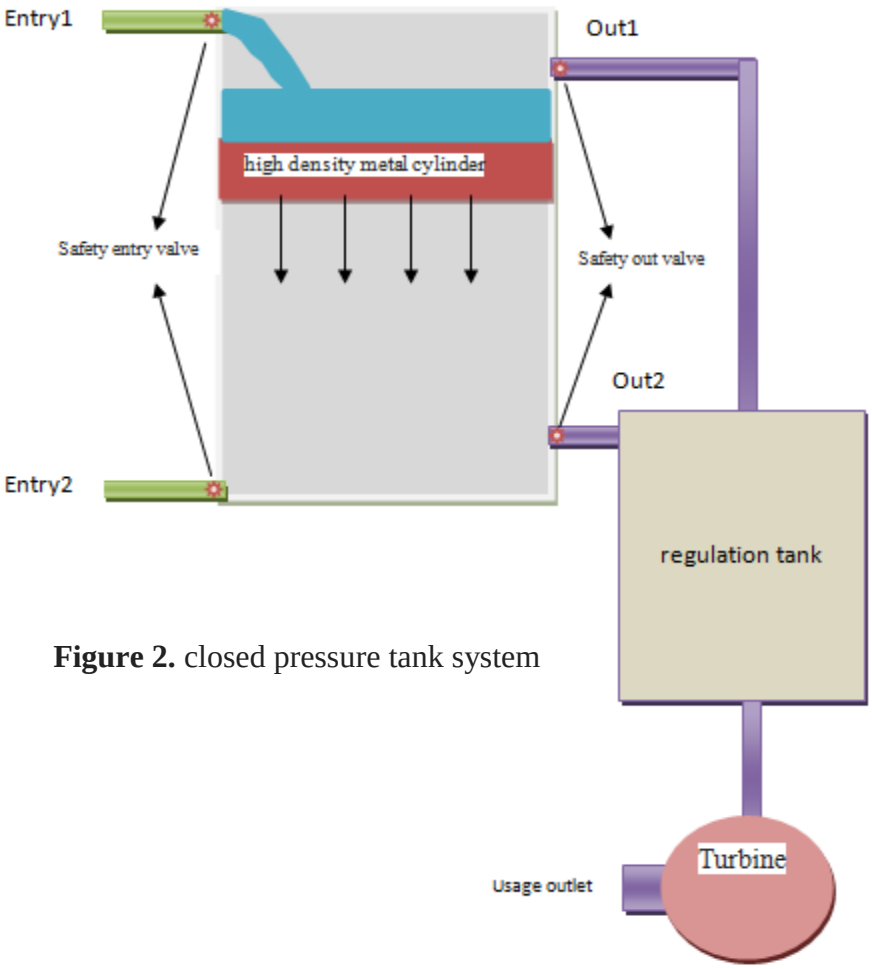

Figure 2. closed pressure tank system

2.2. CLOSED PRESSURE TANK SYSTEM ACTION STEPS.

The first operation occurred when the cylinder started to move from the top of the tank to the bottom of it. This movement happened because of the gravity causing a gap of theoretical zero pressure in the top of the tank. There are two openings in the top of the tank, one of them is entry and one of exit but there are two safety valves fixed on both of the openings. The safety valve serves the purpose of the exit in the case of exit opening and the purpose of the enter in the case of entry. Because of the decrease in the pressure as there is a safety valve on

the exit opening, the water starts to enter the tank. After a particular period the cylinder reaches the bottom of the tank, the water bottom reaches the exit opening ,thus the water leaves the tank. After a particular period the tank is almost empty. The platform reverses the top of the tank to the bottom then the same operation is repeated from the opposite part. The exit openings provide the regulation tank with the liquid. For the rotation of the tank done by the platform the required dynamic energy can be gained from a turbine being fixed after the regulation tank. In this case all of the system elements are fixed higher than the destination level to provide a sufficient height for the turbine to gain the required energy.

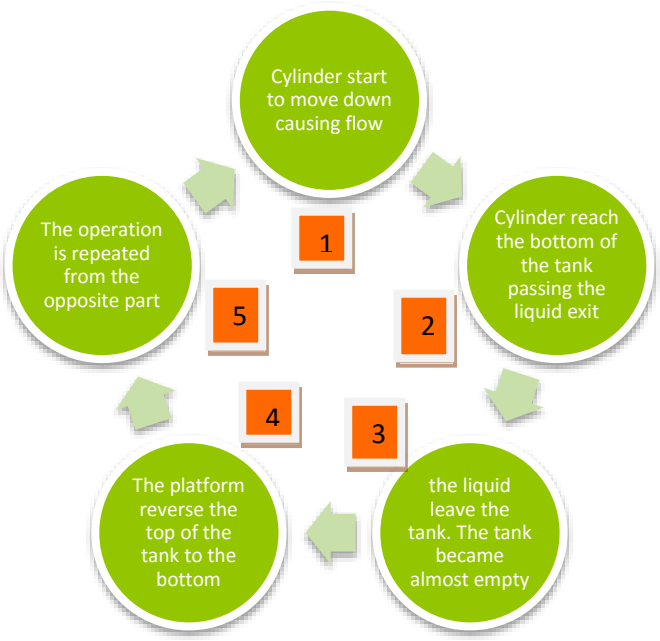

Figure 3. closed pressure tank operations cart.

3. CONCLUSION

The optimum value of the pressure for the destination point can be dived from the relationship shown in the condition of the flow **(P2=(P1- g* ρ *(h2-h1)))**. If we consider the pressure for the starting point to be equal to the atmospheric pressure and the pressure at the close pressure tank equal to zero theoretically then, **P1- P2= Δ p= atmospheric pressure =g* ρ *(h2-h1).** The condition of the flow can be expressed as **atmospheric pressure >g* ρ *(h2-h1)** thus, It is clear now that this method is not possible for high level differences as thevalue of the multiplication of water density with magnitude ofthe acceleration due to gravity with the level difference must be less than the atmospheric pressure.

4. REFERENCES

Zhi-guang, Z., Bing-qin, Y., Li-wen, Z. and Sheng-lian, Y., 2011, April. Research on type selection of pump used in pumping irrigation well. In *2011 International Conference on Consumer Electronics, Communications and Networks (CECNet)* (pp. 5195-5198). IEEE.

Free, R., 2012. Process Component Function and Performance Criteria. *Process Plant Equipment: Operation, Control, and Reliability*, pp.355-411.

Chandel, S.S., Naik, M.N. and Chandel, R., 2015. Review of solar photovoltaic water pumping system technology for irrigation and community drinking water supplies. *Renewable and Sustainable Energy Reviews*, *49*, pp.1084-1099.

Mimmi, G.C. and Pennacchi, P.E., 1997. Involute gear pumps versus lobe pumps: a comparison.

Tong, S.H. and Yang, D.C., 2000. On the generation of new lobe pumps for higher pumping flowrate. *Mechanism and machine theory*, *35*(7), pp.997-1012.

Hartley, F.T., Hartley and Frank T., 1999. *Micromachined peristaltic pumps*. U.S. Patent 6,007,309.

Tamari, Y., 1993. *Innovative pumping system for peristaltic pumps*. U.S. Patent 5,215,450.

Gülich, J.F., 2008. *Centrifugal pumps* (Vol. 2). Berlin: Springer.

Wilson, K.C., Addie, G.R., Sellgren, A. and Clift, R., 2006. *Slurry transport using centrifugal pumps*. Springer Science & Business Media.

Karassik, I. and McGuire, J.T. eds., 2012. *Centrifugal pumps*. Springer Science & Business Media.

Karassik, I. and McGuire, J.T. eds., 2012. *Centrifugal pumps*. Springer Science & Business Media.

Pritchard, P.J. and Mitchell, J.W., 2016. *Fox and McDonald's introduction to fluid mechanics*. John Wiley & Sons.

Badeer, H.S., 1985. Elementary hemodynamic principles based on modified Bernoulli's equation. *Physiologist*, *28*(1), pp.41-46.

Segletes, S.B. and Walters, W.P., 2002. A note on the application of the extended Bernoulli equation. *International journal of impact engineering*, *27*(5), pp.561-576.

Saleta, M.E., Tobia, D. and Gil, S., 2005. Experimental study of Bernoulli's equation with losses. *American journal of physics*, *73*(7), pp.598-602.

Kay, J.M., Nedderman, R.M. and Nedderman, R.M., 1985. *Fluid mechanics and transfer processes*. CUP Archive.

Fay, J.A., 1994. *Introduction to fluid mechanics*. MIT press.

THE EFFECT OF CHANGE IN ANGLE BETWEEN ROTOR ARMS ON TRAJECTORY TRACKING QUALITY OF A PID CONTROLLED QUADCOPTER

PID KONTROLLÜ QUADCOPTER'IN YÖRÜNGE İZLEME KALİTESİ ÜZERİNE ROTOR KOLLARI ARASINDAKİ AÇI DEĞİŞİKLİĞİNİN ETKİSİ

Öğr. Gör. Yüksel ERASLAN*

İskenderun Teknik Üniversitesi, İskenderun Meslek Yüksekokulu, İnsansız Hava Aracı Teknolojisi ve Operasyonları Programı

Enes ÖZEN

Doktora Öğrencisi, Erciyes Üniversitesi, Fen Bilimleri Enstitüsü, Uçak Mühendisliği

Doç. Dr. Tuğrul OKTAY

Erciyes Üniversitesi, Havacılık ve Uzay Bilimleri Fakültesi, Uçak Mühendisliği Bölümü

Özet

Quadcopter, gezinme uçuşu ve yüksek manevra kabiliyeti ile yapısı basit ancak kontrol açısından karmaşık olan dört rotorlu insansız hava araçlarıdır. Keşif, kurtarma, gözlem ve kargo gibi birçok askeri ve sivil uygulamada aktif rol alan bu hava araçlarının artan popülaritesi, bu alanda birçok farklı tasarımın geliştirilmesine yol açmıştır. Özellikle son zamanlarda geçiş geometrileri olan hava araçlarının hem deneysel, hem de sayısal hem de analitik olarak birçok disiplin tarafından incelendiği görülmektedir. Dönüşüm geometrileri olan quadcopterlerden, yıkılan binalardaki kurtarma operasyonları veya mağara araştırma çalışmalarında olduğu gibi ulaşılması zor dar alanlardan yararlanabilir. Dönüşümün etkinliğini aktif ve pasif olarak iki sınıfa ayırmak mümkündür. Aktif geçiş, hava aracının uçuş sırasında şeklini değiştirme kabiliyeti olarak tanımlanır ve pasif geçiş, uçuştan önce geometrik şekli manuel olarak değiştirme yeteneğidir. Aktif ve pasif geçiş, özellikle rotor kollarının uzunluğu ve dört rotorlu quadcopterin üzerindeki rotor kolları arasındaki açılar, hava aracının performansını artırmaya katkıda bulunabilir. Rotor kolu uzunluğunun değiştirilmesi ile hava aracının boyutları simetrik veya asimetrik olarak büyütülebilir veya küçültülebilir ve rotor kolları arasındaki açısının değiştirilmesi ile hava aracının en boy oranı değişebilir ve büyük avantajlar olabilir. Çevre koşullarına uyum sağlayarak elde edilir. Dönüştürme kabiliyeti ile quadcopterlerin morfolojik olarak X, O, T şekilleri gibi farklı konfigürasyonlara dönüştürülmesi mümkündür. Bu çalışmada, bir PID (oransal-integral-türev) kontrolör ile kontrol edilen X morfolojisi olan bir quadcopter üretilmiştir, rotor kolları arasındaki açının değişmesine bağlı olarak yörünge izleme kalitesi değişikliği tartışılmıştır.

Anahtar Kelimeler: Quadcopter, PID Denetleyicisi, Rotor Kolları Arası Açı, Yörünge İzleme Kalitesi.

Abstract

Quadcopters are unmanned aerial vehicles with four rotors, which are simple in structure but complex in terms of control, with the ability of hovering flight and high maneuverability. The increasing popularity of these aircraft, which take an active role in many military and civilian applications such as reconnaissance, rescue, observation and cargo, have resulted in many different designs to be developed in this field. Especially in recent times, it is seen that aircraft with morphing geometries have been examined by many disciplines both experimentally, numerically and analytically. Quadcopters with morphing geometries can benefit in narrow-section areas that are difficult to reach, such as in rescue operations in collapsed buildings or in cave research studies. It is possible to divide the morphing activity into two classes as active and passive. Active morphing is defined as the ability of the aircraft to change shape during flight, and passive morphing is the ability to manually change geometric shape before flight. Active and passive morphing, especially on the length of the rotor arms and the angles between the rotor arms on quadcopters with four rotors, can contribute to improve the performance of the aircraft. With the change of the rotor arm length, the dimensions of the aircraft can be enlarged or lessen symmetrically or asymmetrically, and with the change of the angle of the angle between rotor arms, the aspect ratio of the aircraft can change and great advantages can be achieved by adapting to the environmental conditions. With the morphing ability, it is possible that the quadcopters can be transformed into different configurations such as X, O, T shapes morphologically. In this study, a unique quadcopter with X morphology controlled with a PID (proportional-integral-derivative) controller is produced, the trajectory tracking quality change depending on the change of the angle between rotor arms is discussed.

Keywords: Quadcopter, PID Controller, Angle between Rotor Arms, Trajectory Tracking Quality.

1. INTRODUCTION

Unmanned aerial vehicles (UAV) are fixed wing or rotary wing systems. They are aircraft operated autonomous or by commands transmitted from the ground control station. Tricopter, quadcopter and hexacopters are the most popular rotary wing UAV's. Unmanned aerial vehicles have become a popular topic thanks to the development and accessibility of electronics, software and material technology. Civilian and military use of these vehicles exists due to meet various needs especially for outdoor scenarios, and some of indoor applications such as cave, rescue in destroyed buildings, intervention in terrorist activities (Debinez *et al.* 2017). These applications includes traveling among small cracks or gaps, often in confined spaces, which causes very difficult, possibly crushing, situations for traditional quadcopters (Falanga *et al.* 2018).

These vehicles can converted into compatible with indoor uses with image identification, sensor fusion, and artificial intelligence applications (Bai *et al.* 2019). This can be done with changing the shape of quadcopters, preventing collisions and providing shapes that are more

appropriate. In four-rotor unmanned aerial vehicles, shaping is done by methods such as arm extension-shortening or changing the angles between the arms (Wallace 2019). This can be used as a morphing control element to change flight dynamics (Prisacariu *et al.* 2011). If morphing is done before the flight of the quadrotor, it is called as passive morphing and if it occurs during flight, this type is called as active morphing (Oktay and Sal 2016).In another similar system, they are morphing wings that mimic the wings of birds (Di Luca *et al.* 2017).

In this study, a X configuration quadcopter design, mathematical modeling and flight simulation were performed and the results were compared. These studies were prepared by examining the previous studies. O. Kose and T. Oktay designed an asynchronous morphing design for the yaw movement of the quadrotors. In their studies (Kose and Oktay 2019), they developed the quadrotor dynamic modeling in Matlab/Simulink environment using the state space model. O. Kose and T. Oktay designed a quadrotor for their longitudinal, lateral and hover flight. In their study (Kose and Oktay 2019), they derived the quadrotor dynamics with the Newton-Euler method and worked on linear modeling. The authors, who made their simulations in the Matlab / Simulink environment, used separate PID controllers for the quadrotor longitudinal, lateral and hovering flight. They also included atmospheric turbulence in their simulations for all quadrotor flights. O. Kose and T. Oktay designed an asynchronous morphing design for the quadrotors (Kose and Oktay 2019). The authors drew quadrotor morphing and non-morphing states as a full model in Solidworks program. In the drawn models, they obtained the quadrotor inertia parameters in cases with and without morphing by using solid body dynamics. On the other hand, inertial parameters stated that the state space model approach varies as an input matrix element. They made simulations for longitudinal and lateral flight using varying inertial parameters and PID control algorithm. They have demonstrated that, morphing for the longitudinal flight at the same morphing rate does not affect the flight, but that morphing for the lateral flight affects the flight with the design performance criteria and graphics. The actively morphing aircraft X1 (unfolded) and X2 (folded) can fly in two different configurations. General information is given about the dynamics of quadcopter. Geometry was calculated separately for X1 and X2 configurations. In the next section, the force, torque and torque equations on the aircraft are generated. In the next section, the created equations are simulated in Matlab / Simulink environment by considering the loads of the aircraft under different values, and the results are compared. In the last chapter, general thoughts about the results and preliminary values and roadmap is created for the next studies.

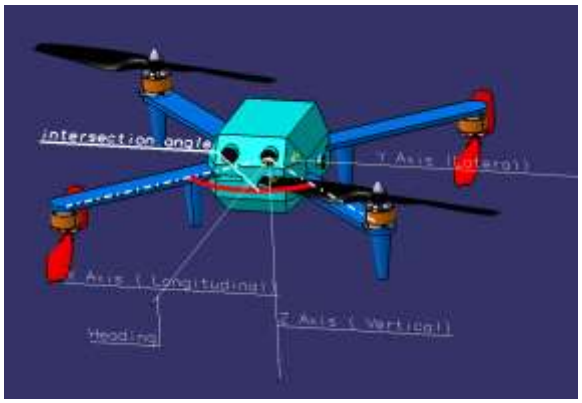

Figure 1. Morph Quadcopter

2. QUADCOPTER FEATURES

Quadcopter that can change the angle of intersection of the arms are connected with a scissor at center. Intersection angle named differently in other studies. Like these; adjustable angle quadcopters (Falanga *et al.* 2018), bisector angle (Debinez *et al.* 2017), scissor-joint angle (Debinez *et al.* 2017), intersection angle (Bai *et al.* 2019) is preferred in this study. Two rotors are placed on the arm ends. The rotor drives the propeller, resulting in forces and moments. The turning directions of the propellers are placed according to the wing edge and body configuration. X configuration are generally preferred for quadcopters. X configuration was preferred in this study. X cofigurations are more stable and maneuvrability is significantly higher than others.

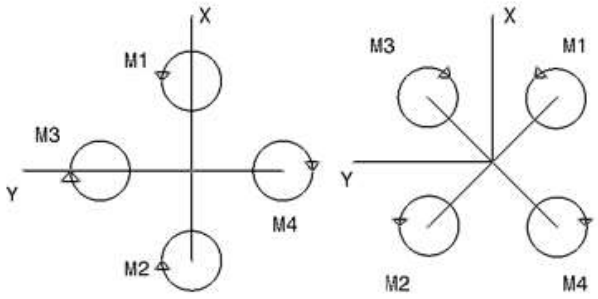

Figure 2. Quadcopter + and X Configurations

Propeller and rotors are placed as 1-2-3-4; propeller 1 and 2 rotate in the opposite direction of clockwise (CCW), while propeller 3 and 4 rotate in the direction of clockwise (CW). In this way, the torques that occur are reset, tail rotors such as helicopters are not needed to balance the vertical axis.

The Quadrotor consists of a flight controller for controlling the engine and propellers, external power regulator, receiver that transmits commands and transmits it to the controller, battery that supplies power to the system, and the body that carries all of them. Quadcopter features are given in table 1.

Table 1. Quadcopter Features

Type of Aircraft	Multi-Rotor
Mtow	1000 gr
Wide X1 - X2	575 mm – 370 mm
Length X1 – X2	575 mm – 685 mm
Morphing time	0.5 sn
Propeller	10X4
BLDC	1000 Kv
Flight Controller	PixHawk 1

The balance and control of the quadcopter during flight is more difficult than fixed wing aircraft. The system is unstable because lift and thrust are produced by the propellers. Flight controllers regulate rpm of the rotors according to the commands received, ensuring that the desired orientations are based on the user's commands or autonomous flying.

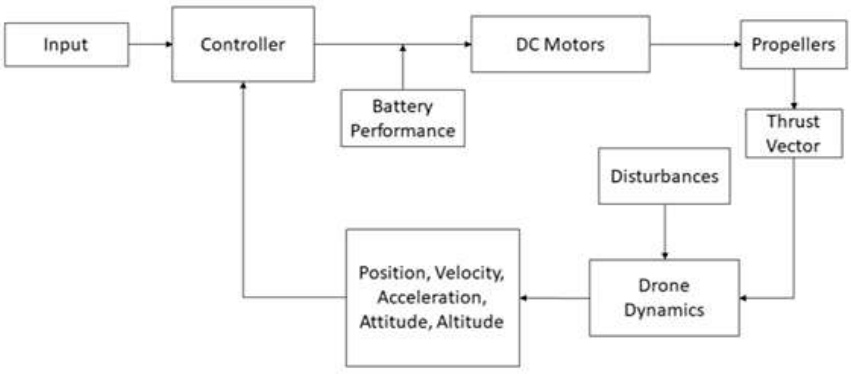

Figure 3. Flight Control Scheme

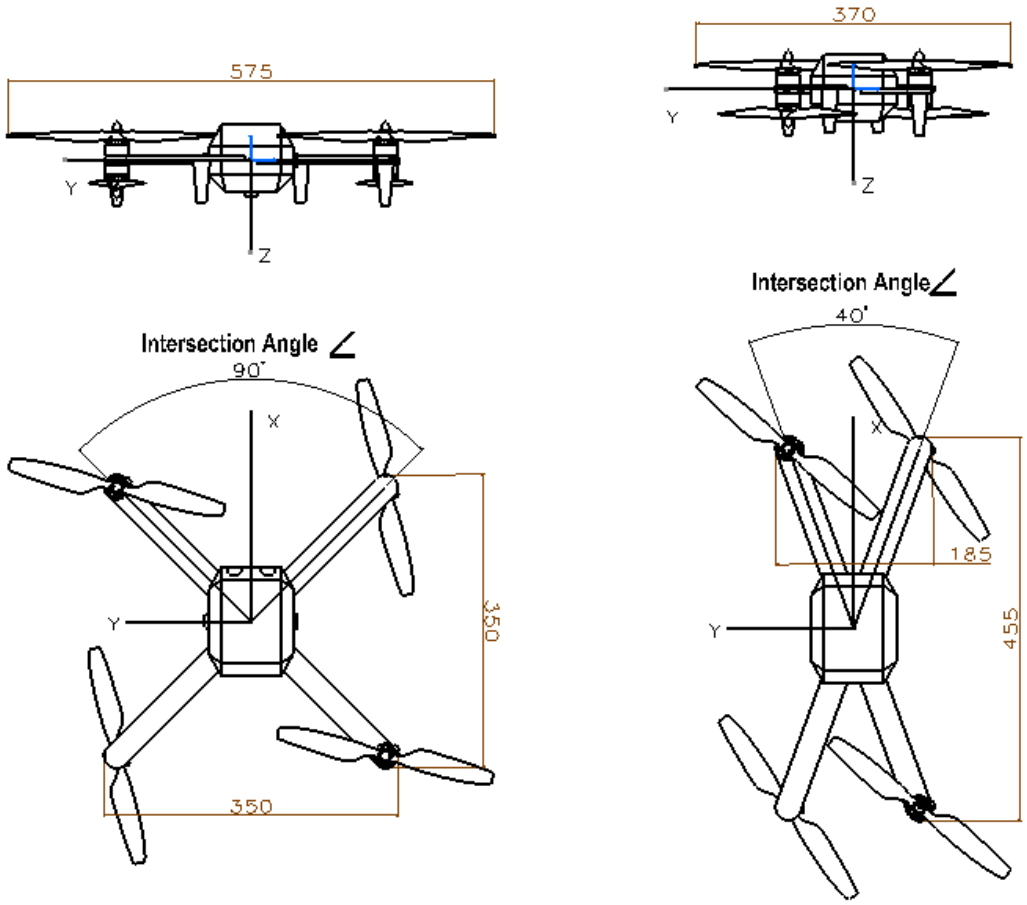

Figure 4. X1 Configuration X2 Configuration

Table 2. Quadcopter X1 ve X2 Configurations Geometry

Symbol	**Description**	**Value (X1)**	**Value (X2)**	**Unit**
∠	Intersection Angle	90	40	degree
m	Mass of Quadcopter	1	1	Kg
l	Arm Length	0.45	0.45	m
lx	X Length	0.35	0.455	m
ly	Y Length	0.35	0.185	m
I_x	Moment of Inertia of X axis	0.01	0.002	Kgm^2
I_y	Moment of Inertia of Y axis	0.01	0.017	Kgm^2
I_z	Moment of Inertia of Z axis	0.02	0.019	Kgm^2

Differences between the geometric measurements between the X1 (unfolded) configuration and the X2 (folded) configuration and the moments of inertia were shown in table 2. According to the angular momentum formulation, the decrease in inertia causes the torque force required for rolling to decrease. This affects the aircraft's stability. Therefore, the system is suitable for use in closed environments, where the effects of wind and other external forces are minimal. This was also examined in the Matlab/Simulink environment. Behavior satisboured.

3. QUADCOPTER DYNAMICS

Quadcopter dynamic calculations are need to examine the mathematical model of the aircraft switching between two different configurations and to examine what different loads the changing system adapts to different configurations. Two axis sets are used to determine the movements of the aircraft. The system has 6 degrees of freedom and 12 states.

- Quadcopter position with respect fixed axis **(*x, y, z*)**
- Linear velocities with respect body axis ***(u, v, w)***
- Angular rates of the body axis ***(p, q, r)***
- Euler angles ***(Ø, θ, ψ)***

In order to study the motion of our drone in Space we need to predict its translational and rotational motion in 3D (x,y,z). According to the 2nd law of Newton, the sum of external forces applied to an object of mass m is equal to its mass multiplied by its acceleration:

$$F=ma \tag{1}$$

Similar rules apply to rotational movements such as:

$$M = I\alpha \tag{2}$$

For quadcopter's movements in space; roll, pitch, yaw and altitude. The rolling movement around the longitudinal axis (X) is produced by the Mx moment. The pitching movement around the lateral axis (Y) is produced by My moment and the yaw movement around the vertical axis (Z) is produced by the Mz moment.

3.1. Linear Dynamic Motion

Acceleration is derived from the variant of the [u, v, w] linear velocity components on the body axis set.

Linear Velocity of Quadcopter;

$$\frac{d}{dt}\begin{bmatrix} x \\ y \\ z \end{bmatrix} = S\begin{bmatrix} u \\ v \\ w \end{bmatrix};\ V=[u\ v\ w]^T \tag{3}$$

Linear Acceleration of the Quadcopter;

$$F=m\frac{d}{dt}\mathrm{V} \Rightarrow \begin{bmatrix}\dot{u}\\ \dot{v}\\ \dot{w}\end{bmatrix}=\frac{F}{m} \quad (4)$$

3.2. Angular Dynamic Motion

Euler angles achieve an angular velocity from derivative. Angular velocity of the quadcopter;

$$\frac{d}{dt}\begin{bmatrix}\emptyset\\ \theta\\ \varphi\end{bmatrix}=\begin{bmatrix}p\\ q\\ r\end{bmatrix} \; ; \; \omega=[\mathrm{p\ q\ r}]^{\mathrm{T}} \quad (5)$$

Angular acceleration of the Quadcopter;

$$M = I\frac{d}{dt}\omega \Rightarrow \begin{bmatrix}\dot{p}\\ \dot{q}\\ \dot{r}\end{bmatrix}=\frac{M}{I} \quad (6)$$

The force and moment generated by the propulsion of propellers on the quadcopter creates linear and angular movements. The force produced by the propellers is eqn.(1) is achieved by the square of the angular speed of the rotors and the coefficient of the thrust .

$$F_i = b\omega_i^2 \; ; \; \mathrm{i} = 4 \quad (7)$$

The moment produced by the propellers is eqn. (2) is achieved by the square of the angular speed of the rotors and the d-moment coefficient.

$$M_i=d\omega_i^2 \; ; \; \mathrm{i}=4 \quad (8)$$

Since the quadcopter has 4 rotors, the total push generated creates the lifting force.

$$\text{Thrust:} \quad U_1 = b(\omega_1^2+ \omega_2^2+ \omega_3^2+ \omega_4^2) \quad (9)$$

The rpm differences of the rotors create moments that cause rotation on the axes on the body. These perform rolling, pitching and yaw movements.

$$\text{Roll:} \quad U_2 = bl/\sqrt{2}(-\omega_1^2+ \omega_2^2+ \omega_3^2- \omega_4^2) \quad (10)$$

$$\text{Pitch:} \quad U_3 = bl/\sqrt{2}(\omega_1^2- \omega_2^2+ \omega_3^2- \omega_4^2) \quad (11)$$

The moments created by the propellers ensure that the aircraft remains constant around the z-axis. The opposite direction of the propellers eliminated the need for a stabilizing tail rotor like in helicopters. The moment produced by the propellers is obtained by the square of the angular velocity and the constant of momentum. Force and moment constants are obtained from propeller theory.

$$\text{Yaw:} \quad U_4 = d(\omega_1^2- \omega_2^2- \omega_3^2- \omega_4^2) \quad (12)$$

The relationship between the rotation speeds of the propellers and the forces and torques and dynamic movements are shown in equations (9), (10), (11) and (12). These are shown in matrix form, equation (13) is also shown.

$$\begin{bmatrix} U_1 \\ U_2 \\ U_3 \\ U_4 \end{bmatrix} = \begin{bmatrix} b & b & b & b \\ \frac{-lb}{\sqrt{2}} & \frac{lb}{\sqrt{2}} & \frac{lb}{\sqrt{2}} & \frac{-lb}{\sqrt{2}} \\ \frac{lb}{\sqrt{2}} & \frac{-lb}{\sqrt{2}} & \frac{lb}{\sqrt{2}} & \frac{-lb}{\sqrt{2}} \\ d & d & -d & -d \end{bmatrix} \begin{bmatrix} \omega_1^2 \\ \omega_2^2 \\ \omega_3^2 \\ \omega_4^2 \end{bmatrix} \quad (13)$$

4. SIMULATION

Quadcopter modeling was implemented in the Matlab-Simulink program. Before this study was done, the necessary formulations were created to run in the background. These; motor, battery, propeller, thrust, torque, dynamic motion equations and their relations.

The preferred engine in this study is 1000 kV and this is the RPMxV unit. It is the relationship between voltage value and motor performance. This equation;

$$RPM=-2.6931*V^3+1000*V \quad (14)$$

The eqn.(15) used for propulsion;

$$Thrust = C_T*p*n^2*D^4 \quad (15)$$

C_T = propolsion coefficient of the propeller

p = denstiy of air

n = rpm of propeller

D = diameter of propeller.

The relationship of C_t with the rpm of the propeller;

$$C_t=2*10^{-15}*RPM^3-4*10^{-11}*RPM^2+3*10^{-7}*RPM+0.1013 \quad (16)$$

The relationship between the torque values obtained by the rotation of the propellers and rpm;

$$Torque=4*10^{-14}*RPM^3+8*10^{-12}*RPM^2+3*10^{-6}*RPM \quad (17)$$

The relationship between torque and current; Torque = KT * I. In this case, the equation that gives the relation of the current with the number of turns;

$$I=1000*(4*10^{-14}*RPM^3+8*10^{-12}*RPM^2+3*10^{-6}*RPM) \quad (18)$$

In the Matlab / Simulink program, considering the flow chart in fig. (4), the control scheme was designed based on the determined mathematical equations. The results of the compilations and configuration adjustments, data and graphics obtained from the program were compared.

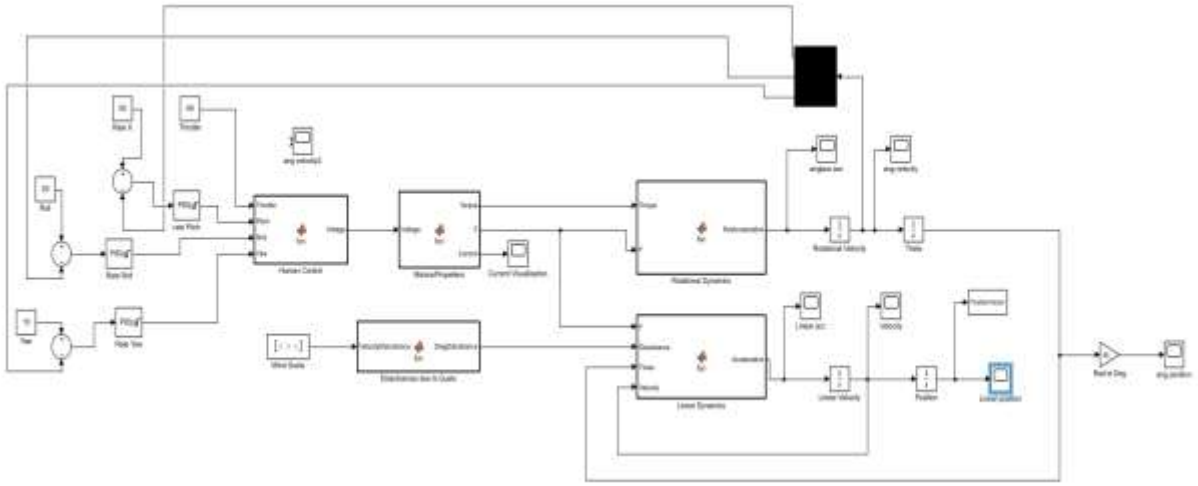

Figure 6. Quadcopter PID Flight Control Diagram

5. CONCLUSION

The geometric results of the quadcopter configuration changes examined together with the environment modelling. In addition, the short passage of the 650mm minimum width aircraft in the X1 configuration was provided.

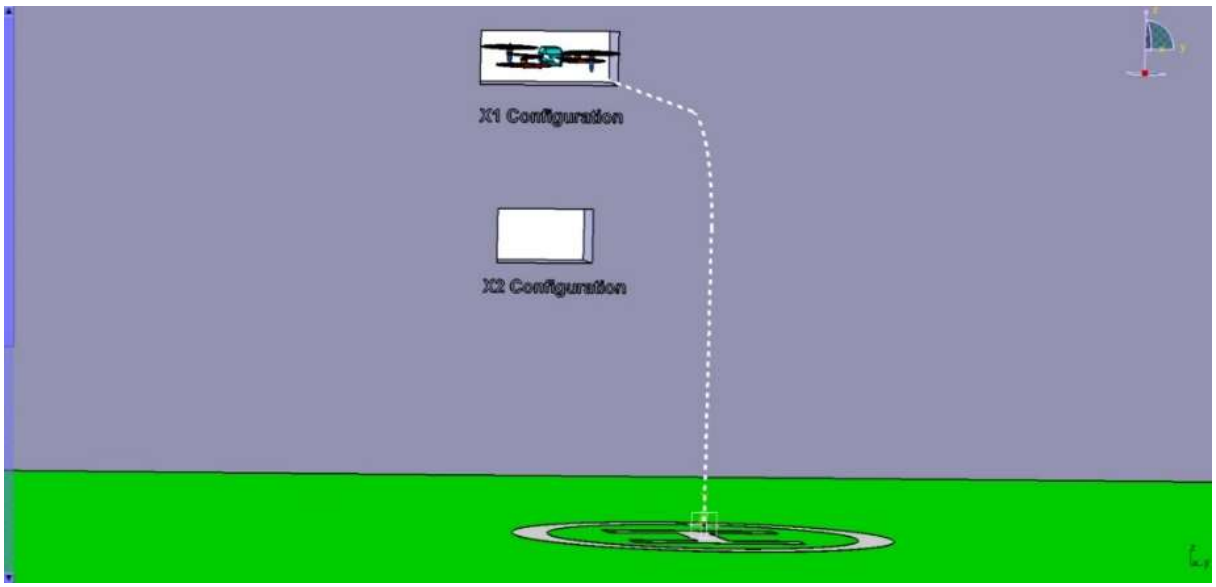

Figure 7. X1 Configuration Flight Simulation Modeling

A short transition was provided in the X2 configuration from the narrower second area, which has a width of 450 mm. The transition between the configurations and the geometric and dynamic load differences caused by this transition were realized with minimum effects thanks to the flight control system.

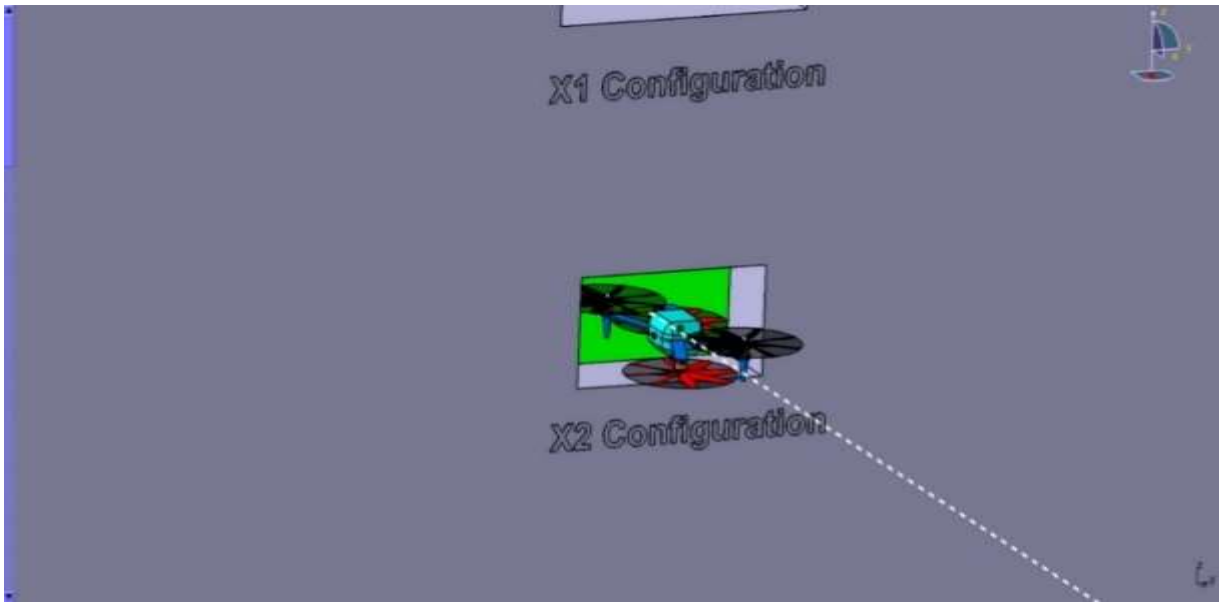

Figure 8. X2 Flight Simulation Modelling

The trial platform prepared and the experiences gained will enable military and civilian applications to be carried out more efficiently, and can be used as a guide in similar transformation and certification studies in civil transportation.

REFERENCES

1.Desbines, A., Expert, F., Boyron, M., Diperi, J., Viollet,S., Ruffier, F. (2017). X-Morf: A crash-separable quadrotor that morfs its X-geometry in flight. 2017 Workshop on Research, Education and Development of Unmanned Aerial Systems (RED UAS)

2.Falanga, D., Kleber, K., Mintchev, S., Floreano, D., Scaramuzza, D. (2018) The Foldable Drone: A Morphing Quadrotor that can Squeeze and Fly. *IEEE Robotics And Automation Letters. Preprint Version.* Accepted November, 2018

3.Bai, Y., Gururajan, S. (2019). Evaluation of a Baseline Controller for Autonomous "Figure-8" Flights of a Morphing Geometry Quadcopter: Flight Performance. *Drones 2019,* 3, 70

4.Wallace, D. (2016). Dynamics and Control of a Quadrotor with Active Geometric Morphing. *Computer Science* Published 2016

5.Prisacariu, V., Sandru, V., & Rău, C. (2011). Introduction morphing technology in unmanned aircraft vehicles (UAV). Paper presented at the International Conference of Scientific Paper, AFASES.

6.Oktay, T., & Sal, F. (2016). Combined passive and active helicopter main rotor morphing for helicopter energy save. Journal of the Brazilian Society of Mechanical Sciences and Engineering, 38(6), 1511-1525

7.Di Luca M, Mintchev S, Heitz G, Noca F, Floreano D. (2017). Bioinspired morphing wings for extended flight envelope and roll control of small drones. *Interface Focus* 7: 20160092.

8.T.Oktay and K. Oğuz, "Non Simultaneous Morphing System Design for Yaw Motion in Quadrotors," *Journal of Aviation*, vol. 3, no. 2, pp. 81-88, 2019.

9.O. Kose and T. Oktay, "Dynamic Modeling and Simulation of Quadrotor for Different Flight Conditions," *European Journal of Science and Technology*, no. 15, pp. 132-142, 2019

10.O. Köse and T. Oktay, "Non Simultaneous Morphing System Desing for Quadrotors," *Avrupa Bilim ve Teknoloji Dergisi*, no. 16, pp. 577-588,2019.

МЕДИЦИНСКОЕ СТРАХОВАНИЕ В УКРАИНЕ И ТУРЦИИ: СРАВНИТЕЛЬНАЯ ХАРАКТЕРИСТИКА

А. В. Кириченко

Кандидат экономических наук, доцент

Аннотация. В статье проанализировано опыт украинского и турецкого медицинского страхования и их особенности. С учетом турецкого опыта в сфере медицинского страхования обосновано необходимость внедрения обязательного медицинского страхования в Украине.

Ключевые слова: медицинское страхование, добровольное медицинское страхование, обязательное медицинское страхование.

Необходимость реформирования системы здравоохранения Украины не вызывает сомнения, ведь по показателю расходов на здравоохранение на одного человека наше государство занимает 89 место в мире (среди 184 стран), а по показателю продолжительности жизни - 108 место [1].

Украинская система здравоохранения финансируется ограничено на уровне 3,3-3,8% ВВП, хотя законодательством определено, что должно быть не менее 5% ВВП, правда и 5% - это мизерная сумма. Для сравнения: в среднем государства-члены Организации экономического сотрудничества и развития (OECD) тратят на сферу здравоохранения 9% ВВП. Безоговорочным лидером по этому показателю являются США - 17,2% ВВП, далее следует Швейцария - 12,4% и Германия - 11,3%. Самые низкие среди стран OECD расходы на здравоохранение в соотношении к ВВП у Турции - 4,3%. Стоит отметить, что даже 4,3% ВВП в Турции - это значительно больше украинских желанных 5%. Поскольку ВВП у нас разные [2].

Согласно ожиданиям общемировой объём расходов на здравоохранение будет расти и дальше. Прогнозы предсказывают дальнейший рост расходов на 5,4% ежегодно в течение 2017-2022 гг., с 7,7 триллионов долларов США до 10,1 триллионов долларов США [7].

Для Украины такие расходы на медицину непосильные, поэтому именно медицинское страхование - это единственный путь выхода здравоохранения Украины из глубокого экономического и социального кризиса [3, с. 86]. Сегодня в Украине более 90% людей, которые не имеют медицинского страхования, то есть перспективы развития системы медицинского страхования в Украине велики, поскольку потенциальных потребителей страховых услуг много [5, с. 111].

Цель исследования – исследовать проблемы и тенденции развития украинского и турецкого медицинского страхования.

С целью определения целесообразности внедрения медицинского страхования, а также определения, какой именно вид медицинской системы предпочитают украинцы, были

проведены исследования, результаты которых показали, что практически все опрошенные имеют представление о преимуществах медицинского страхования, из них 12% предпочитают современную медицинскую систему, обязательное социальное медицинское страхование - 24%, смешанный вид медицинской системы - 43% опрошенных. Люди, которые не имеют интереса к виду медицинской системы - 21%. Итак, можно сделать вывод, что большинство людей хотят видеть в Украине смешанный вид медицинской системы [5, с. 110-111]. Сравнительная характеристика украинского и турецкого медицинского страхования и их особенностей приведена в таблице.

Таблица. Сравнительная характеристика украинского и турецкого медицинского страхования*

<table>
<tr><td>Показатель</td><td colspan="3">Украина</td><td colspan="3">Турция</td></tr>
<tr><td>Финансирование здравохранения, % ВВП</td><td colspan="3">3,5</td><td colspan="3">4,3</td></tr>
<tr><td>Право граждан на медицинскую помощь</td><td colspan="3">49-я статья Конституции Украины</td><td colspan="3">60-я статья Конституции Турции</td></tr>
<tr><td>Средняя продолжительность жизни
Мужчины
Женщины</td><td colspan="3">71,8
66,7
76,7</td><td colspan="3">75
72,7
77,5</td></tr>
<tr><td rowspan="2">Взносы на социальное страхование %, всего
в т.ч. на обязательное медицинское страхование</td><td>Работодатель</td><td>Работник</td><td>Всего</td><td>Работодатель</td><td>Работник</td><td>Всего</td></tr>
<tr><td>22

-</td><td>0

-</td><td>22

-</td><td>22,5

7,5</td><td>15

5</td><td>37,5

12,5</td></tr>
<tr><td>Обязательное медицинское страхование</td><td colspan="3">Практическое введение обязательного медицинского страхования началось 1 января 2018 г. на основе утвержденной медицинской реформы.</td><td colspan="3">С 1 января 2012 г. стала действовать система обязательного страхования, которая дает возможность бесплатного лечения во всех государственных больницах, а также предоставляет скидку на обслуживание в частных клиниках.</td></tr>
<tr><td>Добровольное медицинское страхование</td><td colspan="3">Добровольное медицинское страхование развивается медленно (по последним данным, только около 6% украинцев имеют соответствующие полисы). Чаще всего медицинскую страховку для своих работников оформляют компании, таким образом обеспечивая для них покрытие расходов на лечение. При оформлении страхования предлагают различные пакеты медицинских услуг. Чаще всего в них входит: оплата лекарств; плановая и экстренная стационарная помощь; неотложная помощь; обслуживание в</td><td colspan="3">Дает возможность обслуживаться не во всех клиниках. Бесплатные медицинские услуги предоставляют только учреждения, сотрудничающие с страховой компанией. Обычно такие страховки не покрывают долгосрочное лечение от хронических, психологических, венерических заболеваний. Также не предусмотрена помощь в случаях, выходящих за рамки страховых событий. Таким образом, за лечение травм, полученных в результате митингов, военных действий и других подобных</td></tr>
</table>

	поликлиниках; стоматология (плановая и экстренная).	событий, придется платить самостоятельно.

*Построено автором на основе [2; 4; 8; 9; 10; 11; 12].

В Украине в 2018 г. новая модель финансирования здравоохранения введена на первичном звене медицинской помощи, где работают семейные врачи, терапевты, педиатры. На высших уровнях – вторичной (специализированной) и третичном (высокоспециализированном) она вводиться постепенно к 2020 г.

Для введения новой системы финансирования здравоохранения создана Национальная служба здоровья Украины (НСЗУ), которая перечисляет бюджетные средства медицинским учреждениям и врачам-ФОПам за оказание медицинской помощи населению. НСЗУ заключает соглашения со всеми медицинскими учреждениями и гарантирует финансирование в соответствии с количеством пациентов, которым в этих заведениях будет оказана медицинская помощь. Финансирование осуществляется на условиях предварительной оплаты [1].

Проанализировав турецкий опыт медицинского страхования стоит отметить, что с 1 января 2012 г. в Турции стала действовать система обязательного медицинского страхования, которая распространяется не только на граждан страны, но и на иностранцев, которые проживают в Турции больше года. Она была создана, чтобы устранить беспорядок в системе здравоохранения и дать относительно свободный доступ к медицинским услугам всем людям.

Система обязательного медицинского страхования затрагивает не только медицинскую сферу, но и социальную, так как медицинская страховка также покрывает все расходы связанные с травмами которые можно получить на производстве. Самый распространенный вид медицинской страховки в Турции – государственная (обязательное медицинское страхование). Данный вид страховки дает возможность бесплатного лечения во всех государственных больницах, а также предоставляет скидку на обслуживание в частных клиниках.

Кроме медицинских услуг, государственная страховка в Турции предусматривает различного рода выплаты: по выходу на пенсию, инвалидности, безработицы. Кроме государственного страхования распространен еще один вид страховки – частный (добровольное медицинское страхование). Последний вид страховки дает возможность обслуживаться не во всех клиниках. Бесплатные медицинские услуги оказывают только учреждения, сотрудничающие со страховой компанией. Система обязательного страхования оплачивает все виды медицинских услуг в государственных больницах, и дает право на скидки в некоторых частных учреждениях. Следовательно, данная страховка покроет и долгосрочное лечение от хронических заболеваний, и расходы на лекарства, выписанные врачом.

Добровольное медицинское страхование обычно не покрывает долгосрочное лечение от хронических, психологических, венерических заболеваний. Также не предусмотрена помощь в случаях, выходящих за рамки страховых событий. Таким образом, за лечение травм, полученных в результате митингов, военных действий и других подобных событий, придется платить самостоятельно.

Ни частное, ни государственное страхование не покрывает полностью расходы на медпрепараты, но их можно приобрести со значительной скидкой, если они выписаны врачом и есть в наличии рецепт. При наличии государственной страховки придется оплатить лишь 20% начальной стоимости лекарств [11].

Имеющаяся в Украине система здравоохранения нуждается в срочном выполнении процесса реформирования. Учитывая положительный турецкий опыт внедрения обязательного медицинского страхования нужно подготовить как законодательную, так и материальную базу, согласовать все механизмы, чтобы в дальнейшем не достичь еще худшего состояния, учесть все преимущества и риски, также создать Единый государственный банк медицинского страхования, который будет аккумулировать все поступления и распоряжаться ими.

Общеобязательное медицинское страхование будет способствовать увеличению финансовых поступлений в отрасль здравоохранения и оптимизации их использования; обеспечению качественной медицинской помощи каждому гражданину; финансированию медицинских учреждений в соответствии с объемом и качеством предоставляемых ими услуг, что будет способствовать повышению оплаты труда; обеспечению финансовой независимости медицинских учреждений; переходу к контрактным условиям в системе здравоохранения; усилению конкуренции между государственными и частными лечебными учреждениями; дальнейшему развитию добровольного медицинского страхования [5, с. 113; 10, с. 1143].

Список использованной литературы

1. Бойко С.Г. Диверсифікація джерел фінансування охорони здоров’я / С.Г. Бойко [Електронний ресурс]. – Режим доступу – https://niss.gov.ua/doslidzhennya/analitichni-materiali/socialna-politika/diversifikaciya-dzherel-finansuvannya

2. Дорогие лекарства: как государство и фармкомпании могут гарантировать их доступность // Экономическая правда [Электронный ресурс]. – Режим доступа – // https://www.epravda.com.ua/rus/columns/2019/08/7/650359/

3. Кириченко А. В. Розвиток соціального страхування в Україні: Монографія. – К.: ЦП “КОМПРИНТ”, 2017. – 197 с.

4. Медичне страхування: коли добровільне стане обов'язковим і як це працюватиме [Електронний ресурс]. – Режим доступу – https://24tv.ua/health/medichne_strahuvannya_koli_dobrovilne_stane_obovyazkovim_i_yak_tse_pratsyuvatime_n1166692

4.Міщук І. Сучасний стан обов'язкового медичного страхування в Україні та шляхи його розвитку / І. Міщук, І. Віннічук // Підприємництво, господарство і право. – 2019. – № 2. – С. 110-114.

5.Офіційний сайт Держаної служби статистики України [Електронний ресурс]. – Режим доступу – // www.ukrstat.gov.ua

6.Прогноз тенденцій розвитку світової галузі охорони здоров'я в 2019 році [Електронний ресурс]. – Режим доступу – // https://www2.deloitte.com/ua/uk/pages/life-sciences-and-healthcare/articles/global-health-care-sector-outlook-2019.html)

7.Рівень життя в Туреччині [Електронний ресурс]. – Режим доступу – https://news.eurabota.ua/uk/turkey/migration/zhyttya-v-turechchyni/#3

8.Система социального обеспечения в Турции [Электронный ресурс]. – Режим доступа – // http://www.invest.gov.tr/ru-RU/investmentguide/investorsguide/employeesandsocialsecurity/Pages/TurkishSocialSecuritySystem.aspx

9.Сокирко О.С. Розвиток медичного страхування: зарубіжний досвід та можливості його використання в Україні / О.С. Сокирко, І.А. Кобзар, І.С. Ханалієва // Економіка і суспільство. – 2018. – № 19. – С. 1139-1145.

10.Як організовано медичне страхування в Туреччині [Електронний ресурс]. – Режим доступу – https://poradnuk.com.ua/kraini-svitu/europe/turkey/medychne-strakhuvannya-v-turechchyni.htm)

11.Trading Economics [Электронный ресурс]. – Режим доступа – // www.tradingeconomics.com

БИОЛОГИЯЛЫҚ ҚОСПАЛАРДЫ ҚОЛДАНЫП ЙОГУРТ ДАЙЫНДАУ ӘДІСІ

Исаев Ғ.И., Бостанова А.М., Ыдырыс Б.А.

Қ.А.Ясауи атындағы Халықаралық қазақ-түрік университеті, Түркістан қ.

Аннотация

Бұл мақалада Йогурттың араласқан культураларын пайдаланған кезде S. Thermophilus және L.delbruecrii –дің қышқыл түзу жылдамдығы басқа штаммаларға қарағанда жоғары екені анықталды. Жұмыс нәтижесінде бұл екі микроорганизмдердің арасындағы байланыстың басты негізгі валина культурасын жасау L.delbruecrii, бірақ құрамының өзгеруіне байланысты жыл бойына сүтте басқа аминқышқылдарының жеткіліксіз екендігі байқалды.

Кілттік сөздер: Йогурт, S. Thermophilus, L.delbruecrii, штамм, бифидобактерия, ассоциативтік өсу, грамм салмақты, анаэробты, гетероферментативті, қимылсыз, спорасыз таяқшалар.

ҚР Президентінің Қазақстан халқына арналған жолдауында, ауыл шаруашылығындағы мына мәселелерге тоқталып өткен. Негізгі міндетіміз – ауыл шаруашылығының өнімділік деңгейін көтеру, жердің тозуының алдын алу, еліміздің су және басқа табиғи ресурстарын пайдалану тиімділігін арттыру, сонымен қатар ескірген аграрлық технологиялардың қолданылуына, аграрлық ғылымның кенжелеп дамуына тосқауыл қою, сондай-ақ ұсақ шаруа қожалықтарының бытыраңқылығын еңсеру мәселелерін жүйелі түрде шешу. Алға қойылған міндеттердің ауқымында ауыл шаруашылығының барлық салаларына сапалы талдау жүргізіп, өркендеу қажет болатын бағыттарды айқындауға міндетті. Бүкіл дүние жүзіндегі жедел дами бастаған, ауыл шаруашылығындағы өнімдердің жаңа рыногы – экологиялық таза өнімдер алуда өз үлесімізді қосу. Ескірген агротехнологияларды алмастыруды және жоғары технологиялық агроөнеркәсіп құруды қарастыруы қажет [1].

Қазіргі кезде бифидобактериялардың әртүрлі нәрселерден алынған 30 түрлі штаммы теңестірілген – адамдардан, жануарлар мен құстардан, ағын сулардан алынған, олардың ішіндегі алтауы адамдардан алынған Bifidobacterium adolescentis, breve, bifidum, infantis, lactis және longum бактериялары ферменттелген сүт өндірісінде «биопродуктылар» жасауға қолданылады. Адамнан алынған Bifidobacterium animalis адам жасушаларында нық тұрады, сондықтан қандай бактерия түрлерін йогурт жасауға қолданатынын білу әлі де болса тереңірек зерттеулерді қажет етеді. Бактериялардың сипаттамаларының теңестірілуі төменде көрсетілген:

- грамм салмақты, анаэробты, гетероферментативті, қимылсыз, спорасыз таяқшалар, көлемдері 0,5-1,3×1,5-8 мкм;

- бұл бифидобактериялардың клеткалары анаэробты ортада триптиказды-фитон ашытқылы ортасында өскен, өзіне тән формасы мен құрылымы бар (қысқа және ұзын, ұзын және жіңішке, бірнеше қисықтардан және сирек тармақталған);

- пептидогликан қабырғасы-бұл ұйымдағы бактериялар олар түрлеріне қарай әртүрлі болады, күрделі молекулалық тізбектен тұрады N –ацетилмурамды қышқыл және N-ацетилглюкозамин екеуі кезектесіп орналасады; Көмірсулардың әр түрлі тәсілмен теңестіріледі. Ең жақсы фермент көзі болып фруктоза -6 – фосфат фосфокетолаза (F6ФФК) «бифидошунт» деген атпен белгілі. Бұл фермент түрлерді теңестіру үшін қолданылады, бірақ барлық штаммаларды бірдей мөлшерде теңестіре алмайды. Глюкозаның екі молекуласы, екі молекула лактат пен 3 молекула ацетат түзеді;

- ганин мен цитозин құрамындағы молекулалар (Г+Ц) ДНҚ-да 54-67 моль % болып топтасады:

- көптеген бифидогенді заттар бойдың өсуіне көмек береді [2].

Бифидобактериялардың таяқшалары көбінесе қисық болып келеді, бастары иіліп, аяқ жақтары жуандау болады. Кейбір кездерде жасушалар ұзын және қысқа болып, әр түрлі көлемде болады, жасушалар V-Y немесе X тәріздес болады, бұл түрлердің барлығы да өскен ортаның құрамына байланысты. Қолайсыз ортада жасуша формалары өзгеріп жан –жағына жайылып кетеді. Кейде амин қышқылдарын құйғаннан жасушаның өсу түрлері бұзылатыны анықталған. Осындай жағдайлармен кокка тәрізді жасушалардың B.bifidum түрі ортаға натрий хлоридын құйғаннан кейін ұқсап кеткен. B.longum - өте ұзын, жіңішке болады, B.breve- ең жіңішке және ең қысқа (бифидобактериялардың арасындағы) болып саналады.

Йогурттың ашытқысын- екі микроорганизмнің ассоциациясын симбиоз деп атаған, ол байланыс көптеген зерттеулерде жазылған. Бұндай біріккен жағдайда әр организм бір-біріне пайдалы зат шығарады. S.thermophilus және L.delbruecrii сүтте әрқайсысы бөлек культура болуына байланысты «симбиоз» атын өзгертіп «ассоциативтік өсу» деп атаған тиімді тәрізді.

Йогурттың араласқан культураларын пайдаланған кезде S. Thermophilus және L.delbruecrii –дің қышқыл түзу жылдамдығы басқа штаммаларға қарағанда жоғары. Жұмыс нәтижесіне қарағанда, бұл екі микроорганизмдердің арасындағы байланыстың басты негізгі валина культурасын жасау L.delbruecrii, бірақ құрамының өзгеруіне байланысты жыл бойына сүтте басқа аминқышқылдарының жеткіліксіз екендігі байқалады.

Ассоциативтік өсу теориясы бұл жұмыста зерттелді және L.delbruecrii тармағы bulgaricus, S. thermophilus реттейді, нәтижесінде глицин және глистидин түзеді, сөйтіп мынадай қорытынды шығардық: ең қажеттісі глистидин екен, валин емес. Бірақ глицин мен глистидиннің әсері басқа аминқышқылдарына қарағанда төмен болды. Қорыта

келгенде айтармыз. Еріген азоты жоқ майсыз сүттен жасалған ортада S. Thermophilus-дің өсуін тежейді, басқа аминқышқылдарының өсуіне себепші болады. Олар йогурттың ашытқысындағы ақуызды ыдыратып жібереді. Ондай микроорганизмдерге төмендегілер жатады:

-пептидтер, құрамында лизині бар;

-трипептидтер, құрамында гистидин, метионин және глутамин қышқылдары бар;

-казеин гидролизаты;

-магнийді қосу.

S. thermophilus-дің белсенділігінің артуы лейцинмен және изолейцинмен қосылған кезде 30 және 45ºС болды. Лактобациллдің белсенділігінің көтерілуі стрептококтарға жайлы жағдай жасайды, себепші болатын L.delbruecrii - bulgaricus-дің тармағы. Бұл жұмыста біріккен культивирлеу жасаудың қарсы жақтары да қаралды. Одан мынадай қорытынды жасалды: а) анаэробтық жағдайда белгісіз фактор себепші болады; в) бұл фактор құмырсқа қышқылы болуы мүмкін. Бұлардан басқа, осы авторлар сүтті қыздырып өңдеген уақытта әртүрлі түрлердің әсері болатынын, қарқынды түрде ысытылған сүтте тек заттың өзі себепші болатынын дәлелдеді. Бірақ, йогурт жасау үшін ысытылған сүтке себепші факторлардың S. thermophilus-ден шығатынын мойындайды. L.delbruecrii, bulgaricus тармағының кейбір штаммдары сүтті дақылдандырған уақытта, ысытып 100ºС 15 мин. өңдеген кезде жасушалардың ұзаратынын, ал мембрананы бояу, ол жасушалардың әлі жасалмағанын көрсетті. Бірақ бұл сияқты морфологиялық өзгерістер сүтті 100ºС температурада ысытып 15 минут ұстаған уақытта байқалмады. Сонымен бірге сүттегі натрий формиаты L.delbruecrii-bulgaricus тармағының протеолитикалық белсенділігін арттыруға себепші болды [3].

Йогурт құрамындағы CO_2 мочевинаның гидролизі нәтижесінде пайда болады, және оның маңызы кондуктометриялық әдіспен өлшенеді, ал CO_2 парциальды қысымы арқылы йогурт құрамындағы микроорганизмдердің өміршеңдігін анықтауға болады. Дахиде жасалған CO_2 мөлшері ашыту температурасында 42ºС және 1мл/100 мл ашытқы салған уақытта 450 мкл. Болды, бұл өнімнің органолептикалық көрсеткіштерін көрсетеді. Бұл жұмыста бірінші рет, CO_2 және натрий гидрокарбонаты S. thermophilus – дің өсуіне себепші болып, микроорганизмдердің метаболизмдік функцияларына әсер етеді. Бұдан шығатын қорытынды йогурттың ашуына себепші болатын факторлар L.delbruecrii- bulgaricus тармағы қоректік заттармен қамтамасыз етеді (аминқышқылдармен) S. Thermophilus, кейінгісі лактобацилланың өсуіне жағдай жасайды.

Йогурттағы микроорганизмдердің өсуіне электромагнитті аймақ немесе жоғарғы қабаттағы микроорганизмдерді өсіруге арналған жағдай әсер етеді.

Сүт қышқылының ашуы сүт қышқылды бактериялардың ферменттерімен көміртектердің анаэробты процесінің ыдырауы, сүт қышқылдың және басқа да

өнімдердің пайда болуымен түзіледі. Бұл процеске қатысатын бактериялардың түріне байланысты ашудың соңғы өнімі әр түрлі болады. Мысалға, гомоферментативті сүт қышқылының ашуынан сүт қанты тек сүт қышқылын ғана ыдыратады.

Гетероферментативті ашуда сүт қышқылынан бөлек басқа өнімдер де түзіледі (ұшқыш қышқылдар, спирт, газдар, эфирлер).

Гомоферментативті ашудың қоздырғышы болып мына микроорганизм саналады: Streptococcus lactis-сопақша шар тәрізді, диаметрі 0,5-1,0 мкм, культурада қос-қостан (диплококктар) немесе қысқа тізбекті (стрептококктар), өте сирек бір-бірден кездеседі.

Streptococcus cremoris-жасушалары ұзынырақ тізбекті болып орналасқан; Lactobacillus, bulgaricus – ірі таяқша тәрізді қозғалмайтын, грам оң, жеке жасуша немесе қысқаша тізбек түрінде орналасады.

Йогурттағы бактериофаг қоспасы орталарының морфологиясы

Микро организмдер	**Басы**		**Құйрығы**	**Құйрық ұшы**	**(n=)**
	Құрылысы	**Өлшемі (нм)**	**Ұзындығы(нм) × диаметрі (нм)**		
S. thermophilis	Гексагональды	50-60	217-239×4,8	-	2
	Многогранды	40-60	220-420×8	+	2
	Многогранды немесе	49-50	130-224×8-9	+	14
	Октаэдр	60-65	236-290×10	±	3
	НС	48-70	213-265×11-12	+	59
	Многогранды	57	234×9,5	+	50
	Изометриялық	45-65	220-245×НС	+	120
	Гексогональды	65	230-260×НС	+	24
	Изометриялық				
L.delbruecrii подвида bulgaricus	Гексагональды	56-62	205-215×СН	±	1
	Многогранды немесе октаэдр	44-55	116-160×8-9	-	7
	НС	50-59,4	175-198×5-6,6	-	3
	Гексагональды	48	159×НС	-	1

Микроорганизмдер көмегімен алынатын азық тамақ өнімдерінің спектрі өте үлкен. Бұл – ашыту нәтижесінде алынатын өнімдер-йогурт, нан, ірімшік, сүзбе, шарап, сыра т.б. осы уақытқа дейін тамақ өнеркәсібінде биотехнология бұрынғы игерілген процесстерді жетілдіру мақсатында ғана қолданылса, қазіргі кезеңде өнімді штаммаларды қажетті жағдайларға пайдалану үшін генетикалық зерттеулер жүргізіп, ашыту технологиясының жаңа әдістері ашылып отыр.

Қолданылған әдебиеттер тізімі

1. ҚР Президенті Н.Ә.Назарбаевтың Қазақстан халқына жолдауы // Университет 9009.3-5 бет

2. Богданов В.М. Микробиология молоко и молочных продуктов. – М., Пищевая промышленность. 1976.

3. Горбатова К.К. Биохимия молока и молочных продуктов.- М., Агропромиздат. 1986.